

COMPARISON OF MECHANICAL PROPERTIES OF SEMI SOLID FORMING AND  
HOT FORMING OF A356 ALUMINUM ALLOY

by

Erhan Doğruyol

B.S. in M.E., İstanbul Technical University, 2002

Submitted to the Institute of Graduate Studies in  
Science and Engineering in partial fulfillment of  
the requirements for the degree of  
Master of Science

Graduate Program in Mechanical Engineering  
Boğaziçi Univeristy

2006

## ACKNOWLEDGEMENTS

I would like to express my most sincere appreciation to my thesis supervisor Prof. Sabri Altıntaş for his invaluable support and encouragement throughout this study.

I am grateful to Kurt Neulinger from Salzburger Aluminium for supplying the necessary aluminum alloys for the experimental study.

I gratefully acknowledge the HEMA ENDÜSTRİ A.Ş and ASLAR PRES DÖKÜM A.Ş. for manufacturing experimental set-up and remarkable assistance given for the experimental work.

I am also indebted to my friend Mehmet Günhan Çil and to my parents for their unlimited support and encouragements during the study.

Finally I wish to express special thanks to Nazım Mahmutyazıcıoğlu and Önder Albayrak for their memorable helps and assistance throughout the project.

## **ABSTRACT**

### **COMPARISON OF MECHANICAL PROPERTIES OF SEMI SOLID FORMING AND HOT FORMING OF A356 ALUMINUM ALLOY**

Thixoforming is a forming technology to produce near net shaped complex parts with high mechanical properties especially for automotive industry. The process is based on a discovery made at MIT in the early 1970s. The operation takes place in the semi solid region of the metal and therefore has several advantages such as close dimensional tolerances, lower porosity and better mechanical properties over conventional forming processes. In this study origins and principles of thixotropic behavior of metals were explained with giving examples of previous studies on the subject. The production techniques for obtaining the necessary raw material with fine and globular microstructure were explained and the steps of the forming process were described. In the experimental part of the study semi-solid forming and hot forming experiments were conducted on A356 aluminum alloy, at different temperatures with various holding times. After the production of the samples the effects of the heating parameters on the final microstructure of semi-solid formed products were examined. Finally microhardness and tensile tests were performed on the samples and a comparison of mechanical properties was made between semi solid formed and hot formed samples.

## ÖZET

### **YARI-KATI VE SICAK ŞEKİLLENDİRİLEN A356 ALÜMİNYUM ALAŞIMININ MEKANİK ÖZELLİKLERİNİN KIYASLANMASI**

Yarı-katı şekillendirme özellikle otomotiv endüstrisinde yüksek mekanik özelliklere sahip karmaşık geometrik şekillerdeki parçaların üretilmesinde kullanılan bir yöntemdir. Bu işlem temel olarak 1970 lerin başında MIT de yapılan bir buluşa dayanmaktadır. Şekil verme işlemi malzeme yarı-katı halde iken gerçekleştirilmekte ve bunun sonucunda klasik şekillendirme yöntemlerine kıyasla yakın boyutsal tolerans, düşük gözenek oranı ve daha iyi mekanik özellikler gibi birçok avantaja sahiptir. Bu çalışmada tiktotropik davranışın temelleri ve ilkeleri geçmiş çalışmalardan örnekler verilerek anlatılmıştır. Gerekli küresel mikroyapının temini için uygulanan yöntemler açıklanmış ve şekil verme işleminin adımları sıralanmıştır. Çalışmanın deneysel bölümünde A356 alüminyum alaşımı kullanılarak farklı sıcaklıklarda ve bekleme sürelerinde yarı-katı ve sıcak şekillendirme deneyleri gerçekleştirilmiştir. Parçaların üretiminin ardından deney parametrelerinin yarı-katı şekillendirilmiş ürünler üzerindeki mikroyapısal etkileri incelenmiştir. Son olarak ürünler üzerinde sertlik ve çekme deneyleri yapılarak yarı-katı şekillendirilmiş ve sıcak şekillendirilmiş ürünlerin mekanik özellikleri kıyaslanmıştır.

## TABLE OF CONTENTS

ACKNOWLEDGEMENTS .....	ii
ABSTRACT .....	iii
ÖZET .....	v
LIST OF FIGURES .....	viii
LIST OF TABLES .....	xiii
LIST OF SYMBOLS/ABBREVIATIONS .....	xiv
1. INTRODUCTION .....	1
2. FORMATION OF NON-DENDRITIC STRUCTURES .....	5
2.1. Mechanisms for Formation of Non-Dendritic Structure .....	5
2.2. Origins of Thixotropy .....	11
2.3. Experimental Techniques .....	13
2.4. Rheology of Semi-Solid Alloys .....	14
2.5. Technologies for Production of Non-Dendritic Feedstock .....	19
2.5.1. Mechanical Stirring .....	20
2.5.2. Magneto Hydrodynamic (MHD) Stirring .....	24
2.5.3. Stress Induced and Melt Activated (SIMA) Process .....	27
2.5.4. Spray Casting .....	29
2.5.5. Liquidus Casting .....	31
2.5.6. Chemical Grain Refining .....	34
2.5.7. Ultrasonic Treatment .....	35
3. SEMI SOLID AND HOT FORMING OF ALUMINUM .....	36
3.1. Semi-Solid Metal Forming .....	36
3.2. Rheocasting .....	38
3.3. Thixomolding .....	40
3.4. Rheomolding .....	42
3.5. Thixoforming .....	42
3.5.1. Reheating Process .....	44
3.5.2. Forming Process .....	46
3.6. Hot Forming of Aluminum Alloys .....	50

3.6.1. Rolling of Aluminum Alloys . . . . .	51
3.6.2. Forging of Aluminum Alloys . . . . .	51
3.6.3. Extrusion of Aluminum Alloys . . . . .	52
3.6.4. Common Forging Processes . . . . .	53
3.6.4.1. Press Forgings . . . . .	53
3.6.4.2. Upset Forgings . . . . .	53
3.6.4.3. Roll Forgings . . . . .	53
3.6.4.4. Net Shape Near-Net Shape Forging . . . . .	53
4. EXPERIMENTAL STUDY . . . . .	55
4.1. Materials . . . . .	55
4.2. Experimental Setup . . . . .	57
4.2.1. Semi-Solid Forming and Hydraulic Power Unit . . . . .	57
4.2.2. Heating Unit . . . . .	59
4.2.3. Temperature Control Unit . . . . .	60
4.2.4. Die . . . . .	61
4.2.5. Conveyer . . . . .	63
4.3. Semi-Solid Forming and Hot Forming of A356 Alloy . . . . .	63
4.4. Sample Characterization . . . . .	67
4.4.1. Microstructure Examinations . . . . .	67
4.4.2. Vickers Microhardness Tests . . . . .	68
4.4.3. Tensile Tests . . . . .	69
5. RESULTS AND DISCUSSION . . . . .	72
5.1. Microstructure Examination . . . . .	73
5.2. Mechanical Properties . . . . .	84
6. CONCLUSIONS . . . . .	90
REFERENCES . . . . .	92
REFERENCES NOT CITED . . . . .	100

## LIST OF FIGURES

Figure 1.1.	Special microstructure in semi-solid metal . . . . .	2
Figure 1.2.	Cutting reheated billet with a spatula . . . . .	3
Figure 1.3.	Schematic view of semi-solid forming . . . . .	3
Figure 2.1.	Schematic illustration of evolution of structure during solidification with vigorous agitation: (a) initial dendritic fragment; (b) dendritic growth; (c) rosette; (d) ripened rosette; e) spheroid . . . . .	6
Figure 2.2.	Schematic illustration of dendrite arm fragmentation mechanism: (a) undeformed dendrite; (b) after bending; (c) formation of high angle boundary; (d) fragmentation through wetting of grain boundary by liquid metal . . . . .	7
Figure 2.3.	Schematic illustration of morphological transition from dendritic to spherical via rosette with increase in shear rate and intensity of turbulence . . . . .	10
Figure 2.4.	Diagram showing when the shear rate increases, the agglomerates break up and spheroidise, when the shear rate decreases further agglomeration occurs . . . . .	12
Figure 2.5.	Apparent viscosities versus solid fractions at different shearing rates (left) and cooling rates (right) . . . . .	15
Figure 2.6.	Steady state apparent viscosity versus shear rate in Sn-15Pb alloy for various solid fractions . . . . .	16

Figure 2.7.	Yield stress of semi-solid Sn-15Pb alloy as function of resting time . . .	17
Figure 2.8.	(a) Shear-rate step-up and step-down experiments; (b) shear-stress evolution in shear-rate step experiments . . . . .	18
Figure 2.9.	Schematic view of a mechanical stirring machine . . . . .	21
Figure 2.10.	Schematic view of continuous rheocaster . . . . .	22
Figure 2.11.	Schematic view of stir casting device . . . . .	24
Figure 2.12.	Vertical casting with horizontal electromagnetic flow . . . . .	25
Figure 2.13.	Effects of EMS stirring time on microstructure of A356 alloy: (a) 0 s; (b) 10 s; (c) 20 s; (d) 40 s; (e) 60 s; (f) 90 s . . . . .	26
Figure 2.14.	Schematic diagram of SIMA process . . . . .	28
Figure 2.15.	Cooling slope casting system . . . . .	33
Figure 3.1.	Examples of semi-solid formed products . . . . .	38
Figure 3.2.	Schematic illustration of new rheocasting (NRC) process . . . . .	39
Figure 3.3.	Schematic diagram of thixomolder . . . . .	41
Figure 3.4.	Steps of thixoforming . . . . .	43
Figure 3.5.	Microstructure of reheated alloy . . . . .	45
Figure 3.6.	Induction heating of cylindrical work piece . . . . .	46
Figure 3.7.	Schematic view of the thixoforming press . . . . .	48

Figure 4.1.	Solid fraction of A356 alloy as a function of temperature . . . . .	56
Figure 4.2.	Microstructure image of the raw material . . . . .	57
Figure 4.3.	Hydraulic unit . . . . .	58
Figure 4.4.	Main body . . . . .	59
Figure 4.5.	Ring heater used for pre-heating the die . . . . .	60
Figure 4.6.	Temperature control unit . . . . .	61
Figure 4.7.	Die used to produce the specimens . . . . .	62
Figure 4.8.	Closing the bottom hole of the die . . . . .	62
Figure 4.9.	Conveyer . . . . .	63
Figure 4.10.	General view of the experimental set up . . . . .	64
Figure 4.11.	Transferring the heated billet to the die cavity . . . . .	65
Figure 4.12.	Removal of the sample from the die . . . . .	66
Figure 4.13.	Prepared specimen in bakalite . . . . .	67
Figure 4.14.	Tensile test specimen . . . . .	70
Figure 4.15.	Image of the tensile test specimen . . . . .	71
Figure 5.1.	Formed specimen . . . . .	72

Figure 5.2.	Microstructure of surface portion of sample S1 (x100) . . . . .	73
Figure 5.3.	Microstructure of mid-portion of sample S1 (x100) . . . . .	74
Figure 5.4.	Microstructure of surface portion of sample S2 (x100) . . . . .	74
Figure 5.5.	Microstructure of mid-portion of sample S2 (x100) . . . . .	76
Figure 5.6.	Microstructure of surface portion of sample S3 (x100) . . . . .	76
Figure 5.7.	Microstructure of mid-portion of sample S3 (x100) . . . . .	77
Figure 5.8.	Microstructure of surface portion of sample S4 (x100) . . . . .	78
Figure 5.9.	Microstructure of mid-portion of sample S4 (x100) . . . . .	78
Figure 5.10.	Microstructure of mid- portion of sample S5 (x50) . . . . .	79
Figure 5.11.	Microstructure of surface portion of sample S5 (x100) . . . . .	80
Figure 5.12.	Microstructure of mid-portion of sample S6 (x50) . . . . .	81
Figure 5.13.	Microstructure of surface portion of sample S6 (x100) . . . . .	81
Figure 5.14.	Eutectic microstructure of sample S6 (x500) . . . . .	82
Figure 5.15.	Microstructure of sample S7 (x500) . . . . .	83
Figure 5.16.	Microstructure of sample S8 (x100) . . . . .	83
Figure 5.17.	Microstructure of sample S9 (x100) . . . . .	84

Figure 5.18.	Vickers microhardness values of samples S1, S2 and S3 through height. ....	85
Figure 5.19.	Vickers microhardness values of samples S1, S2 and S3 through width. ....	85
Figure 5.20.	Vickers microhardness values of samples S4, S5 and S6 through height. ....	85
Figure 5.21.	Vickers microhardness values of samples S4, S5 and S6 through width. ....	86
Figure 5.22.	Vickers microhardness values of samples S7, S8 and S9 through height. ....	86
Figure 5.23.	Vickers microhardness values of samples S7, S8 and S9 through width. ....	86
Figure 5.24.	Average Vickers microhardness values of the samples . . . . .	87

**LIST OF TABLES**

Table 4.1.	Chemical composition of A356 aluminum alloy used in the study in weight percent . . . . .	55
Table 4.2.	Chemical composition of A356 aluminum alloy in weight per cent . . .	56
Table 4.3.	Specifications of the forming unit . . . . .	59
Table 4.4.	Forming parameters of the specimens . . . . .	66
Table 5.1.	Shape factor (F) values of the samples . . . . .	82
Table 5.2	Tensile test results of the products . . . . .	88
Table 5.3.	Mechanical properties of A356 aluminum alloy . . . . .	89

**LIST OF SYMBOLS/ABBREVIATIONS**

A	Particle cross sectional area
E	Young modulus
$E_c$	Coil electromagnetic force
$f_s$	Solid fraction
F	Shape factor
$I_c$	Coil current
$I_w$	Current in work piece
N	Number of turns
P	Perimeter of the particle
$\varepsilon$	Strain
$\sigma$	Stress
$\Phi$	Flux
DC	Direct chill
EMS	Electromagnetic stirring
MHD	Magneto hydrodynamic
MMC	Metal matrix composite
NRC	New rheocasting
RSBN	Reaction bonded silicon nitride
SIMA	Stress Induced and Melt Activated
SQC	Squeeze casting
SSF	Semi solid forging
SSM	Semi-solid metal
SSR	Semi-solid rheocasting
TSRM	Twin screw rheomolding

## 1. INTRODUCTION

Semi-solid processing is a novel method of forming complex-shaped components in the semi-solid state. An alloy as a semi-solid slurry has a much higher viscosity than when fully liquid, thereby retaining laminar flow and filling a die more evenly, facilitating near net-shape forming with a single processing step.

Mascara, honey and certain kinds of paint are all thixotropic. When they are sheared they flow, when allowed to stand they thicken up again; their viscosity is shear rate and time dependent. Such behavior in semi-solid metallic alloys is discovered in the early 1970s at the Massachusetts Institute of Technology (MIT). If the material is stirred continuously during cooling from the fully liquid state to the semi-solid state the viscosity is significantly lower than if the material was cooled into the semi-solid state without stirring. Stirring breaks up the dendrites which would normally be present so that the microstructure in the semi solid state is non-dendritic, which is spheroid particles well insulated from each other by a continuous layer of eutectic liquid. Typical microstructure is shown in Figure 1.1 where the lighter areas are the primary globular grains and the darker region is the eutectic structure. The spots inside the grains are the entrapped liquid phase inside the primary structure [1].

It is this microstructure which is a requirement for thixotropic behavior and for semi-solid processing. When such a semi-solid microstructure is allowed to stand, the spheroids agglomerate and the viscosity increases with time. If the material is sheared, the agglomerates are broken up and the viscosity falls. In the semi-solid state, if the alloy is allowed to stand it will support its own weight and can be handled like a solid. As soon as it is sheared, it flows with a viscosity similar to that of heavy machine oil [2]. This is the behavior which is exploited in semi-solid processing and which is illustrated in Figure 1.2 where the alloy can be cut and spread like butter [3].

This behavior is attractive because it provides an efficient net shape forming method that competes favorably with casting and solid state forming. The thixotropic properties

will permit the material to be handled by robotic devices in the semi-solid condition, allowing processing automation and precision controls while increasing productivity compared to other production methods.

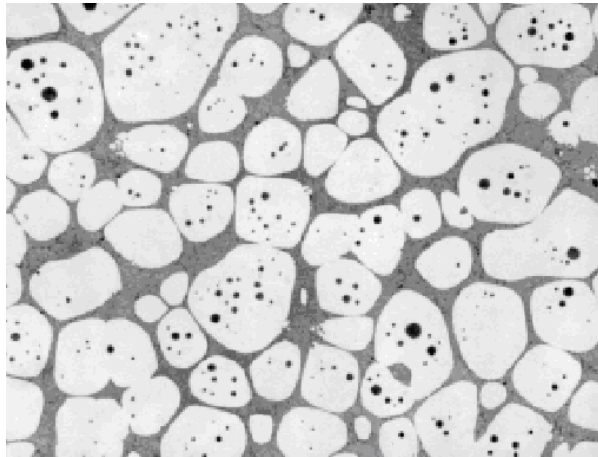


Figure 1.1. Special microstructure in semi-solid metal [1]

Thixoforming has become an important forming technology during the last years. In contrast to the classical die casting and forging processes, the alloy is processed in the semi-solid state, with globular grains suspended in the liquid phase [4]. The thixoforming process is a three step process. The first stage is the raw material production which has a non-dendritic microstructure. In the second stage the metal is reheated to the semi-solid temperatures as quickly and homogeneously as possible. After the reheating process the material consists of fine globular solid phase in the eutectic liquid. In the last process the forming operation takes place by means of thixoforming or thixocasting. The operation is illustrated in Figure 1.3.

Thixoforming has come to play an increasing role as an alternative to classic manufacturing techniques such as casting and forging. One reason for this is the growing demand for high-strength aluminum components for lightweight automotive designs. A necessary condition for the manufacture of low-cost lightweight aluminum parts is the ability to process this expensive material into near net shape components of complex geometry and high strength. Thixoforming provides the engineer with a vastly broader range of design options than forging possibly even broader than conventional casting processes [5].



Figure 1.2. Cutting reheated billet with a spatula [3]

In the automotive sector there is a trend to use different aluminum alloys for parts with complex geometry. In the automotive industry, lightweight materials are very important with respect to reducing fuel consumption and protecting the environment. For this purpose, heavier cast iron and steel parts have been replaced with lightweight aluminum castings in the automotive industry around the world. Particularly from a manufacturing point of view, for lighter and more advanced functional products semi-solid die casting provides a substantial potential as an innovative net shape manufacturing process. With manufacturing costs now on a level with high-grade casting applications, high mechanical component qualities can be achieved, and applications in the field of highly-integrated safety critical components have become possible.

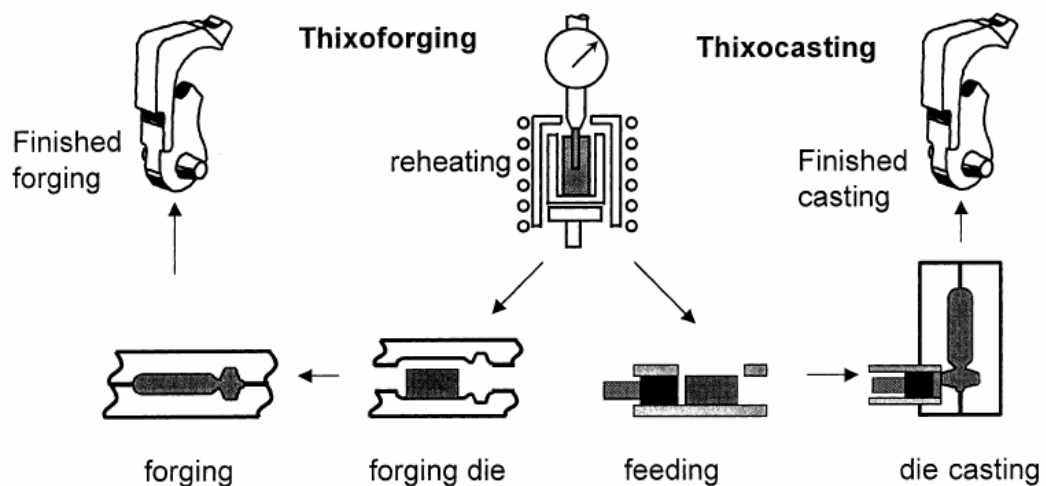


Figure 1.3. Schematic view of semi-solid forming [4]

Commercially, thixoforming is used to produce automotive components on a mass production scale, but only with conventional casting alloys such as A356 and A357, for the most part produced by magneto hydrodynamic stirring (MHD) stirring. There is a considerable interest in extending its application to the higher performance wrought specification aluminum alloys. Nowadays, the known fields of application of forging- and extrusion forming processes are somewhat restricted for technical and economical reasons. In these manufacturing processes, the raw material must be in the full solid state, which makes the plasticity requirement mandatory: materials presenting low deformation ability would require prohibited pressures to be formed. Therefore, only alloys with considerable ductility find commercial application in the forged or extruded state, even though such processes usually demand high pressures and consequent high energy demands. The utilization of raw material in the semi-solid condition can make feasible the forming by forging and by extrusion of low ductility alloys: those which could not be formed in conventional processes. Due to the flow behavior of the semi-solid metal characterized as thixotropic, it can be handled as a solid, even when containing a high solid fraction and it presents low resistance to deformation under pressure. Such a behavior means lower energy requirements for forming when compared to conventional solid forming processes, leading to lower investment costs on machinery [6]. Thixoforming processes, or semi-solid metals (SSM) processing, can potentially produce high quality, near-net-shape products, due to the better accommodation of globular structures, compared to dendritic material, and are reported to have less internal porosity.

## 2. FORMATION OF NON-DENDRITIC STRUCTURES

Nearly all metal alloys of commercial importance solidify dendritically, either with a columnar or with an equiaxed dendritic structure. In both equiaxed and columnar structures, the dendrites themselves evolve greatly during solidification, as a result of ripening due to surface energy. The structure becomes gradually coarser during solidification as a result of remelting of dendrite arms of smaller radius. In accordance with expected ripening kinetics, it is found that final dendrite arm spacing bears in approximately cube-root relationship to the local solidification time or, inversely to the cooling rate. The increase of dendrite (above about  $f_s=0.5$ ) arm spacing takes place only during the initial portion of the solidification time. In later stages of solidification liquid-solid surface area can be most effectively reduced by the filling of spaces between rod like arms to form plates [7].

### 2.1. Mechanisms for Formation of Non-Dendritic Structure

Vigorous agitation, as solidification begins, results in formation of new grains (Figure 2.1a). The early growth of each dendrite fragment then continues dendritically, as shown in Figure 2.1b. With continuing shear and time during solidification, the dendrite morphology becomes that of a rosette (Figure 2.1c), as a result of ripening, shear and abrasion with other grains. Ripening proceeds during further cooling (Figure 2.1d). In addition the reduction of the interfacial energy between particles and liquid provides the driving force for spheroidization of the particles. Oswald ripening would also take place, wherein solutes diffuse from small particles to larger particles effect, resulting in the coarsening phenomenon. Stirring would enhance the ripening by accelerating solute diffusion. At this stage a rosette type of structure would form due to bending and plastic deformation of the dendrites. Two competing mechanisms also prevail, which are structure agglomeration due to bond formation among particles caused by impingement and reaction, and subsequent structure breakdown due to shearing and particle collision. As the stirring time increases, the structure evolution is governed by the balance among the dendrite fragmentation, Oswald ripening and structure agglomeration and breakdown. As

particles become further spheroidise, the dendrite fragmentation mechanism become less and less prevalent. A second rosette type of structure due to particle coalescence may develop when the agglomeration mechanism dominates over the breakdown mechanism. In the subsequent stage, a steady state may be reached where the structure agglomeration and breakdown mechanism are balanced, after which Oswald ripening might become the prevalent mechanism [7,8].

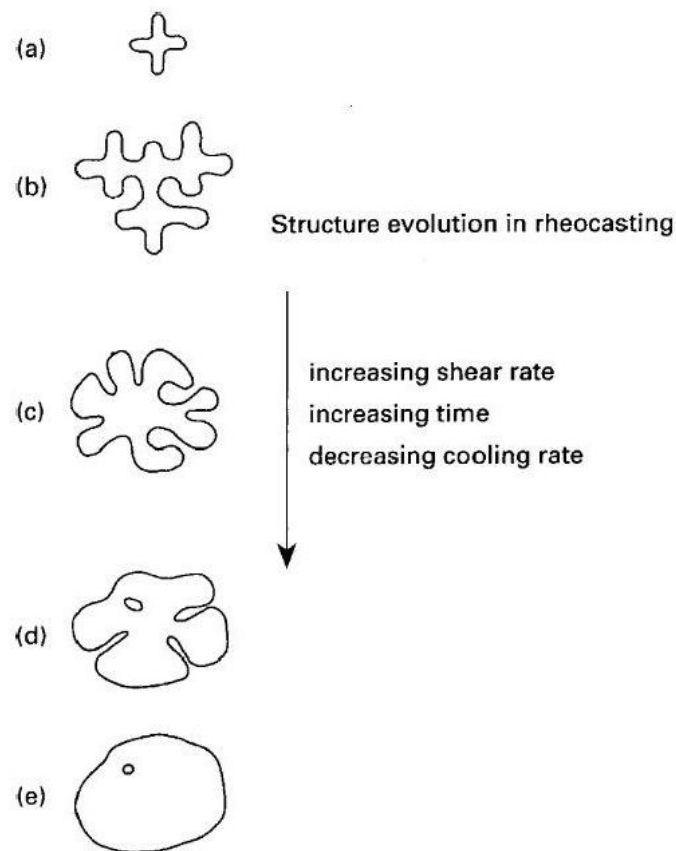


Figure 2.1. Schematic illustration of evolution of structure during solidification with vigorous agitation: (a) initial dendritic fragment; (b) dendritic growth; (c) rosette; (d) ripened rosette; e) spheroid [8]

In the initial stage of stirring, the dendrite fragmentation dominates, for which a higher shear rate would lead to a smaller particle size. In the subsequent stage when Oswald ripening dominates, a higher shear rate would enhance the solute diffusion. Therefore coarsening is accelerated and results in a larger particle size.

To explain the observed fine particle size and non-dendritic morphology under forced convection several mechanisms have been proposed. These include: dendrite arm fragmentation, dendrite arm root remelting, and growth controlled mechanisms. Any proposed mechanism has to address two basic aspects of solidification under forced convection, namely, grain refinement and morphological transition. It should be mentioned that solid particles with any morphology in the semi-solid state would, with prolonged isothermal holding, spheroidise by a ripening process under the driving force for reduction of interfacial free energy, even under full diffusion control.

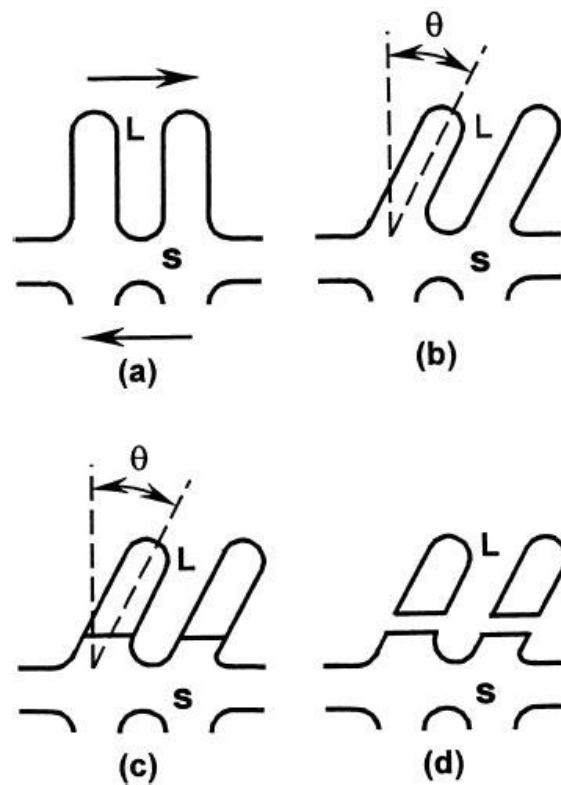


Figure 2.2. Schematic illustration of dendrite arm fragmentation mechanism: (a) undeformed dendrite; (b) after bending; (c) formation of high angle boundary; (d) fragmentation through wetting of grain boundary by liquid metal [4]

To explain the observed grain refinement by melt stirring, Vogel *et al.* [9] have proposed a dendrite arm fragmentation mechanism to account for grain multiplication, as schematically illustrated in Figure 2.2 [4]. Dendrite arms bend plastically under the shear force created by melt stirring. Plastic bending introduces large disorientations into the dendrite arms in the form of ‘geometrically necessary dislocations’. At high temperature,

such dislocations rearrange themselves to form high angle grain boundaries through recrystallisation. Any grain boundary with energy greater than twice the solid/liquid interfacial energy is then wetted by liquid metal, resulting in the detachment of dendrite arms.

Secondary dendrite arms can detach at their roots because of remelting due to solute enrichment and thermosolutal convection. Temperature fluctuations in the MHD rheocasting process play a significant role in the structural evolution. Vigorous stirring prevents the establishment of stable diffusion fields for continued dendrite evolution. Eventually, smooth rounded shapes are expected out of solidification [8].

The intensity of shear is expected to determine the fluid flow characteristics in the melt. At low and intermediate shear rates the flow is essentially laminar, and it is unlikely that a laminar flow can interact with the secondary dendrite arms to exert a bending moment. In fact, under a laminar flow, the secondary dendrite arms are not expected to experience any relative fluid motion at the solid/liquid interface. But the intensity of laminar flow will certainly determine the thickness of diffusion boundary layer around a growing particle, and therefore determine the growth morphology of the solid. At a high shear rate, the flow characteristics change to turbulence, and liquid penetration into the interdendritic region is likely to take place. The turbulence flow enhances relative particle motion. This would bring about a significant change in the solidification structure; as solute transport away from the secondary dendrite arms would take place [4].

Based on the above considerations, Qin and Fan [10] found that the penetration of the liquid phase into the interdendritic region results in a relative change in growth rate along the solidification interface. With increasing intensity of turbulent flow, the local growth rate increases laterally and at the root of dendrite arms, resulting in the formation of rosettes and even spheres at sufficient intensity of turbulence. It has been concluded that turbulent flow stabilizes the solidification interface. Turbulent flow can enhance crystal growth more effectively than laminar flow.

Under intensive turbulent flow, the solidification morphology is spherical even at the very early stage of solidification [11]. The size, shape factor, and density of the solid

particles are almost constant with increasing isothermal shearing time. The particle size distribution was found to be very close to that of randomly dispersed monospheres [12]. In the low shear rate region, increasing shear rate increases particle density and decreases particle size, while in the high shear rate region both particle size and density reach a plateau. This demonstrates the importance of turbulent flow as regards the formation of spherical morphology. The important findings from these investigations are:

- Turbulent flow is crucial for the formation of spherical particles during solidification under forced convection
- The observed rosette and spherical particle morphologies are more likely to be a growth phenomenon during solidification under forced convection.

Furthermore, it is generally observed that melt stirring accelerates crystal growth during solidification. Under full diffusion control, spheroidization of the initially dendritic structure in the semi-solid state usually takes a few tens of minutes or even up to a few hours while formation of spherical particles takes only a few minutes under predominantly laminar flow conditions [13]. This process requires only a few seconds under intensive turbulent flow conditions, even with a fully dendritic structure before stirring. It can be understood from these findings that turbulence flow is essential for the formation of non-dendritic structure.

The experimentally observed grain refinement under high shear rate and high intensity of turbulence was explained by a copious nucleation mechanism [4]. Under the intensive mixing action, both temperature and composition fields inside the liquid alloy are extremely uniform. During the continuous cooling under forced convection, heterogeneous nucleation takes place at the same time throughout the whole liquid phase. The intensive mixing action disperses the clusters of potential nucleation agents, giving rise to an increased number of potential nucleation sites. In fact, this situation not only occurs under intensive turbulent flow, but also applies to nucleation under forced convection in general. However, it seems that laminar flow is much less effective for homogenizing the temperature and composition and for dispersing the potential nucleation agents. Consequently, laminar flow is less powerful for structural refinement and spheroidization of the solid particles than the turbulence flow.

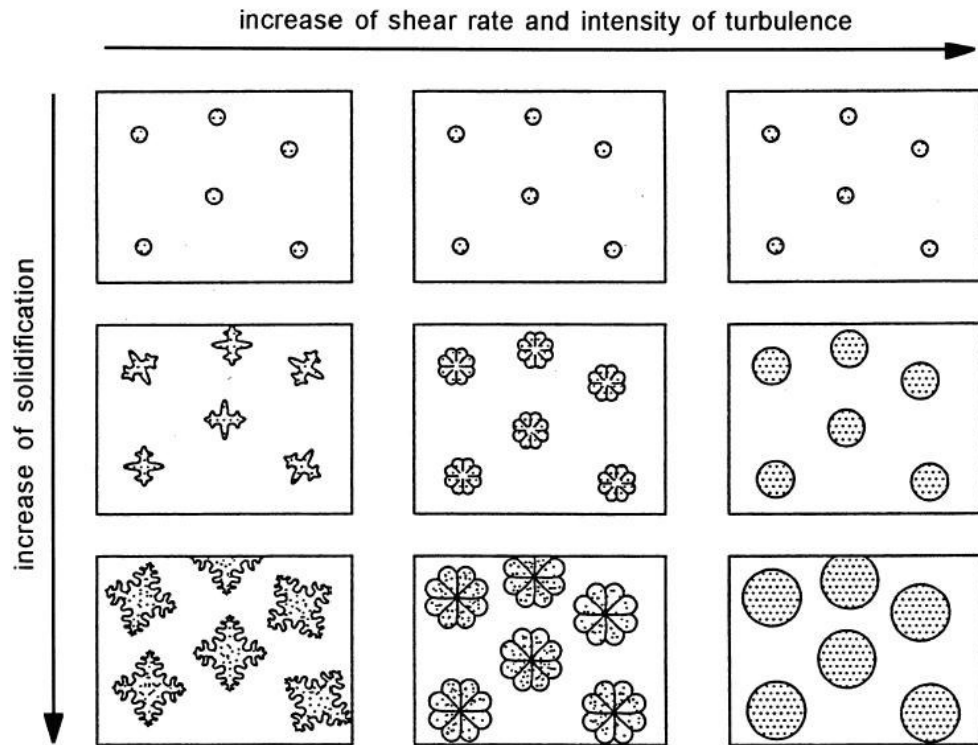


Figure 2.3. Schematic illustration of morphological transition from dendritic to spherical via rosette with increase in shear rate and intensity of turbulence [4]

The understanding of the microstructural evolution obtained from the above investigations [4,11,12,13] can be schematically illustrated in Figure 2.3 and can be summarized as:

- Forced convection promotes crystal growth due to enhanced mass transport during solidification
- Laminar flow changes the normal dendritic growth morphology to rosette, while turbulent flow changes the growth morphology from rosette to sphere
- It appears that the observed rosette and spherical morphologies under forced convection are more likely to be a growth phenomenon rather than resulting from a mechanical fragmentation mechanism
- The structural refinement under intensive stirring is most probably caused by a copious nucleation mechanism, which is facilitated by homogeneous temperature and composition fields and well dispersed heterogeneous nucleation agents. However, at

lower shear rates, the dendrite arm remelting and fragmentation mechanisms may also be of significance.

## 2.2. Origins of Thixotropy

A liquid like semi-solid metal (SSM) slurry is considered as a suspension in which interacting spherical solid particles of low cohesion are dispersed in a liquid matrix. In a simple shear flow field, the dynamic interactions between solid particles result in the formation of agglomerates. Under viscous forces, collisions between agglomerates lead to the formation of new agglomerates of a larger size, and at the same time agglomerates also break up giving rise to agglomerates of smaller size (Figure 2.4). As a result the viscosity decreases. The viscosity is both time and shear rate dependent with a dynamic equilibrium between agglomeration and disagglomeration at a microstructural level. Each shear rate has a characteristic agglomerate size distribution. When the shear rate is changed, over a period of time the agglomerate size distribution will tend towards that characteristic of the new shear rate, with the viscosity changing proportionally. It is believed that it is the state of agglomeration which determines the rheological properties of SSM slurries, whereas the external flow conditions, such as shear rate and shearing time, affect the rheological properties by changing the state of agglomeration [14].

In semi-solid metallic systems, the agglomeration occurs because particles are colliding and, if favorably oriented, form a boundary. By 'favorable orientation' is meant the fact that if the particles are oriented in such a way that a low energy boundary is formed, it will be more energetically favorable for the agglomeration to occur than if a high energy boundary is formed. If a 3-D network builds up throughout the material, the semi-solid will support its own weight and can be handled like a solid because the globular particles agglomerate by forming solid–solid boundaries. It must be energetically favorable for these boundaries to replace solid–liquid boundaries and thus the solid–solid boundaries tend to be of low energy types. As shear occurs, particles are forced into contact with each other. If it is energetically favorable for a solid–solid boundary to be formed; the two particles will stay in contact. If not, they will separate again. The process will be influenced by the rate of shear in two opposing ways. Increasing the rate of shear will increase the possibility of particle–particle contact but it will decrease the time of contact

and the formation of a new solid–solid boundary [2]. There is a higher proportion of low-angle and twin boundaries present between neighboring particles, and hence a higher degree of agglomeration, than for the unstirred grain refined alloy. Non-dendritic structures revealed low energy special boundaries within the primary particles whose formation has been attributed to the sintering of individual primary particles and growth twinning mechanisms [15].

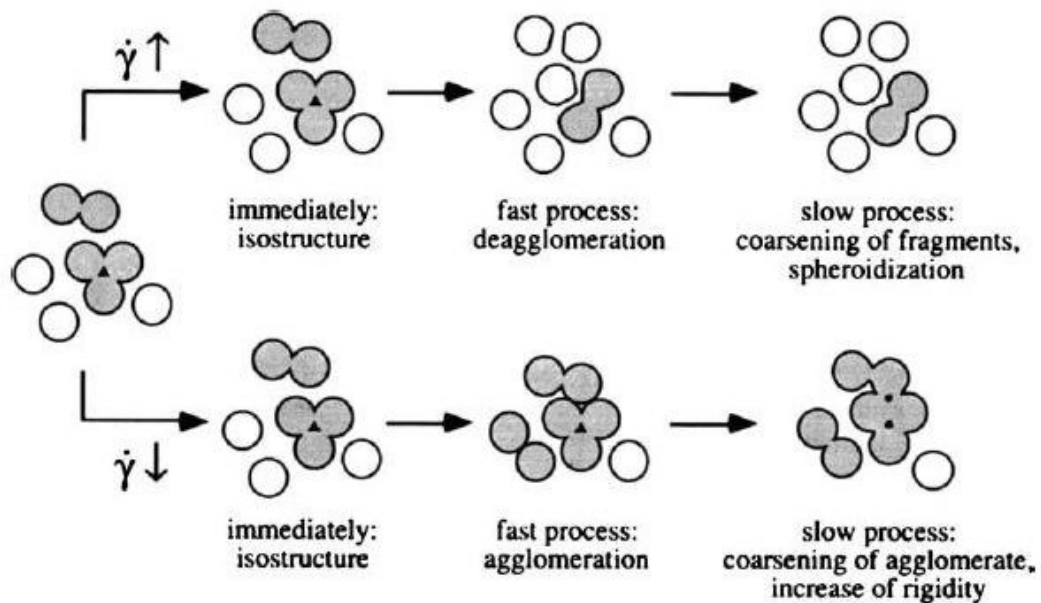


Figure 2.4. Diagram showing when the shear rate increases, the agglomerates break up and spheroidise, when the shear rate decreases further agglomeration occurs [14]

The viscosity in the steady state depends on the balance between the rate of structure build up and the rate of break down. It also depends on the particle morphology. The closer the shape to that of a pure sphere, the lower the steady state viscosity [8]. Contrary viscosity increases with the change of the particles from spheres to dendrites. In addition, if liquid is entrapped within particles, it does not contribute to flow. Thus, although the fraction liquid may take a certain value, governed by the temperature in practice, the effective fraction liquid may be less as some is entrapped within spheroids. As a result entrapped liquid in the primary grains adversely affects the viscosity and result in poor flow behavior of the material.

### 2.3. Experimental Techniques

Semi-solid metal slurries used in SSM processing can be roughly divided into two broad categories, a liquid like slurry contains dispersed solid particles and behaves like a fluid under external forces, while solid-like slurry contains an interconnected solid phase and behaves like a solid exhibiting well defined yield strength. The deformation mechanisms for these two types of slurry are fundamentally different. Semi-solid metal slurries with a solid fraction of less than 0.6 and a globular solid morphology usually exhibit two unique rheological properties, thixotropy and pseudoplasticity [4]. Thixotropy describes the time dependence of transient state viscosity at a given shear rate, while pseudoplasticity refers to the shear rate dependence of steady state viscosity. All the SSM processing techniques rely on either one of those properties or both properties in the same process. Therefore, successful development of SSM processing technologies requires a good understanding of the rheology of SSM slurries.

The concentric cylinder rheometer has been most commonly used for rheological characterization of SSM slurries [16]. In the concentric cylinder rheometer, rheological experiments for SSM slurries are often performed in three different modes [4].

- Continuous cooling and shearing from a temperature above the liquidus
- Transient or steady state experiments from a specified starting condition under fixed solid fraction and shear rate
- Shearing after partial solidification or partial remelting.

The major advantages of this technique include high flexibility in terms of operating mode and well defined flow conditions. This makes it very suitable for understanding the physical mechanisms of SSM rheology. However, this technique is limited to low shear rates and relatively low solid fractions, because too high a shear rate can cause flow instability and too high a solid fraction can lead to wall slippage.

For high solid fractions, above about 0.5, conventional rheometers do not have sufficient torque capability. Other methods must then be used, introducing complexity because the shear rate is no longer constant throughout the material [2].

Compression between parallel plates is the technique used for rheological characterization of SSM slurries with a high solid fraction. In this method, a cylindrical sample with low aspect ratio is compressed between two parallel plates at constant deformation rate or under constant load [17]. In this case, the axial velocity becomes insignificant compared to the radial velocity of the alloy during the later stage of deformation. It should be noted that the stress–strain field in this experiment is highly inhomogeneous due to the presence of friction. Therefore, comparison of results should be made with caution, especially when there are specimen size differences. This technique can be used to investigate SSM slurries with high solid fraction, and to detect the presence of yield stress. However, the flow conditions are complex, it is difficult to define the steady state and, more importantly, it is difficult to prevent solid/liquid segregation.

Capillary die and backward extrusion have also been used to characterize SSM slurries. In such techniques, the flow is pressure driven and is characterized by a variation of shear rate along the cross-section depending on material behavior. Viscosity is usually calculated assuming linear viscous behavior, which may not necessarily be true for all the cases. As in the parallel plate technique, it is not clear whether the steady state is reached; the data obtained are not steady state values, but probably closer to iso-structure data. Moreover, in the presence of strong deviation from linearity or if yield stress is present, plug flow conditions will develop. In this case, the flow conditions near the wall dominate the response of the materials. Therefore, a true viscosity cannot be calculated. Another problem associated with this technique is that it is almost impossible to study thixotropy. Segregation may also occur due to the pressure gradient that develops as a result of the long length required by this test and the increased permeability at the walls. However, since similar flow conditions are present in an actual thixoforming process, the information extracted from such tests can be relevant when comparable values of cross-sections are used [4].

#### **2.4. Rheology of Semi-Solid Alloys**

The first investigation of the rheology of SSM slurries was conducted at MIT (Cambridge, MA, USA) on the Sn-Pb system. They showed that a stirred SSM slurry with a solid fraction higher than 0.2 behaves like a non-Newtonian fluid with an apparent

viscosity orders of magnitude less than that of an unstirred dendritic slurry. It is this first observation which initiated numerous rheological studies on stirred SSM slurries [4]. The rheological phenomena in stirred SSM slurries can be approximately divided into three groups:

- Continuous cooling behavior, which describes the viscosity evolution during continuous cooling at constant cooling rate and shear rate.
- Pseudoplastic behavior, which describes the shear rate dependence of steady state viscosity, or shear thinning behavior.
- Thixotropic behavior, which describes the time dependence of transient state viscosity.

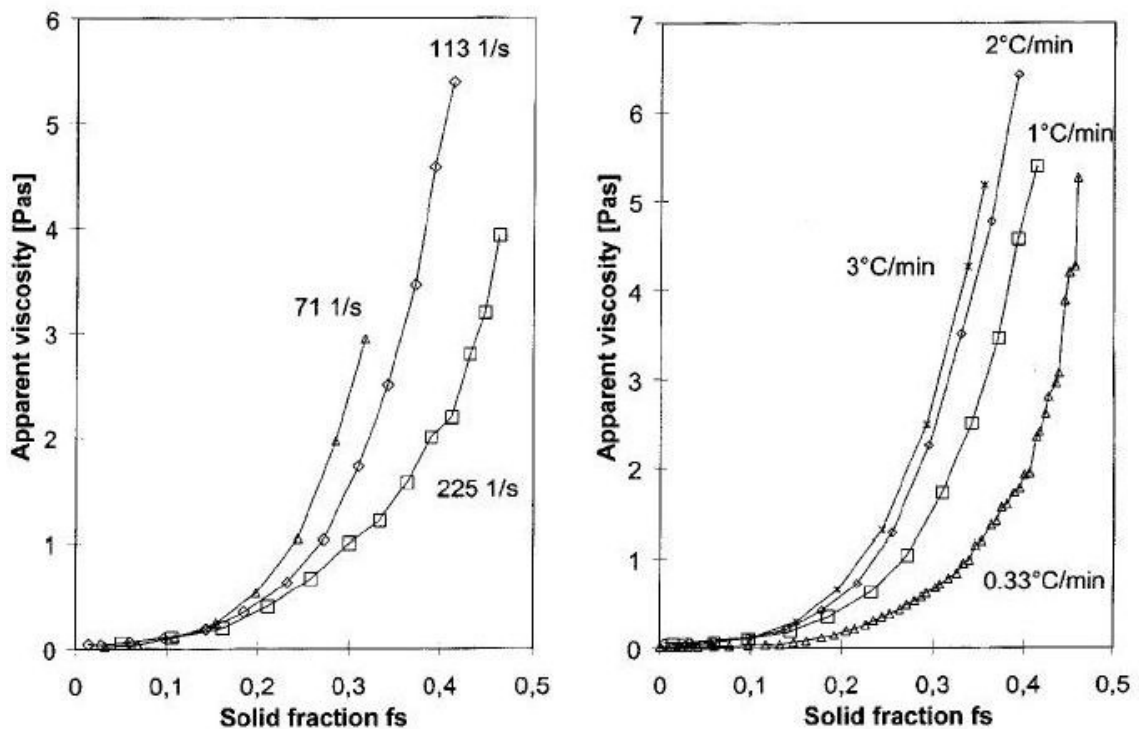


Figure 2.5. Apparent viscosities versus solid fractions at different shearing rates (left) and cooling rates (right) [16]

The continuous cooling behavior gives the first insight of the effects of solid fraction, shear rate, and cooling rate on the rheological behavior of SSM slurries. Figure 2.5 shows examples of results obtained from the continuous cooling experiments on Sn–15Pb alloy [16]. The measured apparent viscosities are plotted versus the solid fraction at different

cooling rates and shear rates. Generally, for a given cooling rate and shear rate, the measured apparent viscosity increases with increasing solid fraction, slowly at low solid fraction and sharply at high solid fraction. At a given solid fraction, the apparent viscosity decreases with increasing shear rate and decreasing cooling rate. This is because both increasing shear rate and decreasing cooling rate promote more spherical particle morphology [16,18].

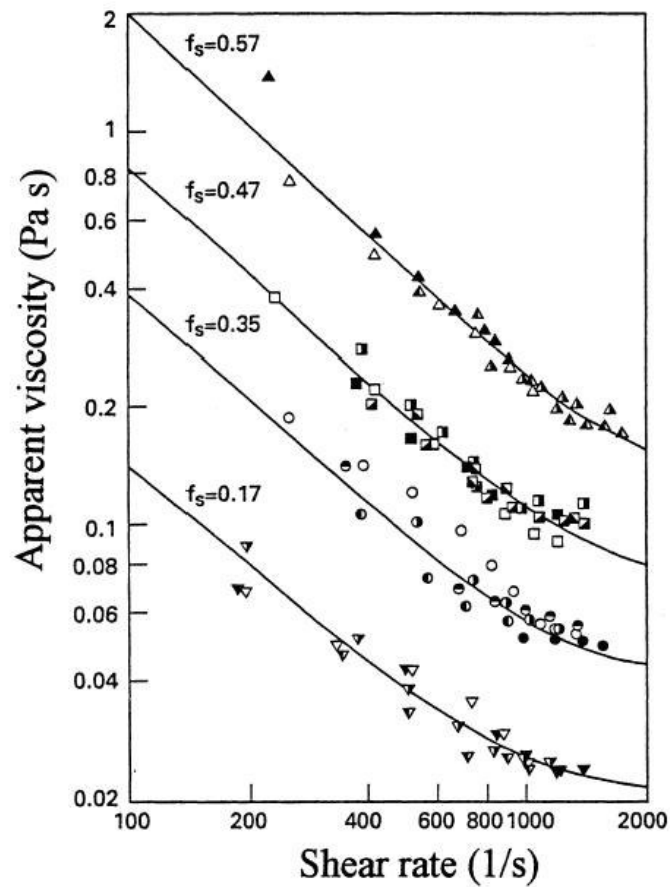


Figure 2.6. Steady state apparent viscosity versus shear rate in Sn-15Pb alloy for various solid fractions [4]

Following the standard model used for general suspensions, Joly and Mehrabian [19] showed on Sn-15Pb alloy that the behavior is shear rate thinning (or pseudoplastic), where the apparent steady state viscosity decreases with increasing shear rate. It is generally accepted that the steady state viscosity at a given shear rate depends on the degree of agglomeration between the solid particles, which in turn is the result of a dynamic equilibrium between agglomeration and disagglomeration of the solid particles [15].

The isothermal steady state experiments lead to more precise rheological characterization. The steady state is usually defined as a state at which the viscosity of SSM slurry with fixed volume fraction and shear rate does not vary with prolonged shearing time. Thus, for a given alloy system, steady state viscosity is a function of solid fraction and shear rate. The shear thinning is more generally demonstrated in Figure 2.6. For a SSM slurry with a fixed solid fraction, the steady state viscosity decreases with increasing shear rate, approaching an asymptotic value when the shear rate becomes infinite [4].

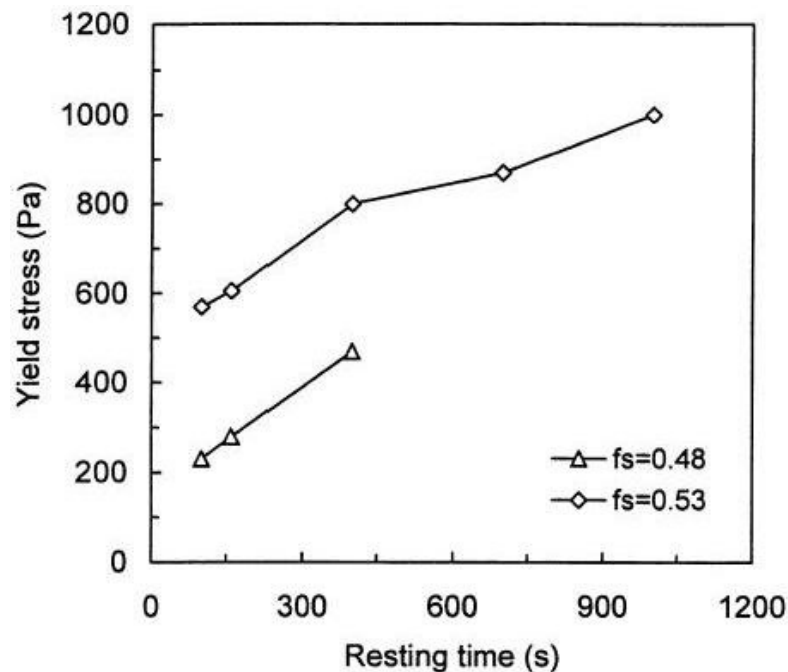


Figure 2.7. Yield stress of semi-solid Sn-15Pb alloy as function of resting time [4]

Another phenomenon associated with steady state behavior is the presence of yield stress. It is generally agreed that many suspensions have a yield point at low shear rate, resulting from the structural formation due to the dynamic interaction between solid particles. The yield phenomenon is generally inherent to the thixotropy. This is the result of agglomeration of solid particles with the help of resting time. More recently, yield stress data for Sn-15Pb SSM slurries as presented in Figure 2.7 as a function of resting time. The strong particle interactions are responsible for the existence of yield stresses, below which the SSM slurries behave like elastic solid. Yield stresses are ideally measured using shear

stress controlled rheometers by applying shear stress ramps and measuring the stress value when the alloy starts to deform [4,15].

In order to characterize the constant structure flow behavior shear-rate ramp decrease experiments are performed on Sn–15Pb alloys [20]. The result of a typical experiment is shown in Figure 2.8. The findings showed that, at increasing shear-rate steps, the apparent viscosity grows immediately with respect to the prior steady state, before approaching a new steady state value that is lower than the previous steady viscosity. The inverse phenomenon is observed at decreasing shear-rate steps.

The break down time is the characteristic time for the slurry to achieve its steady-state condition after a shear rate change from a lower value to a higher value, while the build up time is for a change from a higher shear rate to a lower shear rate. The times for breakdown are faster than those for build up. This is because of the breaking up of ‘bonds’ between spheroidal solid particles in agglomerates is likely to be easier than the formation of bonds during shear-rate drops. During a shear-rate change, the slurry undergoes an initial rapid breakdown/build-up followed by a more gradual process dependent on diffusion. This can be described by a double exponential expression. Immediately after a change in shear rate, the structure remains the same iso-structure. This is followed by a very fast process and then a slow process, associated with diffusion, giving coarsening and spheroidization [2,21].

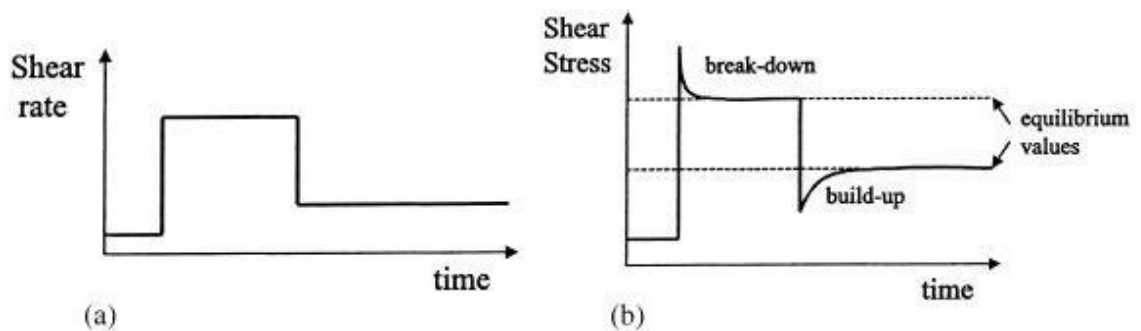


Figure 2.8. (a) Shear-rate step-up and step-down experiments; (b) shear-stress evolution in shear-rate step experiments [20]

## 2.5. Technologies for Production of Non-Dendritic Feedstock

Semi-solid metal forming, forming a metallic alloy at a temperature between its equilibrium liquidus and equilibrium solidus temperatures, is a hybrid metalworking process combining the elements of both casting and forging/extrusion. One of the key elements for the successful operation of a semi-solid forming process is the microstructure of metallic alloy being thus formed. The semi-solid forming process needs a unique microstructure which is different than the conventional alloys.

Conventionally solidified metals can not be utilized in a semi-solid condition, since a structure of dendritic network forms upon solidification in such metals. This kind of an alloy does not show the necessary characteristics for the semi-solid forming process. Cracks and segregates will occur when a conventionally solidified metal is formed in partially liquid-solid state. Therefore raw material of a semi-solid forming process must have a structure comprised of globular or spheroidal grains contained in a secondary phase lower melting alloy matrix. When heated to a semi-solid temperature, the globular solid phase is retained, suspended in a lower melting alloy liquid matrix which is called as eutectic phase. The secondary phase is solid when the metal composition is frozen and is liquid when the metal composition is partially solid and partially liquid. The primary solid particles are generally spheroidal in shape. The primary solid particles are made up of a single phase having an average composition different from the average composition of the surrounding matrix. The primary solids obtained in the composition differ from normal dendritic structures. Normally, solidified alloys have branched dendrites separated from each other in the early stages of solidification and develop into an interconnected network as the temperature is reduced and the weight fraction solid increases. On the other hand, the structure obtained in thixotropic metal slurries consists of discrete primary particles separated from each other by a liquid matrix even up to solid fractions of 80 weight percent. The primary solids have smoother surfaces and less branched structures which approach a spherical configuration compared to normal dendritic structure. The secondary solid which is formed during solidification from the liquid matrix, contains one or more phases with other alloying elements of the material.

The feedstock preparation is the essential step for semi solid forming operations. The objective of feedstock production is to provide a material with a characteristic thixotropic microstructure where a non-dendritic primary phase with a fine grain size is uniformly distributed in a matrix of lower melting point. There are two routes for using the feedstock material. In the rheo-route the feedstock material is directly used for component shaping after obtaining the globular microstructure. In the second method called thixo-route the feedstock material that has a globular microstructure, formed previously from the liquid state and allowed to solidify, is used as a raw material in the solid state for subsequent reheating into the semi-solid state and component shaping.

Nearly all the alloys of commercial importance solid solidify dendritically, with either a columnar or an equiaxed dendritic structure [8]. During dendritic solidification of castings and ingots, a number of processes take place simultaneously within the semi-solid region. These include crystallization, solute redistribution, ripening, interdendritic fluid flow, and solid movement. The dendritic structure is greatly affected by the interdendritic flow and solid movement, which, in conventional solidification, is caused by internal factors such as density difference and heterogeneous distribution of temperature.

The ideal microstructure for a semi-solid slurry before the component shaping process would be an accurately specified volume fraction of fine and spherical solid particles uniformly dispersed in a liquid matrix. A primary goal of slurry preparation is to create such a structure to ensure the favorable rheological characteristics to facilitate the subsequent component shaping process. Technically, this structure can be achieved by a number of different techniques [4].

Thixotropic feedstock production can start either from a liquid alloy through controlled solidification under specific conditions, or from solid state through heavy plastic deformation and recrystallisation.

### **2.5.1. Mechanical Stirring**

The use of mechanical stirring is a direct and cost effective way of altering shear rate. Melt agitation in mechanical stirring is based on the technologies originated at MIT

[22]. The process is commonly generated by means of augers (Figure 2.9), impellers, or multi-paddle agitators mounted on a central rotating shaft. The shear caused by the stirrer during solidification promotes the formation of non-dendritic structure. Shear rate can be roughly estimated by the ratio of the velocity of the impeller extremity to the clearance between the impeller tip and the mould wall.

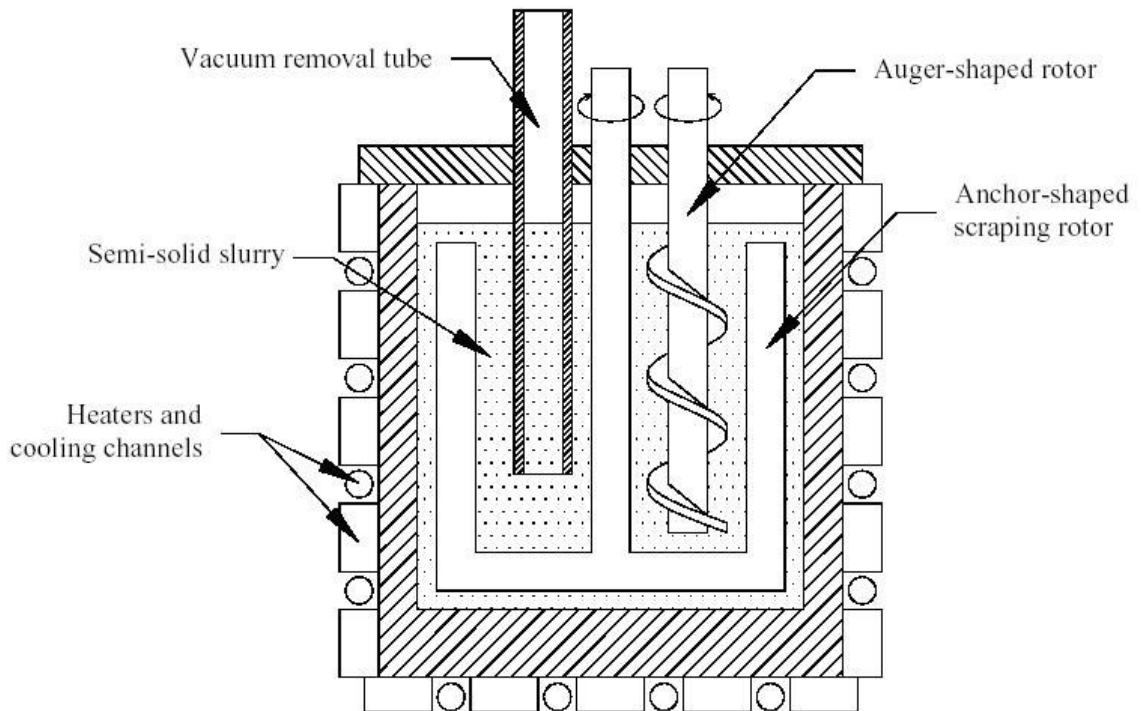


Figure 2.9. Schematic view of a mechanical stirring machine [21]

The mechanical stirring approach was developed from batch process into a continuous process. In the continuous process, superheated liquid in the holding vessel flows down into an annulus between the stirring rod and the outer cylinder where it is simultaneously stirred and cooled. The continuous rheocaster is shown schematically in Figure 2.10. Slurry flows from the bottom of the rheocaster either to be cast directly to shape (rheocasting), or to be solidified as feedstock material for subsequent reheating and thixoforming. The resulting solid particles are usually coarse rosettes [4]. The early version of rheocasting has not reached a commercial stage. Historically, this was attributed to a number of technical difficulties at that time, such as contamination of the melt through oxidation and chemical reaction with the stirring system. Recently, due to the technical and commercial concerns associated with other methods for feedstock production, there has

been renewed interest in this technology. Modifications to the early version of the rheocaster were made to develop a process for feedstock production employing mechanical stirring. In the modified rheocasting process, shearing and solidification are caused to occur in separate volumes, and thus are effectively decoupled. The objective of the modification was to improve the microstructural uniformity in the cross-section of the continuous cast billet.

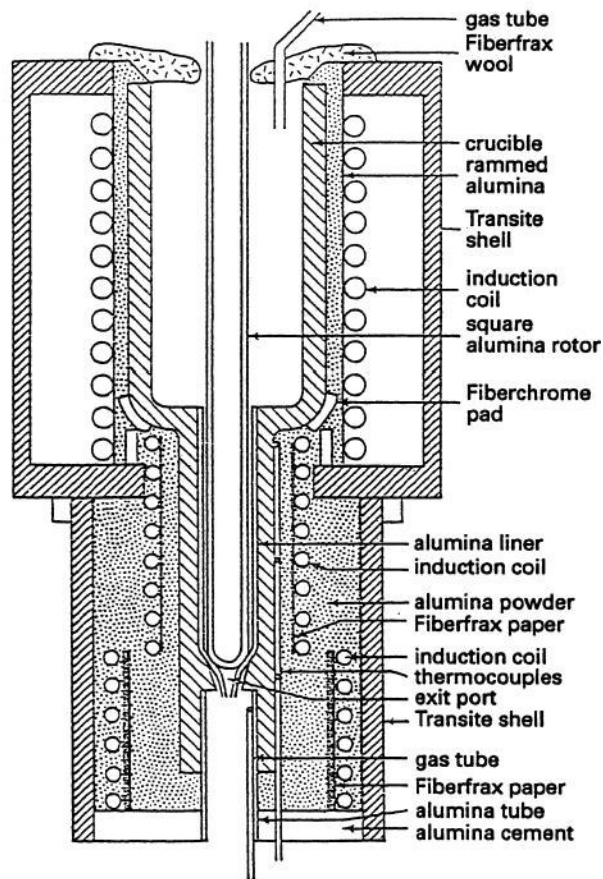


Figure 2.10. Schematic view of continuous rheocaster [4]

In mechanical stirring it is necessary to provide adequate shearing forces to the mixture to create the rounded solid particles and prevent agglomeration of the solids.

It has been conclusively established from experimental observations that solidification under melt stirring produces non-dendritic structures [8]. The early work by Spencer *et al.* [23] on the Sn–Pb system using rotational rheometers confirmed that the solid phase in the semi-solid state has either a degenerated dendritic structure or rosette

morphology. With prolonged stirring time, such particles change to a more or less spherical morphology containing entrapped liquid by a ripening process. Increasing the shear rate accelerates this morphological transition and reduces the amount of entrapped liquid inside the solid particles. The rosette morphology of solid particles has also been observed in many stirred alloys using rod and impeller types of stirrer [9].

For Al–Cu alloys, with applied shear the primary particles grow as rosettes until a certain limit beyond which further growth does not occur but subsequent solidification takes place by formation of more (new) particles. The cell spacing is considerably greater than the secondary dendrite arm spacing from unstirred melt, indicating that stirring promotes crystal growth. With increasing shear rate the average particle diameter decreases, while the particle density increases [4].

Brabazon *et al.* [24] designed a mechanical stir caster and built to produce the various cast morphologies (Figure 2.11). The semi-solid alloy was sheared in a heated tubular zone between a grooved rotor and a crucible. An independent in-line torque meter is positioned between the stirring rotor and the drive motor to enable rheological measurements. The caster furnace is heated by means of four resistance heating elements. One element around the wide reservoir at the top of the crucible and three along the lower narrow section are used to control the temperature in the semi-solid range of the alloy. This configuration enables a maximum temperature of 850 ° C and control of the temperature gradient within the narrow section of the crucible, where the shearing occurred. A linear drive provides lift to the rotor, enabling evacuation of the stir caster after the desired period of shear. The rotor and crucible are both, uniquely, of Reaction Bonded Silicon Nitride (RBSN), which enables these two parts to be easily lapped together during operation of the stir caster. RBSN has good thermal shock resistance, good high temperature strength, does not contaminate the melt, and has a low coefficient of thermal expansion and moment of inertia. An additional external immersion heating element is in the reservoir to provide sufficient molten alloy there for an adequate metallostatic head for stir casting at higher fractions solid. A batch casting trolley, which also holds a plug against the crucible outlet, is used to carry the chill moulds into which the stir cast material poured. Control of stirring speed, stirring time, stirrer height, and the temperature profile of the furnace, is

implemented on a computer which displays the stirring speed, height of the stirrer, temperatures in the furnace, and the torque experienced by the stirrer, on a real time basis.

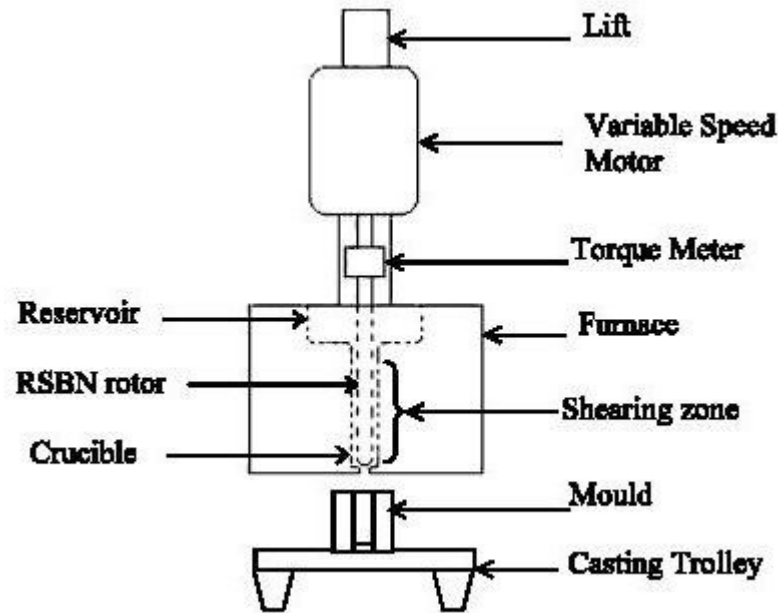


Figure 2.11. Schematic view of stir casting device [24]

### 2.5.2. Magneto Hydrodynamic (MHD) Stirring

To overcome the problems associated with the original rheocasting process using direct mechanical stirring, a magneto hydrodynamic (MHD) stirring process was developed by ITT in the USA [25]. In this technique, rotating electromagnetic fields generate local shear within the continuous casting mould, and continuous billets of solidified non-dendritic alloy can be produced. The stirring is deep in the sump of the liquid, which has previously been filtered and degassed. The contamination, gas entrapment and stirrer erosion involved in mechanical stirring are virtually eliminated in MHD casting. Since the start of this technology for thixotropic feedstock production, it has been subject to intensive research and at present, and MHD stirring is the most widespread route for feedstock production for semi solid forming operations [4].

As illustrated in Figure 2.12 the metal in the mold is stirred vigorously by the dynamic electromagnetic field and as a result the shearing is created. Electromagnetic stirring can be achieved through three different modes: vertical flow, horizontal flow, and

helical flow, with the helical mode being ultimately a combination of the vertical and horizontal modes. In the horizontal flow mode, the motion of the solid particles takes place in an isothermal plane so that mechanical shearing is probably the dominant mechanism for spheroidization. In the vertical flow mode, the dendrites located near the solidification front are recirculated to the hotter zone of the stirring chamber and partially remelted, and therefore thermal processing is dominant over mechanical shearing. At the same time with the stirring, heat removal is established with the conductive heat transfer between the mold wall and the surrounding water [4].

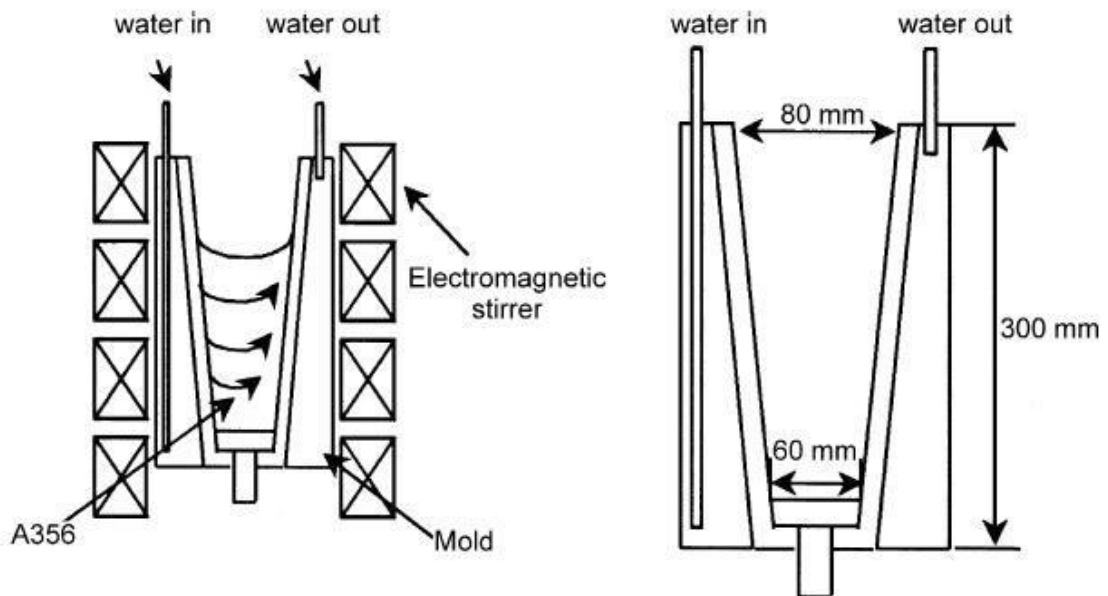


Figure 2.12. Vertical casting with horizontal electromagnetic flow [26]

The continuous casting is made through either a vertical or horizontal arrangement, depending on the casting direction in relation to the gravity direction. While vertical stirring has so far been employed in vertical continuous casting only, horizontal stirring has been used in both vertical and horizontal casting systems. The major advantages of horizontal continuous casting include better economy, continuous production, and low investment costs, but the quality of the billet is influenced by the gravity. On the other hand, the vertical casting system benefits from symmetrical solidification and there is no limitation of the billet diameter. However, the vertical system suffers from drawbacks such as discontinuous production, high investment costs, and high production costs [4].

Electromagnetic stirring (EMS) is widely used because it permits continuous production of ingots and there is no contact between the agitator and the metallic bath. Besides, this type of stirring has very low energy consumption to ingot produced ratio, which justifies its extensive application [27]. The stirring promotes the coarsening of primary particles by the formation and melting of grain boundaries produced either by deformation or by sintering of the primary particles. The initial dendritic structure is fragmented by the stirring of the partially solidified alloy, so that the melting of the grain boundaries is the predominant mechanism during the initial stage of stirring. Long periods of stirring increase the curvature radius of the primary phase solid–liquid interface and the coarsening mechanism takes place [28].

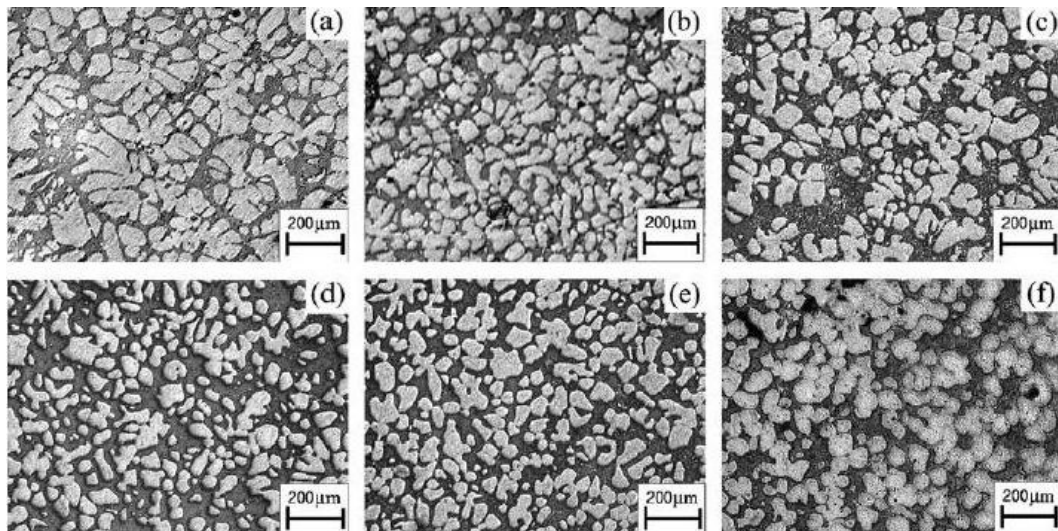


Figure 2.13. Effects of EMS stirring time on microstructure of A356 alloy: (a) 0 s; (b) 10 s; (c) 20 s; (d) 40 s; (e) 60 s; (f) 90 s [28]

In a study of Yang *et al.* [29] the effects of stirring time on the microstructure of A356 was shown in Figure 2.13. It can be erroneously determined that the particles size was influenced so little by the stirring time and no significant grain refinement had occurred as the stirring time was prolonged. But in fact, the size of the primary dendrites was significantly decreased.

The MHD casting process provides the ability to control precisely the shearing action and the rate of heat removal and thus deliver the desired microstructure with a grain size that is normally about 30  $\mu\text{m}$ . This compares favorably with the 100 to 400  $\mu\text{m}$  grain size

produced by mechanical stirrers. Proper control of the casting variables will result in billet properties that meet the quality specifications for MHD billets.

The major difficulties beyond the wide acceptance of MHD technology for thixotropic feedstock production include high production costs (accounting for up to 50 percent of the component cost), lack of microstructural uniformity in the cross-section of the cast billet, and non-spherical (although non-dendritic) with some rosette character remaining particle morphology. Such a microstructural deficiency will cause prolonged reheating time and difficulties during subsequent thixoforming, consequently resulting in a further increase of the production costs [2,4].

### **2.5.3. Stress Induced and Melt Activated (SIMA) Process**

An alternative to the liquid agitation route is the stress induced and melt activated (SIMA) process. This process is based on the scientific understanding that high angle grain boundaries induced by plastic deformation and recrystallisation will be wetted by liquid metal at the semi-solid temperature, resulting in a fine and globular structure. Liquid phase is located at high angle grain boundaries and alloy achieves a microstructure consisting of almost spherical solid particles. These particles are separated by a low melting-temperature liquid phase. Size of these particles depends on [4]:

- Chemical composition of the alloy, which determined the solidus–liquidus temperature interval, microstructure at the beginning of melting.
- Heating rate below the solidus.
- Holding time in the semi-liquid state.

The SIMA process relies on the development of process steps in the basic hot-worked metal alloy extrusions or rolled bars are subjected to additional cold work. When sufficient strain is induced and the material is heated to the semi-solid state, the structure transforms to an extremely fine, uniform, nondendritic spherical microstructure [30]. The semi-solid forging on SIMA processed bar has been demonstrated for a wide variety of alloys, including aluminum, magnesium, copper and ferrous alloys. SIMA processing represents a cost effective and readily available source of small diameter raw material for

semi-solid forging. The process is also technically operable for larger sizes, but the costs of processing are not competitive with those of MHD casting on most metal alloys.

A modification of the SIMA process is made by changing the cold working to warm working at a temperature below the recrystallisation temperature to ensure the maximum strain hardening. With appropriate choice of processing conditions, such as amount of plastic deformation, reheating temperature, and time duration, the resulting solid phase particles are usually fine in size, globular in morphology, and uniform in distribution. The SIMA process produces high quality feedstock for thixoforming and has the potential for wrought alloys and high melting temperature alloys such as steel and superalloys. Small diameter (<38mm) can also be produced by SIMA process [4].

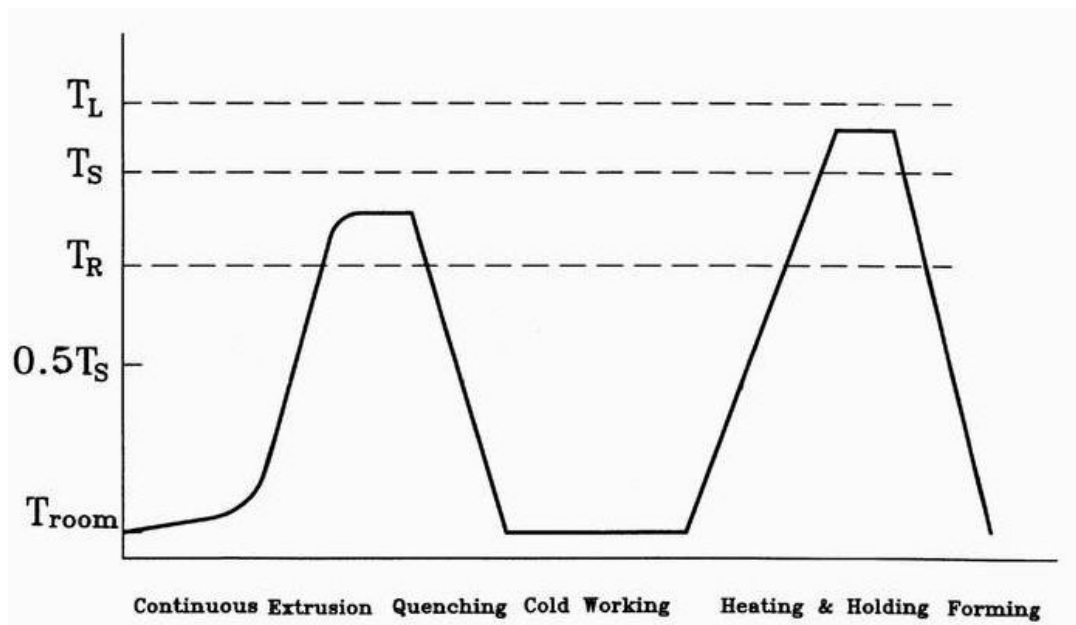


Figure 2.14. Schematic diagram of SIMA process [31]

In SIMA hot worked and quenched billets are cold worked to induce residual plastic strain. Hot working operations include extrusion, rolling, forging, swaging and cold working operations found to be effective include drawing, swaging, rolling and compression or upsetting. The actual strain level will vary with the specific metal or alloy and with the type and conditions of hot working. In the case of extruded aluminum alloy, the strain level should be equivalent to at least a 12 per cent cold worked alloy. Upon completion cold working the billet is reheated to a semi-solid temperature to produce the

globular structure. The specific temperature is generally such as to produce a 0.05 to 0.8 volume fraction liquid, preferably at least 0.10 volume fraction liquid and in most cases a 0.15 to 0.5 volume fraction liquid. As the final step the billet is thixoformed in its semi-solid state. The process is shown schematically in Figure 2.14 [31].

The process has a number of very significant advantages. Casting of the starting billet may be carried out in a single convenient diameter, at one location and reduced to any desirable smaller diameter at the same or a second location using conventional extrusion equipment and technology. The process permits removal of any dendritic exterior skin on the starting billet as part of normal practice prior to extrusion so that the extruded billet exhibits no skin effect. Moreover, the process produces a considerable refinement of the microstructure of the final product, including its size, shape and distribution relative to the starting billet microstructure [31].

However, the SIMA process requires energy and processing intensive steps as plastic deformation and recrystallisation of conventionally cast dendritic materials by thermo-mechanical treatments. As a result of these processes it cost approximately 3 to 5 times more than the MHD stirring process. Therefore the SIMA process is only effective for small applications and for small diameter feedstock. Another disadvantage is that there may be variation in the amount of stored work across the section, resulting in inhomogeneity.

#### **2.5.4. Spray Casting**

Spray casting is another non-agitation process for feedstock production. It is a relatively expensive route but one which can be used to produce alloys, which cannot be produced in any other way, such as aluminum–silicon alloys with greater than 20 weight per cent silicon [32]. Spray forming essentially involves the atomization of a liquid metal stream and collection of the droplets on a former. The resulting microstructure is fine and equiaxed. When heated into the semi-solid state it is ideal for thixoforming operations.

The spray casting process has been investigated extensively over the past two decades and several models have been proposed to describe the process. Various alloys

produced by spray casting have been evaluated experimentally as feedstock materials for semi-solid processing [33]. It is generally believed that spray cast materials are suitable as feedstock for thixoforming, especially for high temperature alloys, such as steels and superalloys.

In the spray forming process, a liquid alloy metal stream is atomized through a nozzle into a spray of fine droplets, of mass median higher than 200  $\mu\text{m}$ , by jets of a high pressure inert gas (nitrogen or argon). The droplets then deposit on to the surface of a growing preform to build up large billets, tubes or rings for down stream processing. The droplets experience cooling during flight, at rates of up to  $10^3$  K/s, such that partial solidification takes place in a significant fraction of droplets. While the large droplets remain fully liquid the small droplets solidify during atomization, those of intermediate sizes become semi-solid. The droplets are collected on a moving substrate and consolidated to form a coherent preform. A second stage of solidification takes place on the substrate at the beginning of the deposition, and subsequently on the upper surface of the preform. Liquid and semi-solid droplets with high liquid fraction splat upon impact, while solid and semi-solid droplets with high solid fraction fragment. A portion of the solid grains undergoes remelting and resolidifies slowly. Typical local solidification time on the preform surface is of the order of 100 s indicating that more than 90 per cent of the solidification time of a spray cast preform occurs in the deposit at high solid fraction. The resulting microstructure comprises very fine equiaxed grains [4,34].

The microstructure of the as-spray formed perform consists of fine equiaxed grains with no microsegregation, but the mechanism by which this microstructure evolves from the dendritic droplets is complex. The dendrites contained within the droplets fragment on impact with the top surface, and then spheroidise and coarsen in a sump of semi-solid material at the top of the growing preform before final solidification [33,34].

Spray-formed hypereutectic Al-Si alloys have a microstructure consisting of fine (less than 10  $\mu\text{m}$ ), approximately uniformly sized silicon crystals in a matrix of aluminum solid solution [2]. On heating into the semi-solid state, the liquid penetrates some of the grain boundaries and produces a microstructure of finely dispersed silicon and primary aluminum spheroidal grains surrounded by liquid, one suitable for semi-solid processing.

Hence, semi-solid processing of these spray-formed materials offers a route to the production of components with the highly desirable properties hypereutectic Al-Si alloys can potentially offer. However, at silicon contents above approximately 27 weight per cent the silicon exists as a continuous three-dimensional (3-D) network with sufficient strength to resist flow. This results in segregation, porosity, incomplete die filling, inhomogeneity, and other deleterious effects. Also, from a practical point of view, further problems occur as the slugs are extremely stiff and consequently appear to contain very little liquid. There then exists the danger of overheating and destroying the aluminum spheroids which is required for thixotropic flow [36].

### **2.5.5. Liquidus Casting**

There have been recent developments in producing feedstock by manipulating the solidification conditions. The new rheocasting (NRC) process [37] is based on this principle with the molten metal at near-liquidus temperature poured into a tilted crucible and grain nucleation occurring on the side of the crucible. The grain size is fine because the temperature is near liquidus. An allied technique is the direct thermal method. In the cooling slope method, liquid metal is poured down a cooled slope and collects in a mould. Nucleation on the slope ensures the spheroid size is fine. With liquidus casting, a high rate of nucleation can be achieved within the entire volume of undercooled melt [2,38].

Liquidus casting, also known as low superheat casting, has been developed recently as an alternative technique for production of thixotropic feedstock. In liquidus casting, melt with a uniform temperature just above its liquidus is poured into a mould for solidification. The resulting microstructures are usually fine and non-dendritic. Upon reheating, the liquidus cast microstructure spheroidises rapidly to produce microstructural features suitable for thixoforming operations. This technique can be used on both cast and wrought aluminum alloys.

The effect of melt superheating was recognized nearly 40 years ago by Chalmers and coworkers. It has been found that reducing the pouring temperature promotes the formation of an equiaxed zone and suppresses the formation of the columnar grain zone. In addition to this lowering the pouring temperature also refines the equiaxed grains. Such

experimental observations can be explained by using the Mullins–Sekerka instability theory, which suggests that an alloy with very small undercooling coupled with a very high saturation of nucleation sites would form an equiaxed structure. However, it seems much effort is still required to establish the exact mechanism for the formation of the fine and non-dendritic structure during liquidus casting [4].

Recently, Fan *et al.* [12] developed a liquidus rheocasting process. In this process, overheated liquid metal is poured into a twin screw extruder where it is continuously sheared and cooled to a temperature around its liquidus before being transferred to a mould for shaping or to a DC (direct chill) caster for continuous casting of thixotropic feedstock billets. The microstructural features offered by the liquidus rheocasting process include fine grain size, spherical particle morphology and much improved chemical and microstructural uniformity. Liquidus casting, with liquidus rheocasting in particular, is gaining more attention as a simple and cost effective technique for feedstock production and seems to have a promising future. However, the major obstacles for industrial application may arise from difficulties related to accuracy and uniformity of temperature control, and consistency and uniformity of resulting microstructure in large scale production [4].

The cooling slope is the simplest process to make the ingot for the thixoforming. Only pouring the melt on the cooling slope and solidifying the metal, the ingot for thixoforming is obtained. Molten metal is poured from the top of a tilting cooler. Gravity accelerates the liquid flow and produces in this flow a shear. The cooling slope is a very simple, compact and cheap piece of equipment with low associated running costs. The equipment and running costs associated with the cooling slope are very low. As a further advantage offered in this route, the casting of the ingot can be synchronized with the act of thixoforming itself, providing more efficiency all around.

However, there is a disadvantage that the solidified metal tends to stick to the slope in the pouring or at the end of the pouring of the melt. When the solid fraction of the metal become higher, adherence of solidified melt at the slope happens during the pouring of the metal. As a result the cooling of the melt that flow on the adherence becomes worse. When the solid rate is low, the adherence of the metal happens at the end of the pouring of the

melt. The cooling slope can be coated by lubricant (BN) to prevent adherence of solidified metal. The use of the lubricant is effective. However, adherence cannot be prevented completely by the use of adherence. The primary crystals of the products are spheroidal, and the general morphology of the ingot microstructures, when heated up to semi-solid condition, is very similar to the microstructures obtained by conventional semi-solid casting routes [39,40]. A schematic view of a cooling slope casting system is shown in Figure 2.15.

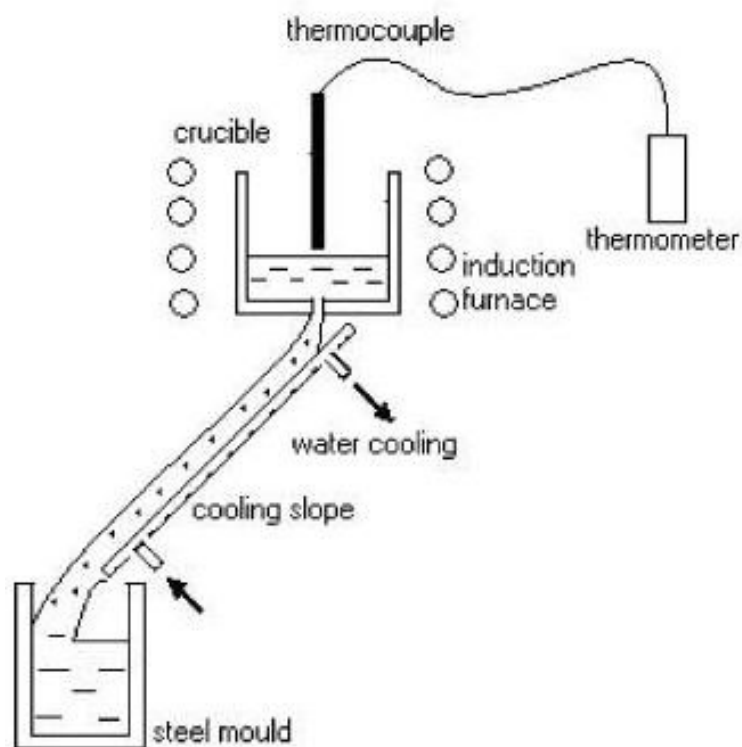


Figure 2.15. Cooling slope casting system [41]

The important factors which affect the microstructure are cooling length of the slope, the angle of the cooling slope and the superheat of the molten metal and the die material.

In another process utilizing low superheat casting, the melt is poured directly into the die and solidified. The need to produce an ingot for further processing by thixoforming can be eliminated since the molten metal can be shaped directly into the semi-solid state by synchronizing the pouring into the die with the thixoforming operation. The size of ingot can be easily varied accordingly by appropriate choice of ladle and die [40].

### 2.5.6. Chemical Grain Refining

Chemical grain refinement is a common practice in continuous casting of aluminum alloys. In most cases, a pre alloyed wire is pro-portioned into the hot metal flow into the launder where it releases heterogeneous nucleation agents, usually titanium and boron based. Owing to the enhanced heterogeneous nucleation rate and suppression of dendritic growth, a fine and equiaxed structure can be achieved. With an appropriate grain refining procedure, such a structure can also be suitable for subsequent reheating and thixoforming. However, chemical grain refining is not used alone, but used in conjunction with other feedstock production methods, such as MHD stirring and liquidus casting.

One disadvantage of the chemical grain refinement method is that nucleation agents are only effective to specific alloy systems. Another is that in some cases these additives will remain present in the product as non-metallic inclusions, which may impair both the process ability of the semi-finished stock and the mechanical properties of the final product [4].

It is generally acknowledged that  $TiAl_3$  constituent meets all the necessary criteria for grain refinement mechanism. The aluminum-titanium binary alloy contains  $TiAl_3$ , but because  $TiAl_3$  is soluble in molten aluminum, it is necessary to add titanium to levels greater than 0.15 per cent in order to retain grain refining effectiveness. However, high level of titanium can rise to coarse intermetallic particles, which are detrimental to mechanical properties [42].

A number of commercial master alloys are available for use of grain-refinement agents. Where it is the practice to add titanium above the peritectic level, that is, in the range of 0.1 to 0.2 per cent, aluminum-titanium binary alloys containing up to 10 per cent Ti can be obtained in the form of cast waffles for furnace additions [42].

In conclusion grain refined alloys can give equiaxed microstructures but it is difficult to ensure the grain structure is uniformly spheroidal and the volume of liquid entrapped in spheroids tends to be relatively high.

### 2.5.7. Ultrasonic Treatment

Application of high power ultrasonic vibration (or ultrasonic treatment) to a solidifying melt for refinement of as cast structure can be traced back to the mid 1970s. Ultrasonic treatment of aluminum alloys, in general, has been studied extensively. In the past few years, there has been renewed interest in this technology as a means for feedstock production. Experimentally, it is well established that application of ultrasonic treatment to a cooling melt at a starting temperature just above its liquidus can produce effectively a fine and non-dendritic microstructure, which is suitable for subsequent reheating and thixoforming operations. They are related to ultrasonically induced cavitations, which produce large instantaneous pressure and temperature fluctuations in the melt. These pressure and temperature fluctuations are likely to induce heterogeneous nucleation in the melt. They are also likely to promote dendrite fragmentation by enhancing solute diffusion through acoustic streaming. However, there is no convincing evidence in the literature as to which mechanism, i.e. heterogeneous nucleation or dendrite fragmentation is more important for grain refinement under ultrasonic vibrations [43].

Regarding the mechanism for the formation of such fine and non-dendritic structure, it is now generally believed that introduction of high power ultrasonic vibration into a liquid alloy can lead to two basic physical phenomena [44]: cavitation and acoustic streaming. Cavitation involves the formation, growth, pulsation, and collapsing of tiny bubbles in the melt. The compression rate of these unsteady bubbles can be so high that their collapsing generates hydraulic waves, thus producing artificial sources of nuclei. The propagation of a high intensity ultrasonic wave involves the initiation of steady state acoustic streaming in the melt. The overall effect of various types of stream is to vigorously mix and homogenize the melt. Therefore, hydraulic shock waves generated by the collapse of cavitation bubbles fragment dendritic arms, and acoustic streams will distribute the dendritic arm fragments homogeneously throughout the melt. When ultrasonic vibration is coupled to the solidifying metal, the structural changes include grain refinement, suppression of the columnar grain structure, increased homogeneity, and reduced segregation [4,43].

### **3. SEMI SOLID AND HOT FORMING OF ALUMINUM**

Present commercial metal forming processes employ either fully liquid metals or fully solid metals. Metal forming processes such as sand castings, die castings, and the like employ fully liquid metals while processes such as forgings, extrusions, etc., employ fully solid metals. Existing cast methods in which a metal is brought to a liquid state and then poured or forced into a mold have a number of shortcomings. In casting, when the liquid changes to solid, shrinkage of about 5 per cent is encountered which initiates stress generations. This stress results in cracking and casting porosity. In addition, the fully liquid melt is highly erosive to dies and molds and the high temperature of the liquid and its erosive characteristics makes difficult die casting of some high temperature alloys. The foregoing shortcomings can be alleviated by casting a controlled semi-solid mixture in the form of thixotropic slurry. Traditionally, forming processes did not employ semi-solid metals because in the conventional solidification of the metals, a dendritic network structure forms when the alloy is as little as 20 per cent solid. Such partially solidified metal cannot be deformed homogeneously without cracking or forming segregates. Because of this reason a material with a non-dendritic microstructure is needed for semi-solid processing.

#### **3.1. Semi-Solid Metal Forming**

At a very basic level, a “semi-solid” material is simply a mixture of a liquid and solid phase. In the context of semi-solid metal processing, a semi-solid is a mixture of rounded solid phase particles suspended in a liquid matrix. These metal mixtures are slurries, much like slush, ketchup, or sand castles mixtures of dispersed solids within a liquid. In a metal alloy, thermodynamics determine at what temperatures a metal is solid, liquid, or partially solid and liquid. For most alloy compositions, there exists a freezing range between the states of solid and liquid where both liquid and solid exist together in the semi-solid state. This is also called as the solidification range of the alloy. This range should be at certain values for the feasibility of semi-solid forming [21].

Deformation of alloys in partly liquid state is one of the latest methods in the forming of metallic products. The process consists in the deformation of the material after it has been heated to a temperature exceeding the solidus point. In such conditions two phases, solid and liquid, coexist in the alloy and their mutual proportion in the entire volume of the material depends on the temperature. Because of the presence of the liquid component, a change in the mechanism of plastic deformation occurs and the conditions of metal flow are affected. In the temperature of the alloy above the solidus point, the liquid component appears at the grain boundaries and makes the plastic deformation to be mainly due to the effect of rotation and relative slip between the grains. The deformation of grains themselves has minor contribution to the metal flow in partly liquid state. Such a mechanism of deformation leads to a decrease of the material's flow strength because the liquid phase located on the grain boundaries fosters displacements of the grains. The resistance to deformation is much lower than in the conventional processes of hot metal forming. All these facts in connection with the compressive state of stress lead to a significant improvement of the workability of partly liquid materials [45].

During any semi-solid forming process, good flow behavior and adequate mould filling are fundamental requirements for the production of sound and defect-free products. Those requirements are fulfilled when a relatively low viscosity of the semi-solid billet can be achieved. In its turn, the attainment of suitable viscosity values depends of the establishment of a particular microstructure, typically non-dendritic, which is a precondition for the success of all semi-solid processing technologies. Due to the higher viscosity than that of liquid, the material flow pattern will not become turbulent flow during die filling. Thus, gas defects such as porosity are diminished, and there will be only small shrinkage defects for on-going solidification.

Even though a die can have complex shapes, the semi-solid forming (SSF) process can manufacture products that can compete with the mechanical properties of aluminum forging parts. Moreover, the applications of the SSF process in the fields of automotive parts and compact electronic parts have been studied actively, because the SSF process has advantages over conventional forming processes in the areas of reduction of forming force, increase of die life, reduction of product defects, and improvement of processes [46].

Figure 3.1 shows a variety of products that are manufactured by semi-solid forming technology.

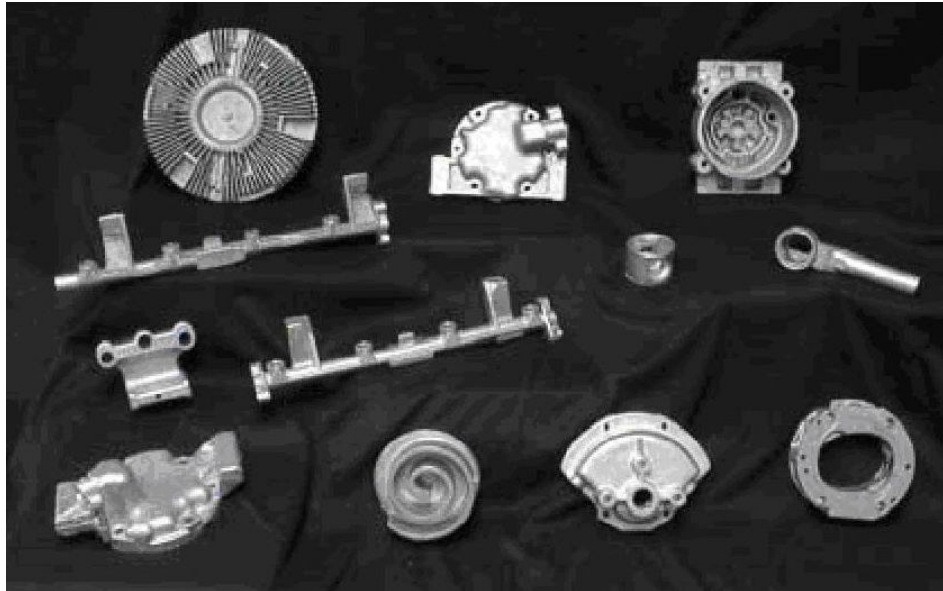


Figure 3.1. Examples of semi-solid formed products [21]

### 3.2. Rheocasting

Rheocasting refers to the process where the alloy is cooled into the semi-solid state and injected into a die without an intermediate solidification step. The non-dendritic microstructure can be obtained by mechanical stirring, by stimulated nucleation of solid particles as in the new rheocasting NRC process or by electromagnetic stirring.

Although rheocasting was identified as the production technology at the very beginning of semi-solid processing research, it has not been commercialized to any great extent so far. This is possibly because of the quality of the semi-solid slurry produced by such stirring processes. Mechanical stirring using either rod or impeller as stirrer results in the formation of very coarse rosettes with a diameter of a few hundred micrometers or approaching millimeter level. The slurries produced under such conditions do not have adequate thixotropic characteristics for successful direct shaping by either a casting or a forging route. In this regard, MHD stirred slurries are not better than mechanically stirred slurries. The MHD stirring process usually gives rise to degenerated equiaxed dendrites, which are inherently unsuitable for direct component shaping unless they are held at semi-

solid temperature for sufficiently long time. However, component shaping directly from SSM slurries is inherently attractive due to its characteristics, such as overall efficiency in production and energy management. The recent effort on the development of so called ‘slurry-on-demand’ processes is in this direction [4].

One of the slurry-on-demand processes is the recently developed new rheocasting (NRC) process, which was patented by UBE Industries Ltd [37].

The NRC process involves pouring molten alloy, at a temperature slightly above the liquidus, into a steel crucible and then controlled cooling to achieve a spheroidal microstructure before transfer to a forming machine. By controlling the slurry temperature (therefore solid fraction), a stable skeleton of the solid phase is formed within a few minutes after pouring. The solid-like slug of cylindrical shape is then heated by induction heating to homogenize the slug temperature before being transferred into the sleeve of the vertical SQC machine, where it is cast into its final shape (Figure 3.2).

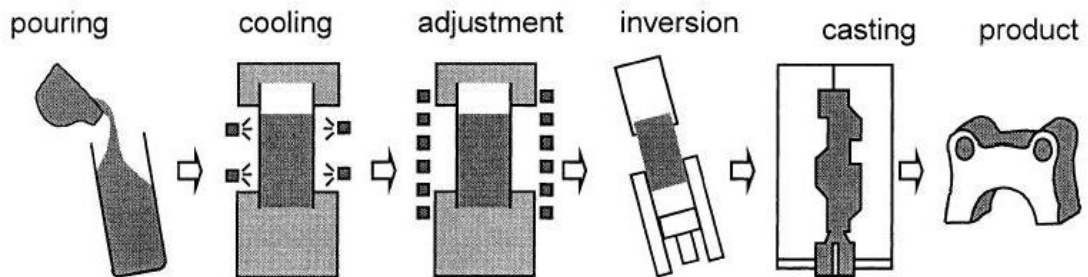


Figure 3.2. Schematic illustration of new rheocasting (NRC) process [4]

There is no need for specially treated thixo-formable feedstock and scrap can be readily recycled within the plant. The NRC route has a lower unit cost than thixoforming, due to the lower starting material cost. It also allows the use of a wider range of alloys; of particular interest are the magnesium alloys, where a thixotropic feedstock material is not readily available in the market place at present.

Rheocasting provides a means to cast very high-strength and high-ductility aluminum structural parts, pressure-tight components, and rangy parts with thin walls at somewhat lower cost than thixo-cast or squeeze cast parts.

Semi solid rheocasting (SSR) is another new process which is patented by MIT [25]. The process is implemented in three stages. In the first stage the molten alloy is held above the liquidus temperature. After that a rotating, cool rod is inserted in the melt and it starts solidification. At final stage the rotating rod is removed, and the quiescent melt is cooled to the casting temperature. SSR is fundamentally different than other rheocasting processes because molten alloy is converted to semi-solid slurry with applied rapid cooling and convection. Desirable, spheroidal microstructures are formed quickly and efficiently from molten alloy right at the liquidus. This gives the SSR process several advantages. The heat removal and convection are controlled with a separate cooling/stirring device, rather than relying upon temperature loss from pouring into a cold vessel. This allows a wider range of incoming melt temperatures and ensures a consistent slurry temperature after the cooling process. During the rheocasting process, heat is removed from the metal before it's transferred to the die casting machine, thus decreasing the cycle time within the die casting machine. In addition cooling occurs within the melt via the spinning rod, thereby ensuring a uniform cooling of the material. Other processes that rely upon heat removal through the outer surface of a container are more susceptible to formation of dendritic skin because of the localized rapid cooling on the surface.

### **3.3. Thixomolding**

Thixomolding is a relatively new process for production of near net shaped components from magnesium alloys in a single integrated machine, as shown in Figure 3.3. The raw material for thixomolding is magnesium alloy chips of 2–5 mm in size obtained during metal working of conventional solid magnesium alloys. A volumetric metering device feeds the magnesium chips into an electrically heated plasticizing and conveying unit where they are partially melted and transformed under continuous shear force into semi-solid slurry. The core of this unit is the screw, which performs both a rotary and translational movement. Upon entering the unit at the feed throat, the chips are forced to pass from the heating zone to the front of the screw while the screw retracts. Once the plasticizing volume corresponds to the weight of the part to be molded, the screw advances at high speed and injects the material into a mould. A non-return valve keeps the material from flowing back from the front of the screw to the in-feed zone. To prevent the

magnesium alloy from oxidizing and igniting as it is heated, an argon atmosphere is usually maintained at the in-feed, displacing the air between the magnesium chips.

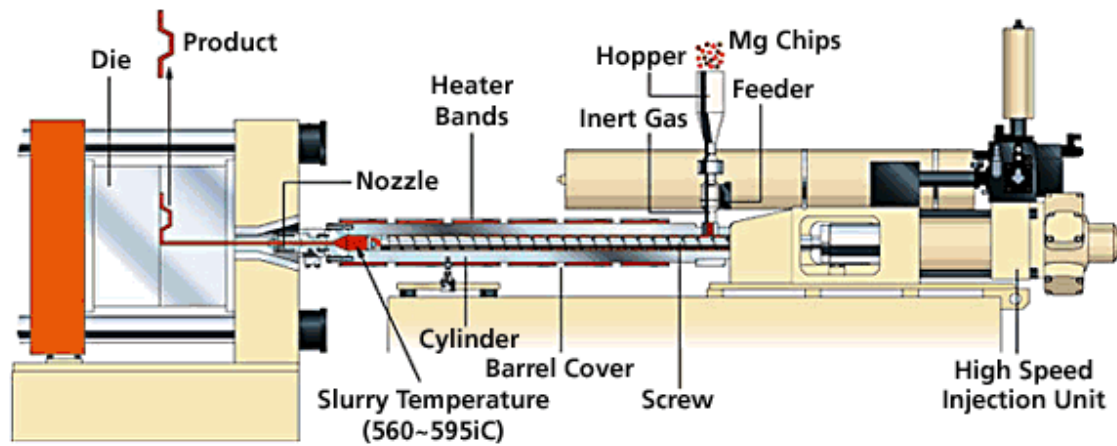


Figure 3.3. Schematic diagram of thixomolder [46]

It is now used by numerous companies, particularly to produce magnesium alloy components, e.g. for portable computers and cameras. Although the process is highly effective with magnesium alloys, aluminum alloys in the semi-solid state attack the screw and the barrel. Strenuous efforts have been made to overcome these problems but it is not clear that a successful commercial outcome has yet been achieved [2].

A major advantage of thixomolding compared with other SSM processing technologies is that it combines effectively the slurry making and component forming operations into a one-step process leading to high efficiency of productivity and energy management. The other advantage of thixomolding is the elimination of liquid metal handling operations, hence creating a cleaner and safer working environment, which is particularly advantageous for processing magnesium alloys. Dimensional stability, low porosity and tighter part tolerances with reduced shrinkage are also obtained with the process. A large number of machines are in operation for producing magnesium castings, particularly for electronic components. At present, this process is limited to relatively low solid fraction and to magnesium alloys for thin wall components [4,48].

### 3.4. Rheomolding

Rheomolding is a new idea of combining rheocasting in an injection-molding-like apparatus to achieve net-shape manufacturing of semi-solid metal parts with lowest porosity. Instead of solid pellets or chips in conventional injection molding or thixomolding, as starting material, rheomolding begins with molten metal in a crucible. As the fluid enters the extruder, it is always subject to cooling along the barrel and begins to crystallize on the cold wall. The screw rotation and the moving fluids will break the dendritic crystals on the wall and form solid particles suspended in the remaining fluids. By adjusting the temperature profile along the barrel and screw rotating speed, one could achieve various degrees of solid fraction and perhaps manipulate particle sizes [49].

Fluid flow in the twin screw rheomolding process (TSRM) is characterized by high shear rate, high intensity of turbulence, and cyclic variation of shear rate. As a consequence of such fluid flow characteristics and the accurate temperature control, the temperature and composition fields inside the barrel are extremely uniform. So far, this technology has been tested using Sn–Pb and magnesium based alloys [12]. The SSM slurry produced by the TSRM process is characterized by fine and spherical particles of uniform size. Such a slurry structure allows direct shaping operations, such as casting, extrusion, and forging [2,4].

### 3.5. Thixoforming

Thixoforming is a general term coined to describe the near net shape forming processes from a partially melted non-dendritic alloy slug within a metal die. If the component shaping is performed in a closed die, it is referred to as thixocasting, while if the shaping is achieved in an open die, it is called thixoforging, as schematically illustrated in Figure 3.4. There are three separate stages involved in the thixoforming process [4]. The first stage is the production of the raw material which has a fine, equiaxed, globular microstructure. The second stage is the uniform heating and partial remelting of the alloy slug so that it is homogeneous throughout. In the last stage, the semi-solid slug is transferred to a forging die or shot chamber by robot handling where it is injected in a controlled manner into a die cavity by a hydraulic ram. After solidification, the shaped

component is removed from the mold for further processing, such as minor machining or grinding. The further processing steps are much lower than other manufacturing techniques.

Thixoforming is the process where suitable material is heated into the semi-solid state and injected into a die. Usually, the liquid content is between 30 and 50 per cent prior to forming. Firstly the specimen is induction heated into the semi-solid state with holding at the semi-solid state for a while in order to achieve the desired microstructure. Secondly when it has reached the appropriate proportion of liquid it is forced into the die for the forming operation. Cycle times are then very comparable with die casting, if not faster because the full solidification range does not have to be gone through.

Most specimen parts and authentic application components produced in the world to date are still made from AlSi7Mg alloy. This material can be semi-solid formed into components weighing from under 10 g to more than 10 kg.

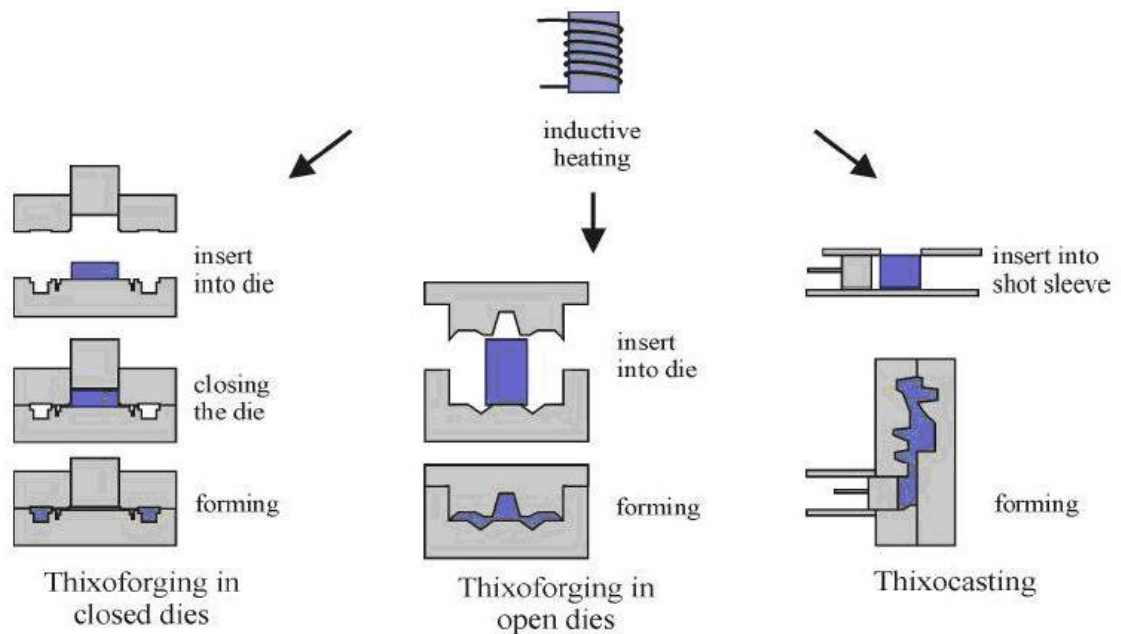


Figure 3.4. Steps of thixoforming [50]

### 3.5.1. Reheating Process

Reheating to the semi-solid state is a particularly important phase in the thixoforming process. It aims to provide semi-solid slug with an accurately controlled solid fraction of fine and spherical particles uniformly dispersed in a liquid matrix of low melting point. In order to obtain good mechanical properties, the eutectic must be completely remelted to achieve this semi-solid microstructure. The important processing parameters during the reheating process include accuracy and uniformity of heating temperature and heating duration. It is the heating temperature that determines the solid fraction in the slug. Too high a heating temperature causes instability of the slug resulting in difficulties for slug handling. At the same time too low a heating temperature leads to unmelted, coalesced, polyhedral silicon phase in the slug in the case of hypoeutectic cast aluminum alloys having a detrimental effect on the rheological properties during die filling parts. A small variation in temperature can cause a large difference in solid fraction. Therefore, temperature accuracy affects the stability of the forming process and the consistency of the product quality. Furthermore, a uniform temperature distribution throughout the slug is important, because a non-uniform distribution of temperature may lead to fluctuation in solid fraction and rheological characteristics, which in turn may cause solid/liquid separation during mould filling. Finally, the heating duration has to be optimized; too long a heating time will cause structural coarsening, while too short a heating time will lead to incomplete spheroidization of the solid particles compromising the rheological properties and leading to difficulties during mould filling [51]. Typical microstructure after reheating is shown in Figure 3.5.

Currently, reheating is achieved mainly by induction heating, although a convection furnace is also used in some cases. Induction heating has advantages over conventional electric furnace heating in that the former reduces the amount of scaling and scrap due to less billet heating time. Induction heating has the advantage of precise and fast heating, which is necessary for SSM processing. On the other hand the relatively low energy efficiency of the induction heating station is a draw-back. Possible improvement of energy efficiency can be achieved by preliminary heating to a critical temperature in a convection furnace followed by induction heating for temperature homogenization. Induction heating is currently implemented in two different ways: vertical and horizontal heating. For

vertical type induction heating, if too much thermal energy and heating time are provided to heat the billet to the required temperature, undesirable phenomena such as liquid segregation, “the elephant-foot effect” by its own weight and an ‘electromagnetic end effect’ may occur.

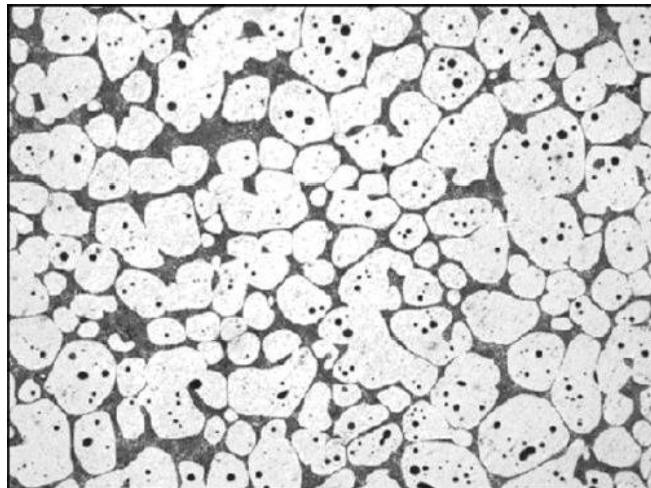


Figure 3.5. Microstructure of reheated alloy [52]

The horizontal heating system is a relatively new development, in which the slug lies in a tray and is heated to the optimal processing state monitored by an automatic control loop. Advantages of the horizontal heating system include reduction of the shape stability problem, possibly using higher liquid fractions and alloys with a short freezing range. For the horizontal-type induction coil, the ‘elephant foot effect’ by its own weight seldom appears and out flow of the liquid decreases remarkably. Horizontal-type induction coils reduce the temperature gradient of the billet and the globular microstructure can be obtained. However, it has a higher system cost and higher space requirement than vertical systems [53,54].

When heating by electromagnetic induction, energy is transferred from a coil to the work piece via an alternating magnetic field. The induced electro-magnetic force ( $E_c$ ) produces a circulating current which, in turn, generates heat (Figure 3.6). The current, and therefore the generation of heat, is concentrated at the surface and its density falls off approximately exponentially with distance from the surface [55].

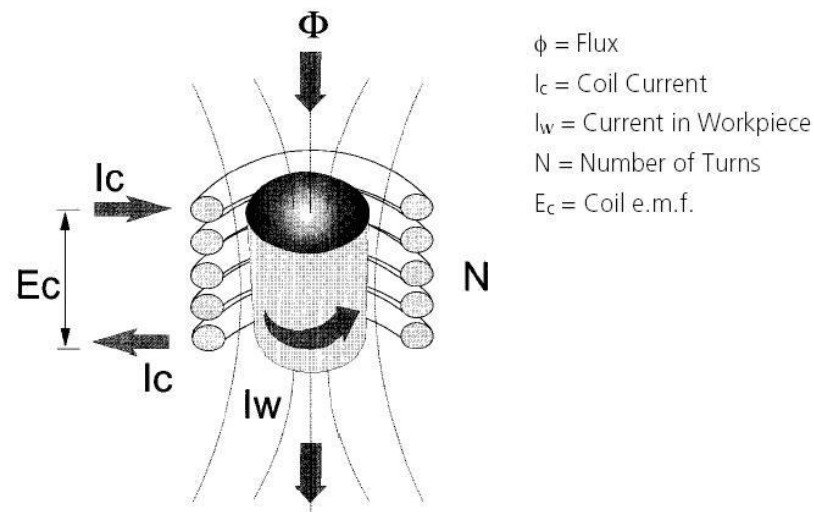


Figure 3.6. Induction heating of cylindrical work piece [55]

The realization of the thixoforming process requires the reheating of the billets in their semi-solid state with a very accurate temperature control. Optimization of the processing parameters is a critical step to ensure a high quality of formed parts. Induction heating can control the billet temperature exactly for a short time but a temperature gradient can arise over the entire cross-sectional area. To obtain a uniform temperature distribution in a cross section of the billet and to reduce the heating time, the design of the induction coil is very important. The temperature of the billet at the edge region is much higher than that at the center region. Reduction of heating times with the same final temperature difference in the billet cross-section can be obtained by the use of multi-stage heating processes [54,56]. In multi-stage heating process firstly the billet is heated to a temperature that is lower than the working temperature and held at that temperature for some time in order to minimize the temperature gradient across the billet. This holding stages maybe two or three. At three stage processes the final holding stage is generally slightly lower than the final temperature. After the final stage the specimen reaches a homogeneous temperature gradient for the forming operation.

### 3.5.2. Forming Process

The forming process takes place either with casting (thixocasting) or with forging (thixoforging). A robot arm transfers the semi-solid slug into the shot chamber and the plunger injects the materials into the die cavity. All the thixocasting machines are real-time

controlled and thus permit a reaction to possible fluctuation during the forming process. At this stage, smooth laminar mould filling is the crucial step for the forming process. This can be achieved by an optimized shot profile tailored for specific alloys and their physical conditions. Another important aspect during the forming process concerns the design of the gating system and die cavity and the correct choice of die temperature. Such a design process has to consider the flow characteristics of the semi-solid metals. The forming process can be optimized through process simulations using various computer modeling techniques [4].

In the forming process, the reheated billet is stable similar to a solid as long as it is not stressed, but flows similar to a liquid when subjected to shear stresses. Compared to plastic deformation in solid state forging the semi-solid metal has almost no flow restrictions. Thus very complex shapes with thin ribs, hollow cross sections, undercuts and difficult mass distribution can be formed in one forming step. In comparison to high quality casting methods, like squeeze casting or vacuum die casting, the unique advantage of thixoforming is, that the solidification shrinkage is significantly reduced which gives the designer more freedom towards thicker cross sections and wall thickness changes. Other process advantages are reduced gas entrapment due to laminar flow and significantly reduced thermal die loading. Compared to castings thixoformed components exhibit none or minimum of porosity and inclusions, which results in high mechanical properties, pressure tightness and the possibility to apply thermal treatment. During the last few years at least the following four categories of components have been identified, for which the thixoforming process maybe of particular interest [5]:

- Components subject to high pressures e.g. brake cylinders
- Thick-walled components subject to high loads
- Thin-walled structural components
- Components made of special materials such as metal matrix composites, which are expensive, difficult to machine and known for their poor casting properties

Forging presses may vary, but the ability to control the forming speed and the pressure precisely is essential if the press is to be used to semi-solid forge a variety of parts. Depending on the part size geometry, alloy and quality specified, forming speeds

may range from a few inches per second to over 1270 mm per second and mold pressures from a hundred pounds per square inch to 140 MPa or more [30]. A schematic view of a thixoforming press is shown in Figure 3.7.

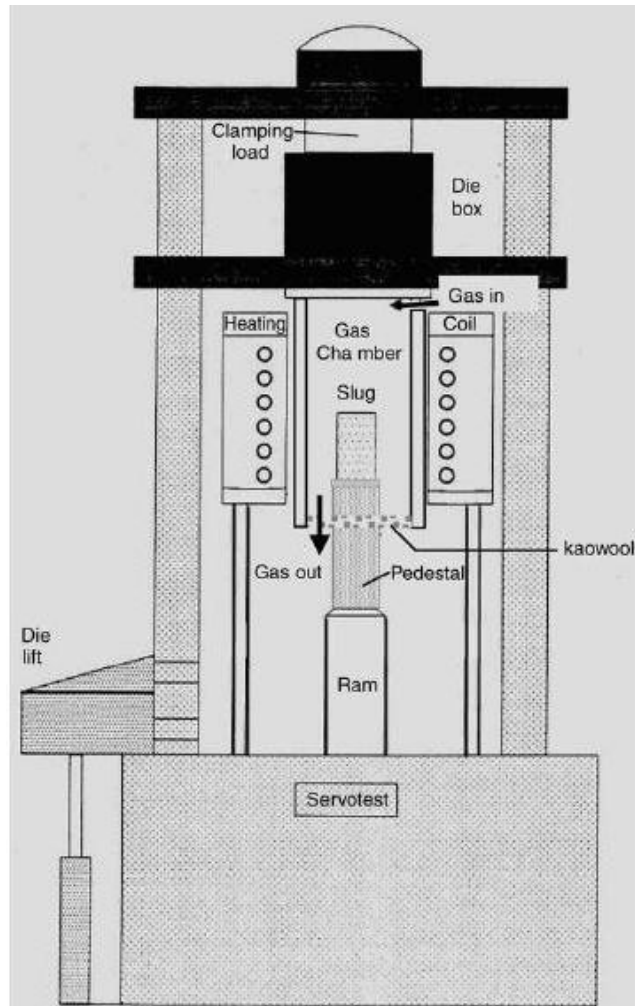


Figure 3.7. Schematic view of the thixoforming press [57]

Flemings [8] has recently summarized the major advantages and disadvantages of the thixoforming process. The main specific advantage of the thixoforming route is that the forming facility is free from handling liquid metal, and the process can be highly automated using approaches similar to those employed in forging and stamping. This basic concept of completely separating the two main parts of the process (forming of the desired structure and forming of the part) has been intuitively appealing and much work has been done in developing this process route industrially. As time progresses, the disadvantages of the thixocasting route are also becoming apparent. It has been difficult to obtain fully

homogenized billets in MHD stirred continuous castings. Typical billets have some degree of inhomogeneity with respect to both structure and composition. There is metal loss during the reheating process, which may amount to as much as 10 per cent of the total part weight. Gates and risers cannot be recycled within the forming facilities, but must be sent back to the ingot producer. Thus, the metal former pays a premium to the continuous caster not only for the unique thixotropic structure in the metal, but also for the recycled materials. Currently, the cost for thixotropic feedstock could account for up to 50 per cent of the total component cost.

The advantages of semi-solid metalworking have enabled it to compete effectively with a variety of conventional processes in a number of different applications. The areas of applications are as automotive, aerospace and some other industries as electronics. Semi-solid forged parts have replaced conventional forgings, permanent mold and investment castings, impact extrusion, machined extrusion profiles, parts produced on screw machines and in usual circumstances, die castings and stampings. Applications include automobile wheels, master brake cylinders, antilock brake valves, disk brake calipers, power steering pump housing, power steering pinion valve housings, engine pistons compressor housings, airbag containment housings, power brake proportioning valves, electrical connectors and various covers and housings that require leak-tight integrity [8,30]. Two key manufacturing advantages of semi-solid working over conventional methods are degree of automation that can be incorporated into the material handling systems, as well as the heating and forging operations and the precision that is routine in the control of the process. In summary, the advantages of the semi-solid working can be summarized as follows [30,58]:

- Laminar flow in die excludes gas entrapment and porosity, (< 0.1%).
- Good combination of strength and ductility.
- Product complexity, close dimensional tolerances, near-net shape, thin walls and excellent surface finish, precision dies produce near-net shape parts that require less machining.
- Low processing temperature and therefore short cycles times and low stress on tooling lead to longer die life.

- Ability to utilize unusual alloys that normally prove difficult in liquid casting processes (wrought compositions, for instance) results in broader parts applications.
- An ability to undergo a T-5 heat treatment without losing ductility, thus often achieving required mechanical properties without the dangers of blistering, distortion or quench stress associated with the full T-6 heat treatment.
- The ability to form hypereutectic Al-Si alloys and MMC's while retaining the desirable size and distribution of primary or second phases developed during billet manufacturing under ideal continuous casting conditions (those phases don't re-melt or dissolve during Semi-solid forming).
- The product consistency that results from using the pre-cast billet that was manufactured under the same ideal continuous processing conditions that are employed to make forging or rolling stock.
- Rapid quench in the forging press avoids expensive solution treatment to obtain higher properties.
- Semi-solid heating requires only 65 per cent of the energy required for casting.

Conversely some disadvantages of semi-solid processing are:

- Specially prepared raw material.
- Higher cost raw materials.
- Few sources of raw material.
- Expensive tooling of special design.
- Special and expensive capital equipment.
- Highly skilled staff required.

### **3.6. Hot Forming of Aluminum Alloys**

Hot working is defined as a mechanical process carried out above the recrystallisation temperature, whilst cold working is performed below that temperature.

When a stress is applied to a metal, it will deform. A small applied stress causes a small deformation or strain and when released the metal springs back to its original

dimensions. This is a non-permanent deformation because the strain was within the elastic limit of the metal. The modulus of elasticity (Young's modulus, E) reflects the relative ease of metals to form elastically. Metals have a high degree of 'plasticity' they can undergo appreciable permanent deformation without fracturing. Plastic deformation begins beyond the elastic limit. If it were not for plasticity, metals would break like glass or other brittle materials. Metals becoming harder and harder as they undergo plastic deformation mainly because the deformation produces conditions that limit the movement of faults (called dislocations) in natural metal crystals. These dislocations allow slip between crystals at much lower stresses than would be required were the crystals without faults. A work hardened metal can be softened by heating it long enough at a sufficiently high temperature so that the grains will recrystallize. The softening occurs simultaneously with reduction of strength and increase in ductility [59].

### **3.6.1. Rolling of Aluminum Alloys**

Rolled aluminum is the most common wrought product. Between 0,15 to 6,3 mm in thickness the rolled product is known as sheet. Above 6,3 mm it is called plate and below 0,15 mm foil. Briefly, the rolling process is performed on ingots or rolling slabs. These are firstly scalped to remove surface defects from the rolling face [59].

Hot rolling is normally performed above the recrystallisation temperature. The lower temperature limit occurs when the metal is still hot enough to be reduced in thickness with each pass through the rolling mill but not cool enough to start cracking. Depending on the alloy, typical temperatures range between 400 and 540 ° C. Lengthening occurs almost entirely in the direction of rolling.

### **3.6.2. Forging of Aluminum Alloys**

Like several other metals aluminum can be forged by conventional forgings hammers and mechanical and hydraulic presses. Generally aluminum alloys require a greater working force for an equal amount of deformation than low carbon steels. Forging hammers from 2 to 222 kN are used for aluminum. Cast or forged blanks are heated to 360 to 480 ° C depending upon the alloy, are hammered repeatedly between two suitably

shaped hammer dies which impart the final forged shape to the forge piece. In press forging a continuous stroke of the press is required. Further strokes using successive die impressions are possible. Mechanical presses of about 2,5 to 90 MN are used. Pressures range from 200 to 500 MPa, depending on the alloy, design and mass of the piece. Typical pieces range from 0,5 to 30 kg. Hydraulic presses are preferred for larger and more complex or precise parts. These presses are available from 4 to 445 MN and can handle from small, thin parts up to large 1 200 kg parts. Mechanical and hydraulic presses can produce close-tolerance forgings requiring a minimum of machining [59].

### **3.6.3. Extrusion of Aluminum Alloys**

Extrusion is the process by which long straight metal parts can be produced. The cross-sections that can be produced vary from solid round, rectangular, to L shapes, T shapes, tubes and many other different types. Extrusion is done by squeezing metal in a closed cavity through a tool, known as a die using either a mechanical or hydraulic press.

Extrusion produces compressive and shear forces in the stock. No tensile is produced, which makes high deformation possible without tearing the metal. The cavity in which the raw material is contained is lined with a wear resistant material. This can withstand the high radial loads that are created when the material is pushed the die.

Hot extrusion is done at fairly high temperatures, approximately 50 to 75 per cent of the melting point of the metal. The pressures can range from 35-700 MPa. Due to the high temperatures and pressures and its detrimental effect on the die life as well as other components, good lubrication is necessary. Oil and graphite work at lower temperatures, whereas at higher temperatures glass powder is used [60].

Typical parts produced by extrusions are trim parts used in automotive and construction applications, window frame members, railings, aircraft structural parts.

### 3.6.4. Common Forging Processes

Forgings are consistent from piece to piece, without any of the porosity, voids, inclusions and other defects. Thus, finishing operations such as machining do not expose voids, because there aren't any. Also coating operations such as plating or painting are straightforward due to a good surface, which needs very little preparation. Forgings yield parts that have high strength to weight ratio-thus are often used in the design of aircraft frame members [61].

A Forged metal can result in the following:

- Increase length, decrease cross-section, called drawing out the metal.
- Decrease length, increase cross-section, called upsetting the metal.
- Change length, change cross-section, by squeezing in closed impression dies. This results in favorable grain flow for strong parts

3.6.4.1. Press Forgings. Press forging use a slow squeezing action of a press, to transfer a great amount of compressive force to the work piece. Unlike an open-die forging where multiple blows transfer the compressive energy to the outside of the product, press forging transfers the force uniformly to the bulk of the material. This results in uniform material properties and is necessary for large weight forgings. Parts made with this process can be quite large as much as 125 kg (260 lb) and 3m (10 feet) long.

3.6.4.2. Upset Forgings. Upset forging increases cross-section by compressing the length, this is used in making heads on bolts and fasteners, valves and other similar parts.

3.6.4.3. Roll Forgings. In roll forging, a bar stock, round or flat is placed between die rollers which reduces the cross-section and increases the length to form parts such as axles, leaf springs etc. This is essentially a form of draw forging.

3.6.4.4. Net Shape / Near-Net Shape Forging. In net shape or near-net shape forging, forging results in wastage of material in the form of material flash and subsequent machining operations. This wastage can be as high as 70 per cent for gear blanks, and even

90 per cent in the case of aircraft structural parts. Net-shape and near-net-shape processes minimize the waste by making precision dies, producing parts with very little draft angle. These types of processes often eliminate or reduce machining. The processes are quite expensive in terms of tooling and the capital expenditure required. Thus, these processes can be only justified for current processes that are very wasteful where the material savings will pay for the significant increase in tooling costs.

## 4. EXPERIMENTAL STUDY

In the following section, the properties of the feedstock material, the components of the experimental set-up and experimental procedure employed throughout this study are explained. In addition to these, the methods that are used to investigate the final samples are given. Finally microstructure images and mechanical properties such as hardness and tensile test results were examined and discussed with comparing the two forming methods used in the study.

### 4.1. Materials

Thixoforming is the forming of metal alloys in the semi-solid state. In order to form an alloy in the semi solid state the feedstock material has to have a fine and globular microstructure. After reheating the feedstock material the microstructure consists of globular grains suspended in a liquid melt. As the forming operation starts the deformation is obtained mainly by the flow of primary grains in the liquid matrix and the deformation of the grains has a minor contribution on forming. The most common method for achieving this microstructure is magneto hydrodynamic stirring (MHD). In this method the melt is stirred intensively with magnetic forces during solidification to obtain a fine grained non-dendritic structure for the thixoforming process.

Table 4.1. Chemical composition of A356 aluminum alloy used in the study in wt percent

A356	Si	Fe	Cu	Mn	Mg	Zn	Ti	Sr
	6,99	0,107	0,006	0,007	0,312	0,008	0,098	0,03

In experimental studies cast aluminum A356 which was fabricated by SAG Austria was used. The alloy was in 76 mm diameter and 100 mm in height. Billets were produced by electromagnetically stirred horizontal casting process. The alloy is used in the automotive industry for producing near net shaped aluminum parts. The A356 is the most popular alloy for semi-solid forming in automotive industry since it has good mechanical properties, high corrosion resistance and welding properties. Another advantage of the

alloy is its wide solidification interval which is a key factor in the semi-solid forming process. The chemical composition of the alloy is shown in Table 4.1.

Table 4.2. Chemical composition of A356 aluminum alloy in wt per cent [62]

	Si	Fe	Cu	Mn	Mg	Ni	Zn	Pb+Sn	Ti	Sr
Minimum	6,5	-	-	-	0.3	-	-	-	-	0.01
Maximum	7.5	0.15	0.03	0.03	0.4	0.03	0.05	0.03	0.2	0.05

The liquidus temperature of this alloy is 614 ° C and the solidus temperature is 554 ° C. The solidification range is 60 ° C. The solid fraction and temperature curve of the alloy is shown in Figure 4.1.

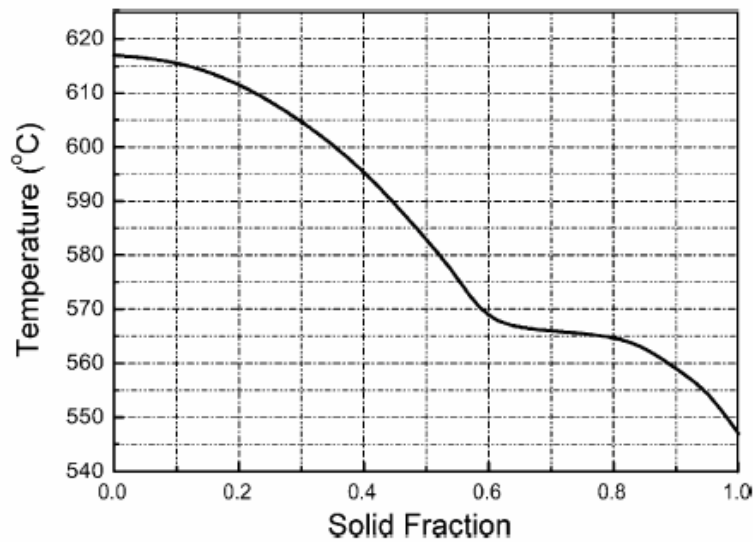


Figure 4.1. Solid fraction of A356 alloy as a function of temperature [29]

The microstructure images of the raw material were taken after supplying from the supplier. The image is shown in Figure 4.2. The raw material have a fine broken non-dendritic structure. It can be observed from the microstructure images that the grains are in the form of ripened rosette like. However the roundness is not perfect.

In addition in the surface region of the billet the grains are rosette like and also there exist dendritic arms. The eutectic structure can be clearly seen in the images. Since these are the images before reheating the eutectic structure is between the grains and there is no

penetrated liquid matrix inside the grain boundaries. The boundaries between the grains and eutectic structure are clear.

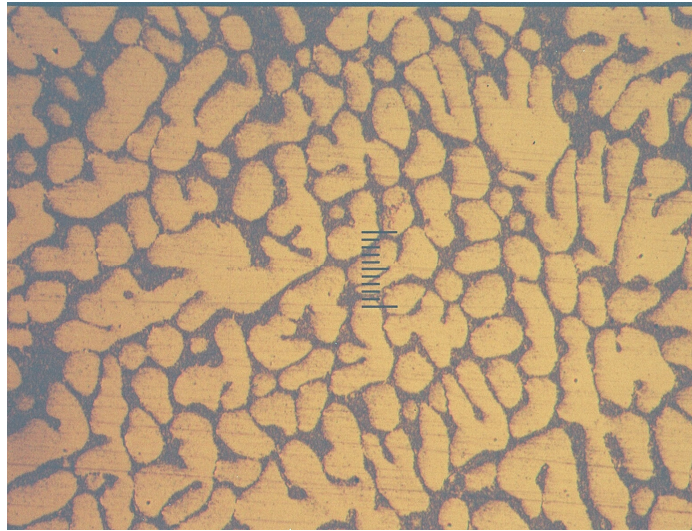


Figure 4.2. Microstructure image of the raw material

## 4.2. Experimental Setup

### 4.2.1. Semi-Solid Forming and Hydraulic Power Unit

The hydraulic press consists of two main elements. The first one is the hydraulic power unit which determines the necessary hydraulic pressure for the system. The view of the unit is shown in Figure 4.3. The hydraulic pump pressurizes the oil by taking motion from the electric motor. The circulating oil in the system is controlled by the directional control valve. When the valve is on free position the oil in the system bypasses through the control valve and returns to the tank. By pushing the control valve the pressurized oil is directed to the upper surface of the hydraulic cylinder and the punch moves down with the pressing force. With the same principle when the valve is pulled the oil is directed to the lower surface of the hydraulic cylinder and the punch moves up. The applied pressure can be controlled by a bolt in the control valve body.

The second main part of the hydraulic press is the main body that holds the punch and the die (Figure 4.4). As it can be seen from the figure the cylinder is placed vertically at the top of the main body. The die is inserted in a hole at the bottom table of the body.

Moreover a plate is fixed to the body in order to support the bottom of the die with two M20 bolts. There is a hole at the centre of the support plate to take the formed samples easily. In order to prevent movement of the die with the injection load two locking blocks are fixed to the main body at the edges of the hole where the die is inserted. The main body generates pressing force by taking necessary pressurized oil from the hydraulic unit.



Figure 4.3. Hydraulic unit

In semi-solid forming operations high ram speed is required in order to minimize the heat loss and maintain good flow in the die. Lower ram speeds may give undesired results such as incomplete die filling due to solidification. Since the experiments are made in the semi-solid state the material solidifies easier than conventional casting operations. Because of this reason the ram speed should be as high as possible to finish the forming operation before solidification of the metal. In order to fulfill these requirements the forming unit has a hydraulic pump of a flow rate of 42 lt/min and a 7.5 KW electric motor to maintain the adequate oil flow and as a consequence high ram speed. The detailed specifications of the system are shown in Table 4.3.



Figure 4.4. Main body

Table 4.3. Specifications of the forming unit

Dimensions of forming unit .....	300 x 300 x 765 mm
Maximum load.....	7.8 ton-f
Speed of the ram.....	Max: 89 mm / sec
Electric motor.....	7.5 KW ; 1440 rpm
Hydraulic pump.....	42 lt/min

#### 4.2.2. Heating Unit

Instead of induction heating, resistance furnace heating was used for heating the billets to the target temperature. Under resistance heating the homogeneity of the temperature is excellent and the temperature may be measured directly. In addition the

primary component cost is much cheaper than induction furnaces. However the risk of grain coarsening may be increased due to the longer duration of heating. By using this technique the feasibility of using resistance heating was evaluated instead of induction heating. Two heating elements were used for heating operations. First one was for heating the billets outside the die and second one was the ring heater which heats the die inside the main body. Vertical tube furnace was used for heating the billets to the semi-solid state. As a result of its small inner space fast and effective heating was obtained in the furnace. The temperature of the furnace was controlled by a K type thermocouple through the temperature controller during the operation.

Preheating the die was done by a 900 W ring resistance as shown in Figure 4.5. It has a built in J type thermocouple and the temperature of the heater was controlled during heating operation by the temperature controller. Because of its perfect roundness and precise inner surface, it contacts equally to every point of the surface of the die and therefore provides excellent heat transfer.



Figure 4.5. Ring heater used for pre-heating the die

#### **4.2.3. Temperature Control Unit.**

Temperature control unit controls the temperature of the furnace and ring resistance heater by utilizing the thermocouples during the operation. Desired temperature levels for both heaters can be adjusted separately by the temperature control unit. It typically consists

of two different thermostats which are connected to the heaters. The control unit can be seen in Figure 4.6.



Figure 4.6. Temperature control unit

#### 4.2.4. Die

Two dies were designed for the experiments. The dies were similar in design but differ from each other in their lengths. The first die was shorter and used in forming samples for microstructural examinations and microhardness tests. The second die was designed longer to produce samples that comply with the standards of the tensile test specimens according to ASTM. Both die concepts consists of 5 parts. These are the main part, moving punch, ejector punch, and two supportive blocks. Figure 4.7 shows all the parts of the die system.

The die had to have high performance since it is designed for pressing operations for both semi-solid forming and hot forming operations. For this purpose the parts of the die were machined from hot work steel. The machining operations were done in conventional lathe. After machining, the parts were heat treated to HRC 56-60. Lastly the set ups were machined in a grinding machine within very small tolerances to fit each other perfectly and prevent possible sticking problems during experiments.



Figure 4.7. Die used to produce the specimens



Figure 4.8. Closing the bottom hole of the die

The main part of the die was inserted in the cavity inside the main body of the forming unit. The punch was assembled in the piston of the hydraulic cylinder. In order to close the bottom hole of the die two parts were used. The first part fits into the bottom of the die and provides excellent closure. The second support part was placed between the first part and main support plate (Figure 4.8).

#### 4.2.5. Conveyer

Convey unit was designed to transfer the heated billets from the furnace to the die. Billets in mushy state are delicate and require special handling in transforming to the die. Another problem is the heat loss during the transformation of the reheated billet to the die cavity. In order to solve both of these problems billets were heated in a cylindrical conveyer made of steel (Figure 4.9). After putting the billets inside the conveyer the upper hole of the unit was closed by ceramic fiber insulator and the whole part was transformed to the furnace. In addition, by using this unit the heated billets did not contact with outside atmosphere directly. As a result oxidation and cooling of the billet were minimized and it ensured enough time to transform the billet to the die for the forming operation. On the surface of the conveyer a thermocouple hole was drilled to measure the temperature of the billet. After transforming the unit to the top of the die the pin was removed and the billet was dropped into the preheated die.



Figure 4.9. Conveyer

#### 4.3. Semi-Solid Forming and Hot Forming of A356 Alloy

The experiments were conducted with thixotropic A356 aluminum alloy which was fabricated by SAG, Austria using the MHD casting method. Supplied billets were cut into pieces and machined to  $\text{Ø} \times h = 15 \times 45$  mm samples in a conventional lathe. Samples for

tensile test specimens were machined to  $\varnothing \times h = 16 \times 90$  mm. A thermocouple hole was drilled on the samples. In order to prevent sticking problem polishing was applied to the samples after machining. The general view of the experimental set up is shown in Figure 4.10.



Figure 4.10. General view of the experimental set up

Before starting the experiments firstly the die with the ring resistance and the punch were assembled to the main forming unit. Support parts were fixed to close the bottom hole of the die. In addition to these, two locking blocks were fixed at the top to prevent the movement of the die under the injection load. To prevent sticking of the samples to the die during the forming operation, special graphite oil was used. After these the cable connections of the ring heater were done. Secondly a sample was put into the convey unit and a K type thermocouple was inserted inside the unit to measure the temperature of the sample during heating. After these the furnace and the thermocouples were connected to control unit.



Figure 4.11. Transferring the heated billet to the die cavity

The furnace and ring heater were set to desired temperatures. Before starting the heating of the elements, the punch was left inside the die to provide the heating of the punch with the ring resistance through the die. This operation minimizes the temperature difference between the die and punch, prevents thermal shock and the dimensional difference between the parts as a result of thermal expansion. After reaching the desired temperatures the convey unit was put inside the hot furnace to provide rapid heating of the sample. Rapid heating is an essential part in thixoforming since prolonged heating times results in grain coarsening. The temperature of the sample was noted during the heating operation. When the sample reached to required temperature the convey unit was transformed to the upper part of the die and the billet was dropped inside the die cavity with the removal of the pin of the conveyer (Figure 4.11).

Afterwards the convey unit was taken away rapidly and the punch moves through the die hole and the forming operation took place at this period. The punch squeezes the sample about 15-20 seconds and at the end of this time it moves back. After the operation, in order to open the hole of the die, the second support part must be ejected first. After ejecting the second part the first support part can be ejected from the hole of the die since it had a fitting. Lastly the specimen could be ejected form the die by the help of the ejector

punch. The final product was dropped through the hole of the support plate. Figure 4.12 shows the removal of the specimen from the die.



Figure 4.12. Removal of the sample from the die

Semi solid experiments were conducted at  $570^{\circ}\text{C}$  and  $580^{\circ}\text{C}$ . Since the eutectic temperature of the alloy is  $574^{\circ}\text{C}$  the effects of the eutectic melting could be seen by using these temperature ranges. Different levels of holding times were used in the investigations. The samples were hold for 3, 5 and 7 minutes at both  $570^{\circ}\text{C}$  and  $580^{\circ}\text{C}$ . Hot forming experiments were done at  $450^{\circ}\text{C}$ ,  $470^{\circ}\text{C}$  and  $500^{\circ}\text{C}$ . The temperature of the die was set to  $300^{\circ}\text{C}$  in both hot forming and semi-solid forming experiments. In order to obtain fast heating condition which is necessary for thixoforming, all the experiments were done after the die, punch and the furnace were heated to target temperatures. The parameters used in the study are shown in Table 4.4.

Table 4.4. Forming parameters of the specimens

Specimen No	S1	S2	S3	S4	S5	S6	S7	S8	S9
Temperature ( $^{\circ}\text{C}$ )	570	570	570	580	580	580	500	470	450
Holding time (minute)	3	5	7	3	5	7	-	-	-

## 4.4. Sample Characterization

### 4.4.1. Microstructure Examinations

Samples cut from the semi-solid and hot formed bars were prepared for metallographic examination. Microstructural examinations were carried out by using an Olympus PME-3 type optical microscope. Olympus C-35AD-4 camera connected to the Olympus microscope was used and collared photographs were taken in three different scales. The microstructure images of the specimens were taken as polished and etched conditions. Etching treatment was carried out using Keller reagent. The composition of the solution was 2.5 ml HNO<sub>3</sub> (concentrated), 1.5 ml HCl (concentrated), 1 ml HF(%48) and 95 ml water. Keller reagent is the most common etchant for Al & Al Alloys, except high Si alloys. The samples were etched for 20 seconds. Figure 4.13 shows a specimen cut, polished, etched and replaced into bakelite for examination. Images of the samples were captured from upper, middle and bottom portions of the samples.

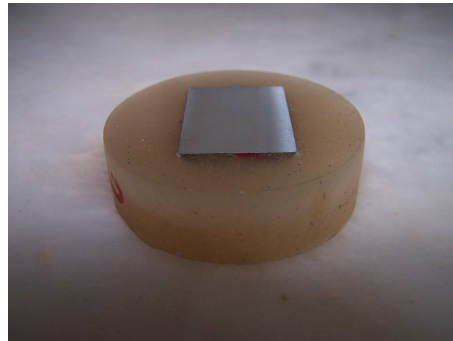


Figure 4.13. Prepared specimen in bakelite

In order to characterize the materials and compare their microstructures in a more quantitative way, extensive image analysis was carried out on the samples. After taking the photographs of the samples the images were analyzed for the determination of the shape factor and grain size. For this purpose Image Tool program was used. With the help of the program perimeters, areas and sizes of several grains were calculated from the images of each sample. After wards, averages of these values were taken as the result. The shape factor  $F$  can be defined as:

$$F=4\Pi A/P^2 \quad (4.1)$$

F= shape factor

A= particle cross sectional area

P=perimeter of the particle

When F is equal to 1, the shape is in the form of exact sphere

#### 4.4.2. Vickers Microhardness Tests

In microhardness testing, an indentation is made by a precision diamond tool at loads from 15 to 1000 gf. The impression length, measured microscopically, and the test load are used to calculate a hardness value. The advantages of the Vickers hardness test are that extremely accurate readings can be taken, and just one type of indenter is used for all types of metals and surface treatments. Although thoroughly adaptable and very precise for testing the softest and hardest of materials, under varying loads, the Vickers machine is a floor standing unit that is rather more expensive than the Brinell or Rockwell machines [63].

The Vickers microhardness tests were performed according to the ASTM E384 standards. The Matsuzawa MHT-2 Vickers Microhardness Testing Instrument was used. Applied load was 100 gf and holding time was 5 seconds. Five measurements through the cross section of height and the center transversal section were made for each sample. At each point 3 measurements were made and the averages of these values were taken as the result. The hardness tests were made on the specimens that were formed in the shorter die.

The equation to calculate the hardness value is given below

$$HV = 1854,4L/d^2 \quad (4.2)$$

L= Load in gf

d = Arithmetic mean of the two diagonals, d1 and d2 in ( $\mu\text{m}$ )

HV = Vickers hardness

#### 4.4.3. Tensile Tests

During a tension test, it is desirable to apply forces to the specimen large enough to break it. The grip region of the specimen must have a large enough area to transmit the force without significant deformation or slipping. There are standard specimen geometries specified by the American Society for Testing Materials (ASTM).

When a load is applied to a solid, deformation occurs. The deformation is elastic if it is completely recovered immediately after the load is removed. Purely elastic deformation is associated with the stretching of primary bonds in materials. Stress is the force per unit area

$$\sigma = F/A \quad (4.3)$$

and strain is the elongation per unit length

$$\varepsilon = \Delta L/L \quad (4.4)$$

The stress and elastic strain are directly proportional and related by the Modulus of Elasticity (or Young's Modulus) which is related to the potential energy well of the interatomic bonds. Hooke's law relates these parameters,

$$\sigma = E \varepsilon \quad (4.5)$$

where E is Young's modulus. It is implicit here that only axial stresses and strains are of interest.

If permanent deformation occurs, it is called plastic. The onset of plastic deformation corresponds to a stress level necessary to initiate the motion of dislocations (a type of defect) in crystalline materials. The stress necessary to produce permanent deformation is the yield strength of the material. Some materials exhibit a sharp yield point, whereas others show a slow change in slope at the end of the elastic range. The yield strength is

conventionally defined as the stress necessary to produce a plastic strain of 0.2 per cent (elongation).

If the hardening rate is too low, a runaway situation called necking develops. This corresponds to the load reaching a maximum, at which point the tensile deformation is inhomogeneous and strain is no longer uniform. The corresponding stress is called the ultimate tensile strength or UTS. The elongation to failure, which is the permanent engineering strain after fracture, is an expression of material ductility. It does not include elastic strain but does include the uniform strain and the localized, necking, strain. The elongation to failure is usually stated as percent strain over a given gauge length.

The yield stress, ultimate tensile stress, and elastic or Young's modulus of a material can all be determined from the engineering stress-strain curve for that material. At small strain values (the elastic region), the relationship between stress and strain is nearly linear. Within this region, the slope of the stress-strain curve is defined as the elastic modulus. Since many metals lack a sharp yield point, i.e. a sudden, observable transition between the elastic region and the plastic region, the yield point is often defined as the stress that gives rise to a 0.2 per cent permanent plastic strain. By this convention, a line is drawn parallel to the elastic region of the material, starting at a strain level of 0.2 per cent strain (or 0.002 m/m.). The point at which this line intersects the curve is called the yield point or the yield stress. The ultimate tensile strength (stress), in contrast, is found by determining the maximum stress reached by the material [64].

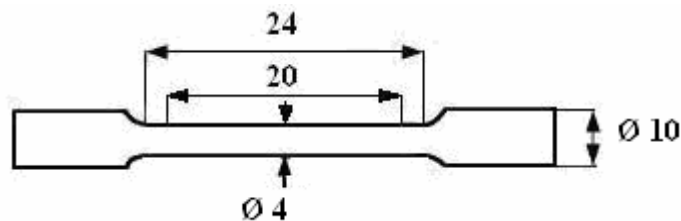


Figure 4.14. Tensile test specimen

After the experiments tensile tests were performed on the specimens which were prepared according to the ASTM E 8M-04 standard [65]. Forming of these products was done in the longer die to fit the standards. Round bar tensile specimens with a diameter of

4 mm were machined from the rod parts of products. The tensile test was carried out on Testometric Micro 500 testing machine. Three tests were made for each parameter. Figure 4.14 and 4.15 show the dimensions and a photograph of the tensile test specimen.



Figure 4.15. Image of the tensile test specimen

## 5. RESULTS AND DISCUSSION

The aim of the experiments is to compare the mechanical properties of the samples that were produced by semi-solid forming and hot forming processes. In addition the effects of reheating temperature and holding time on the microstructure characteristics of semi-solid formed samples were observed.

For the semi-solid forming process, both the coexisting solidus-liquidus phase and the reheating conditions to obtain a globular microstructure are very important. The eutectic phase must be melted completely, and that the reheating time for complete eutectic melting is necessary to obtain a fine globular microstructure. Fine primary grains also favor the manufacture of thin-walled parts and decrease the segregation of the liquid phase. Another advantage of fine microstructure is enhanced mechanical properties.



Figure 5.1. Formed specimen

The raw material used in the experiments was A356 aluminum alloy which was fabricated by SAG, Austria by electromagnetic stirring method. In semi-solid forming experiments two different temperatures and three different holding times were used. Figure 5.1 shows a cylindrical specimen which was formed in the longer die for tensile test. Flashing problem was not observed in the experiments as a result of the tight tolerances. Formed samples were cut into cross sectional parts and micrograph pictures were taken from different regions.

### 5.1. Microstructure Examination

In order to evaluate the morphology of the products microstructure analyses were performed on the specimens. For this purpose, optical micrographs at three different magnifications were used. There is a scale at the center of each image. In the x50 images the length of the scale is equal to 200  $\mu\text{m}$ , in x100 images the scale is equal to 100  $\mu\text{m}$  and in the x500 images the scale is equal to 20  $\mu\text{m}$ .

Samples S1, S2 and S3 were formed at 570 °C with different holding times changing from 3 to 7 minutes respectively. The time to reach the desired temperature was about 8 minutes and heating speed was 68 °C/min. The holding time in sample S1 was 3 minute and Figure 5.2 and 5.3 show the microstructure images after forming, from surface and center sections of the sample. Globularization was not observed in 3 minute holding time at this temperature. As it can be seen from the images, in both the center and surface area of the sample the globularization mechanism was not started and the grain boundaries were not clear. This is because of the insufficient time for eutectic melting. It can be concluded that 3 minutes of holding time was not enough for the formation of globular grains.

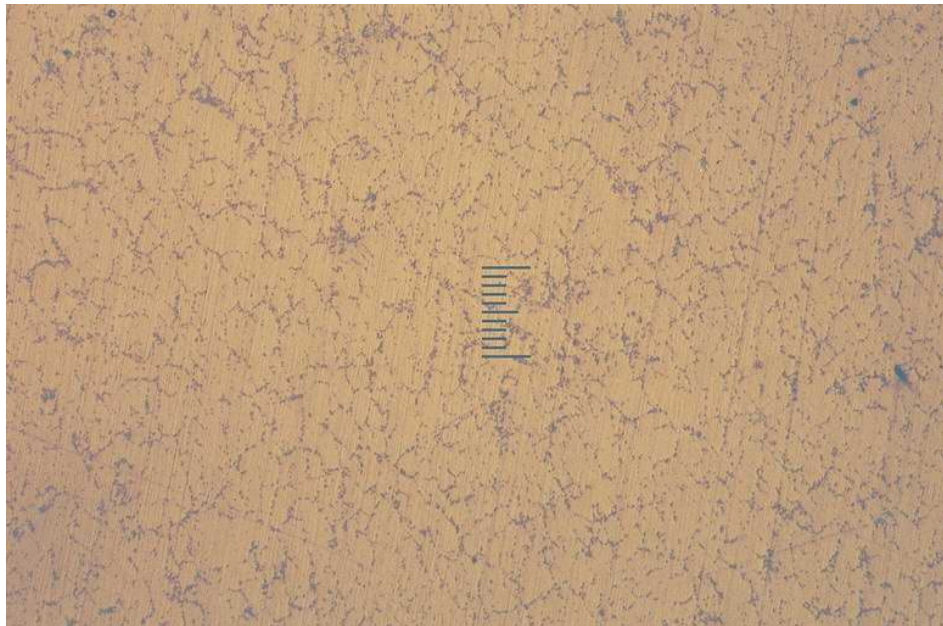


Figure 5.2. Microstructure of surface portion of sample S1 (x100)

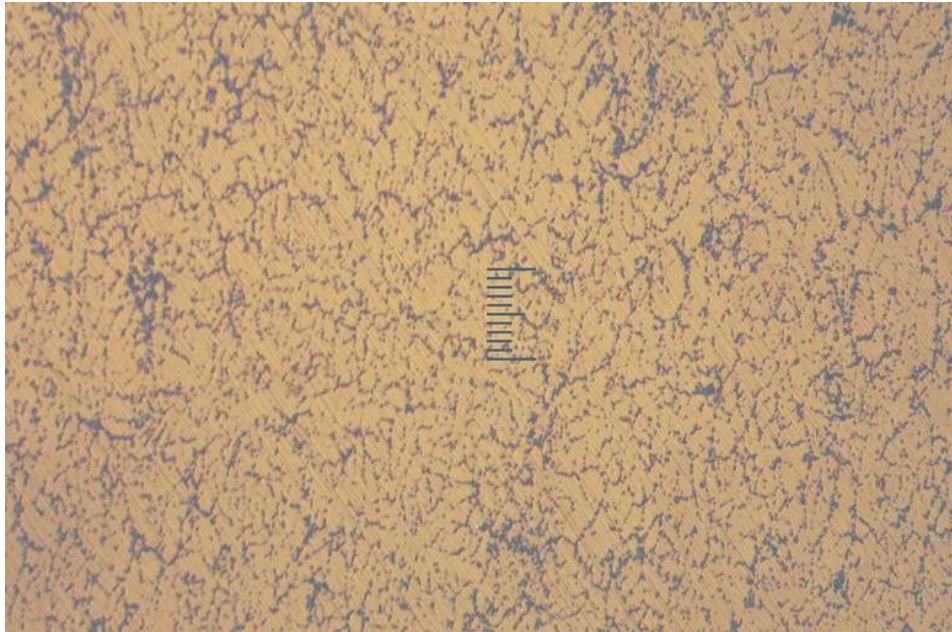


Figure 5.3. Microstructure of mid-portion of sample S1 (x100)

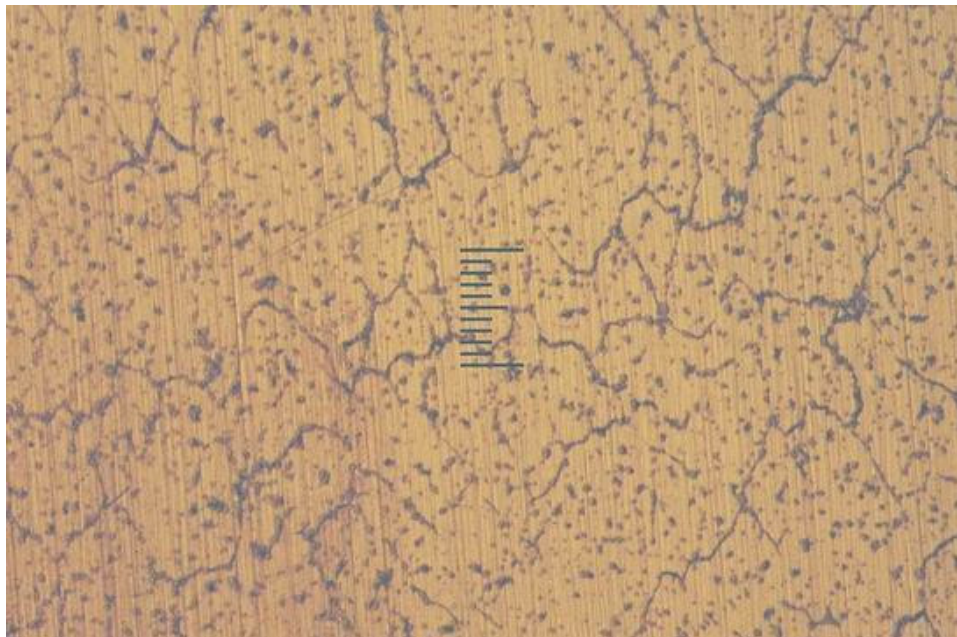


Figure 5.4. Microstructure of surface portion of sample S2 (x100)

Specimen S2 was formed with an isothermal holding time of 5 minute at the same temperature. The images of the formed samples from different regions were shown in Figure 5.4 and 5.5. The effects of increasing isothermal holding time can be observed when compared to the images of the sample S1. It can be seen from the figures that increasing the holding time from 3 to 5 minutes starts the globularization mechanism of the

grains. However this can only be observed in surface sections of the samples. In addition the grain boundaries were not clear in all parts and the grains were not in the shape of exact spheroids. The eutectic structure between the primary grains was not clear because the reheating temperature and holding time were still not sufficient for complete eutectic melting. As a result the forming of the sample was due to the deformation of the grains rather than liquid flow. The observed deformation of the primary grains in the microstructure images confirms this. Average grain size was about 60  $\mu\text{m}$  ranging from 40 to 85  $\mu\text{m}$ .

The center area of the sample did not show such microstructure as the surface part. This could be the consequence of resistance heating method employed throughout the study. Because of heating by convection in the furnace the inner parts remained cooler compared to the surface of the sample and globularization did not occur at inner regions. In view of the heating characteristics of resistance furnace, the occurrence of microstructural evolution, such as, eutectic melting, spheroidization and grain coarsening was not synchronous, but in turn and gradually carried out from the surface to the center of billet during reheating. As a result the surface parts of the samples became globular and eutectic melting occurs earlier than the inner portions. These are the drawbacks of resistance heating and further holding time is needed for homogenous temperature distribution across the billet.

Holding time in specimen S3 was changed to 7 minutes and the reheating temperature kept same as the samples S1 and S2. Figure 5.6 and 5.7 represents the microstructure of the sample S3. The images revealed that the grains were more globular compared to S2. Unlike sample S2 surface and centre parts of the sample showed similar microstructure. This was obtained by the increase in holding time and eventually minimizing the temperature gradient throughout the sample. It is apparent that the liquid phase around the grains was clearer than S1 and S2 but still complete eutectic melting did not take place. The black areas around the collared regions correspond to the eutectic structure. Primary  $\alpha$  phase was found to be non-uniformly distributed through the eutectic phase. The grain sizes range from 40 to almost 120  $\mu\text{m}$  and the average was about 73  $\mu\text{m}$ . It can be noticed from the figures that the eutectic melting started and the grain boundaries were wetted and penetrated by the liquid phase. On the other hand still the deformation

was achieved mainly by the grains rather than the liquid flow. This can be observed from the shapes of the primary deformed grains in the images.

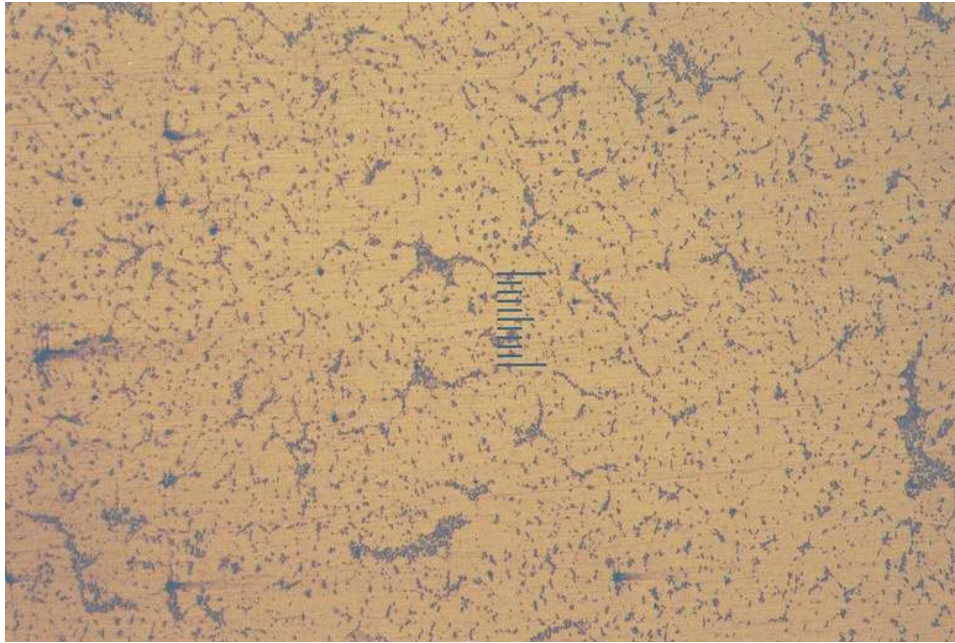


Figure 5.5. Microstructure of mid-portion of sample S2 (x100)

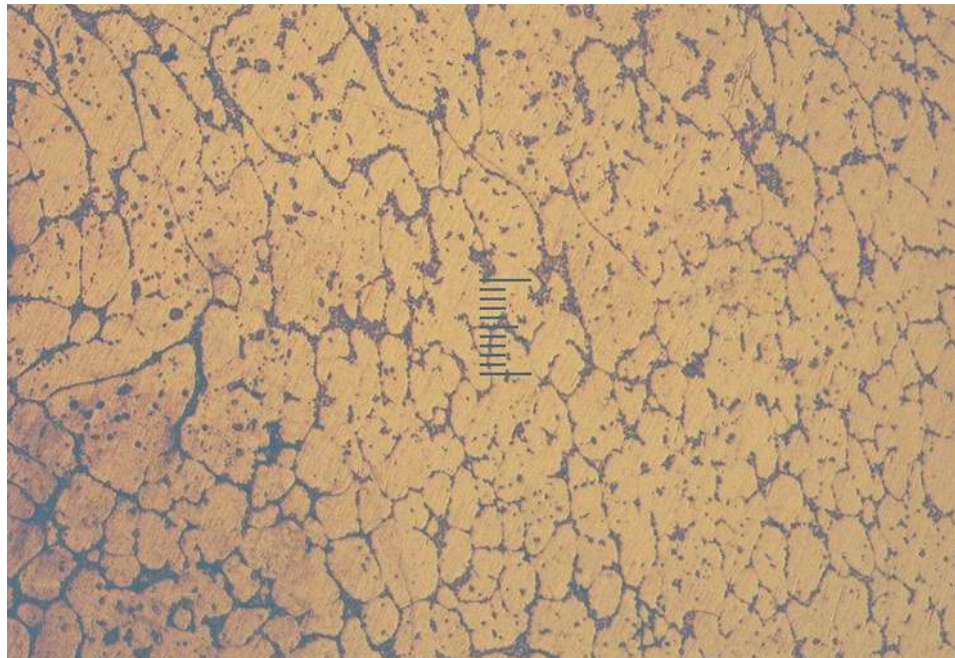


Figure 5.6. Microstructure of surface portion of sample S3 (x100)

It can be concluded from the above findings that at a reheating temperature of  $570^{\circ}\text{C}$  exact thixotropic structure can not be obtained. This is because the reheating temperature in these samples was below the eutectic temperature of A356 which is  $575^{\circ}\text{C}$ . With increasing the isothermal holding time from 3 to 7 minutes the primary grains started to be globular and the eutectic structure became more observable. However the separation between solid and liquid did not occur completely and the globularization was not completed but in progress in samples S2 and S3.

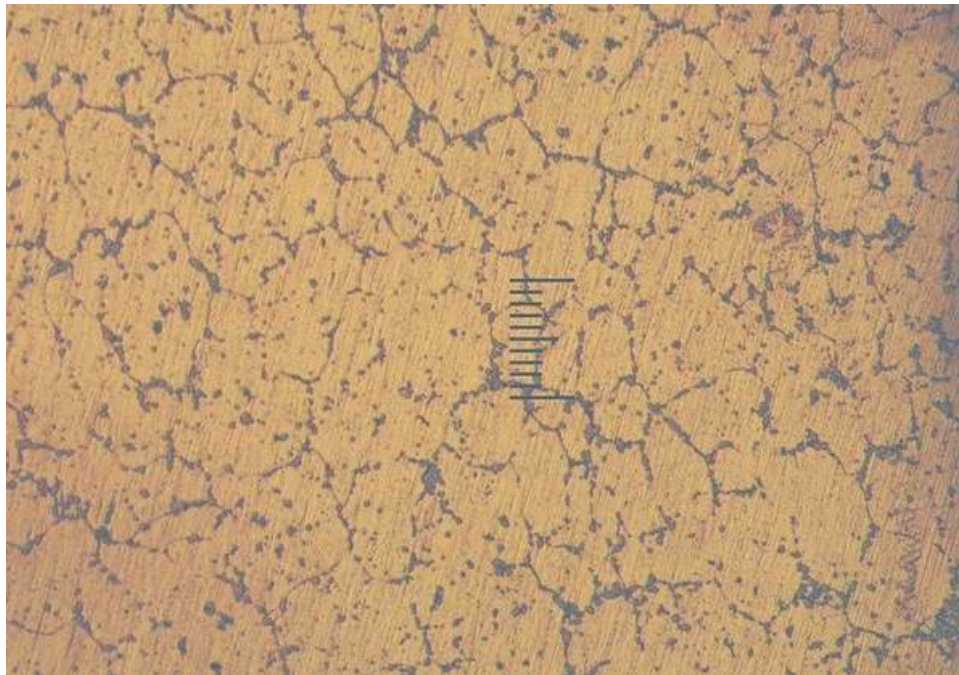


Figure 5.7. Microstructure of mid-portion of sample S3 (x100)

Samples S4, S5 and S6 were formed after reheating the specimens to  $580^{\circ}\text{C}$  and holding for 3, 5 and 7 minutes respectively like the previous samples.

Figure 5.8 and 5.9 represent the microstructure of sample S4. Globularization started on the surface region at this temperature. Unlike the experiments on  $570^{\circ}\text{C}$  the formation of globular grains started to form earlier at this temperature. The grain size was similar to the samples S2 and S3. Size of the primary grains range from  $50$  to  $85\ \mu\text{m}$  and the average grain size was  $68\ \mu\text{m}$ . As it was seen before in the sample S2, centre part of the sample showed no globular grains. Also the grain boundaries were not observable at mid-section. The reason was the lack of heat transfer to the mid portions by convection in the furnace.

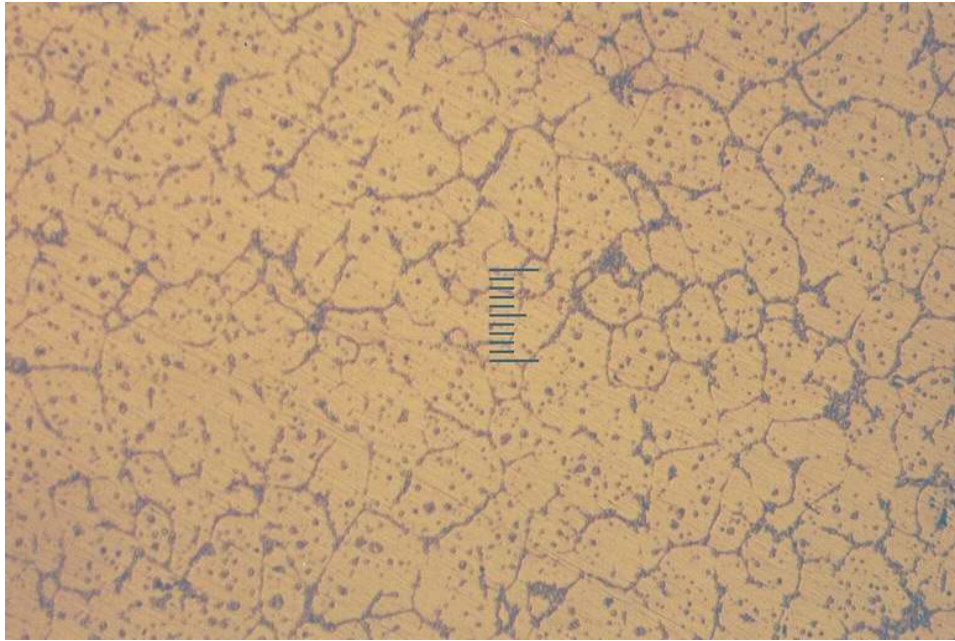


Figure 5.8. Microstructure of surface portion of sample S4 (x100)

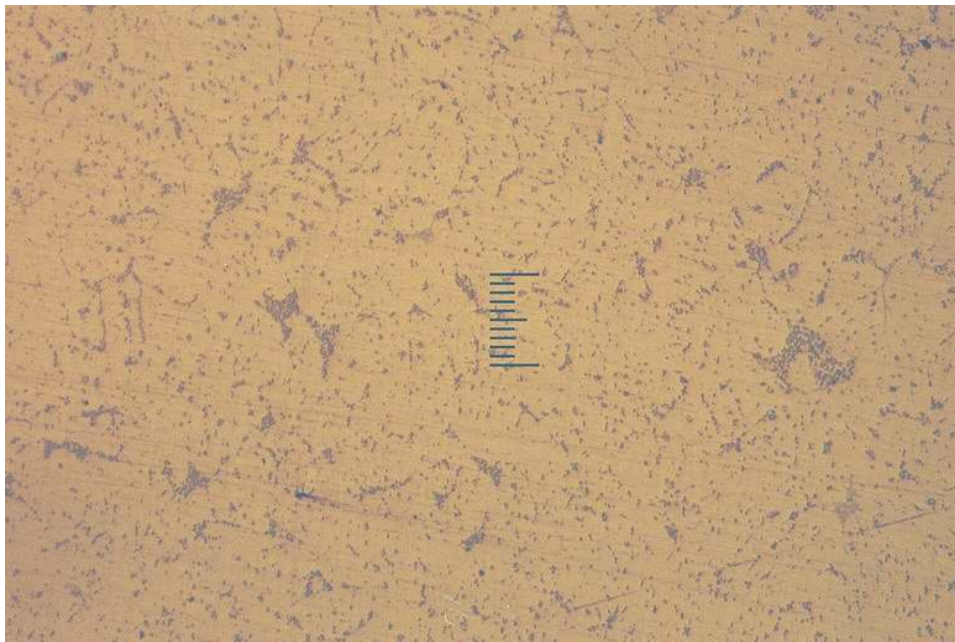


Figure 5.9. Microstructure of mid-portion of sample S4 (x100)

The images of sample S5 are shown in Figure 5.10, 5.11. Globular grains were obtained at this temperature. The eutectic structure was melted since the boundaries between the grains and the liquid phase were clear. Fine, equiaxed, spheroidal grains were dispersed uniformly in the quenched liquid matrix. The structure was homogeneous through the centre to the surface of the sample. This was achieved by the increase in

isothermal holding temperature from 3 to 5 minutes. With increasing the forming temperature to 580 °C homogenous temperature distribution across the sample was achieved earlier than the previous samples as a result of exceeding the eutectic melting point. Completely melted eutectic phase surrounded the primary  $\alpha$  grains and deformation was done mainly due to the effect of rotation and relative slip between the grains by the liquid flow. In other words the deformation of grains has minor contribution to the forming operation and the shape of the grains also confirmed this. Grain sizes range between 50  $\mu\text{m}$  to 100  $\mu\text{m}$ . Average grain size was 72  $\mu\text{m}$  and a significant coarsening was not observed by the increase of the holding time to 5 minutes. Round Si particles were observed between the boundaries. Smaller and globular-shaped Si particles in the products would effectively reduce the stress concentration at the boundary between Si particles and matrix under an applied stress and led to better mechanical properties. It was noticeable from the images that semi-solid forming was accomplished at 580 °C with 5 minutes of holding time.

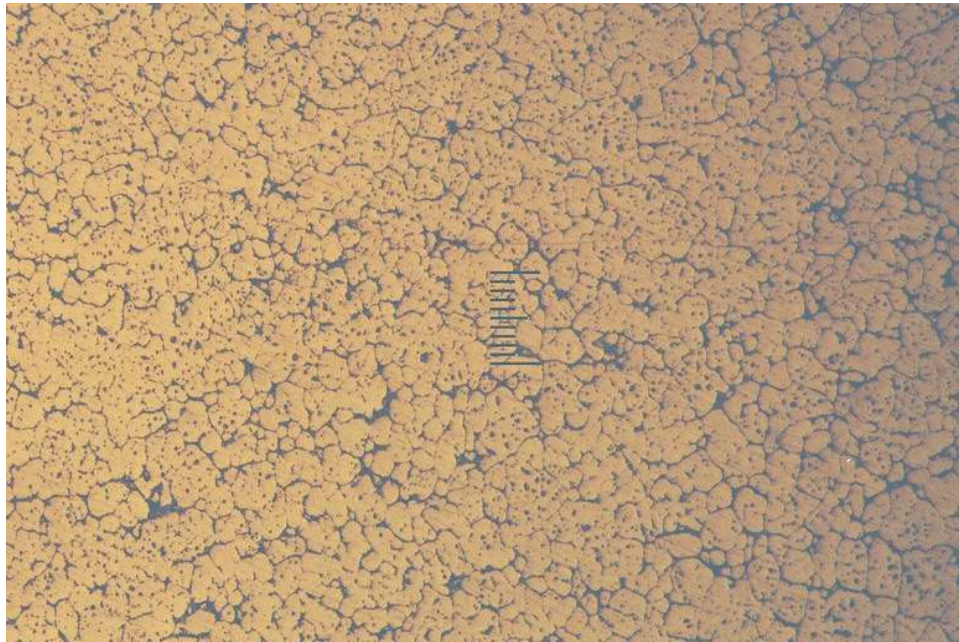


Figure 5.10. Microstructure of mid portion of sample S5 (x50)

The globular grains were also obtained in sample S6. Figure 5.12 and 5.13 represents the microstructure of sample S6. It can be seen from the images that separation between the solid and liquid phase was completed and the primary grains were uniformly distributed in the liquid matrix like the sample S5. The grains have a fine equiaxed and globular microstructure and the boundaries were clear. Grain size was between 60 to 120

$\mu\text{m}$ . Part of the liquid resides inside the solid grains, a result of the grain growth process. This type of liquid adversely affects the ability of the material to deform, since it decreases the amount of interconnected effective liquid available for deformation and results in increased temperature requirements. This was the result of prolonged heating time in resistance furnace heating. However the amount of interconnected liquid available for deformation was adequate. Average grain size below  $100\ \mu\text{m}$  in the reheated state will be sufficient to ensure a homogeneous material flow of the semi-solid alloy and good dimensional stability during die filling [4]. Average grain size was  $80\ \mu\text{m}$ . Figure 5.14 shows micrograph magnified to the scale of 500 to observe the eutectic microstructure obtained under the experimental conditions. Fine and uniform silica particles in the eutectic structure were obtained in the sample. On the other hand changing the holding time to 7 minutes resulted in coarsening of the grains because of coalescence and ripening, compared to sample S5. Therefore 5 minute of isothermal holding time would be appropriate to form the suitable thixotropic structure for semi-solid forming because further heating starts the development of grain coarsening.

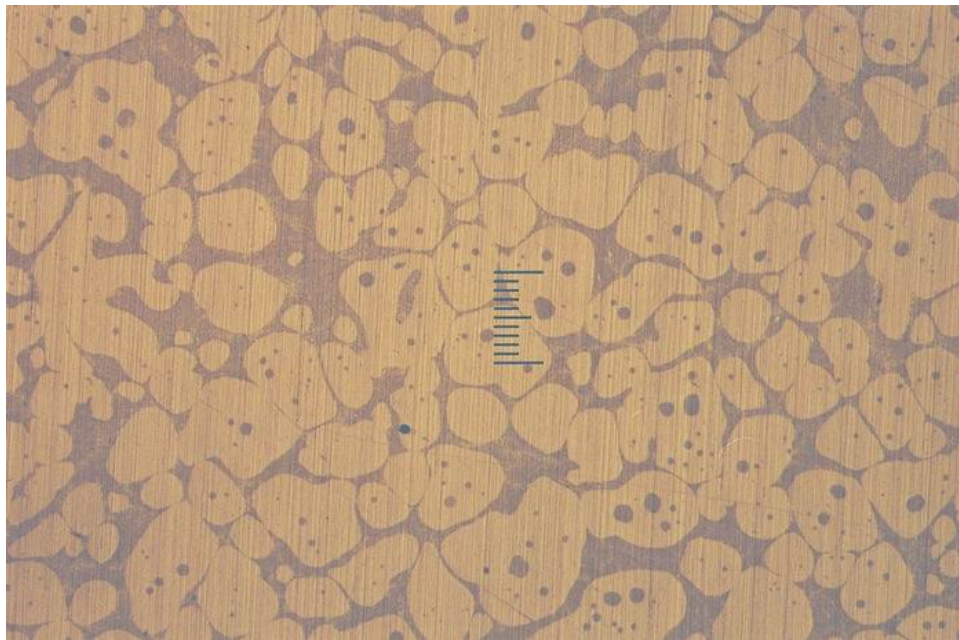


Figure 5.11. Microstructure of surface portion of sample S5 (x100)

As a result fine and globular microstructure was obtained for A357 alloy in samples S5 and S6. Liquid segregation and coarsening in silicon particles which result in undesirable variation in mechanical properties were not observed in the samples. Further

increase in holding time is not necessary because it results in grain growth, poor thixotropic behavior and also decreases in mechanical properties in the products.

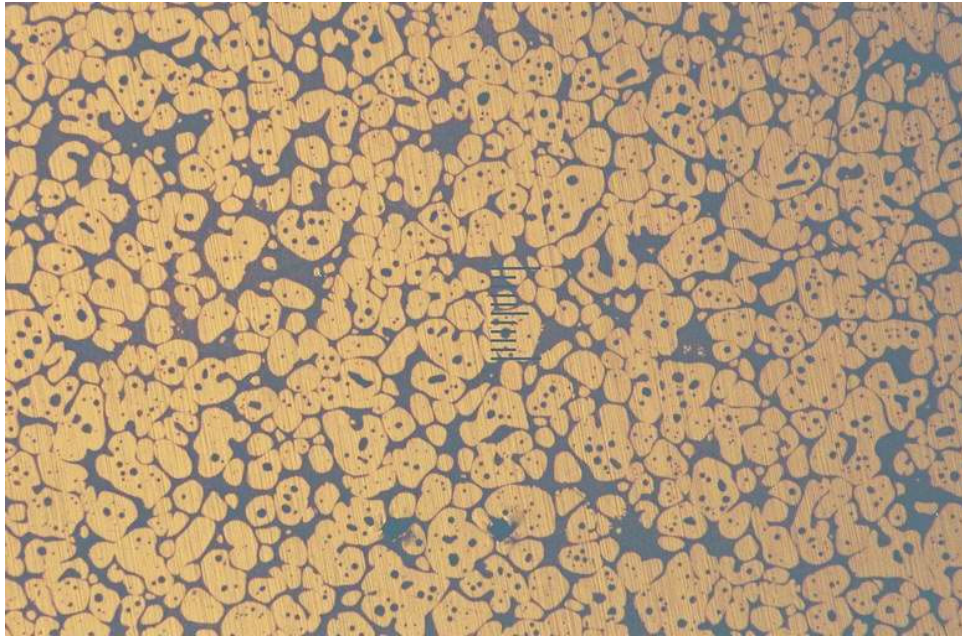


Figure 5.12. Microstructure of mid-portion of sample S6 (x50)

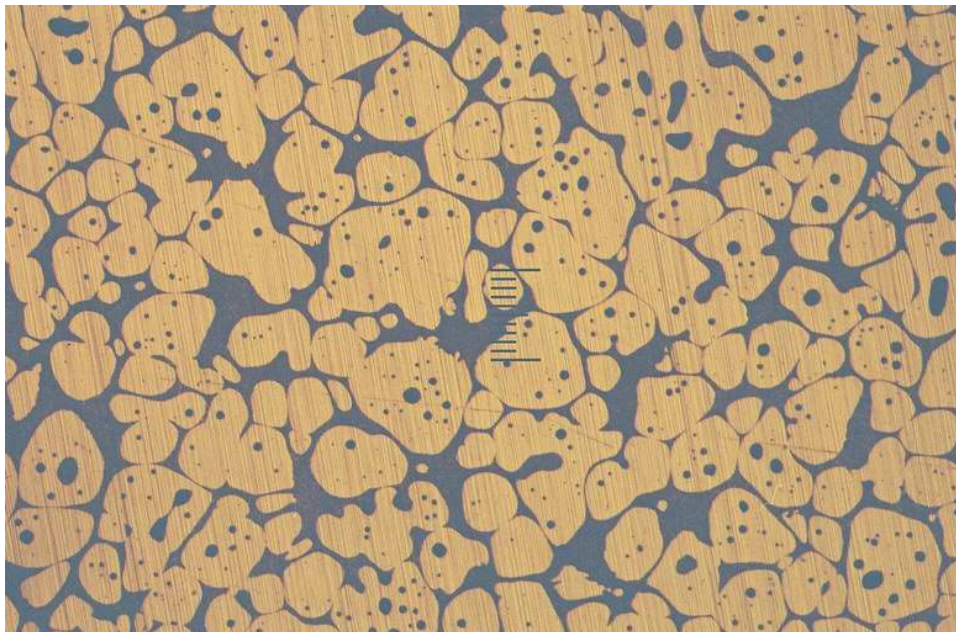


Figure 5.13. Microstructure of surface portion of sample S6 (x100)

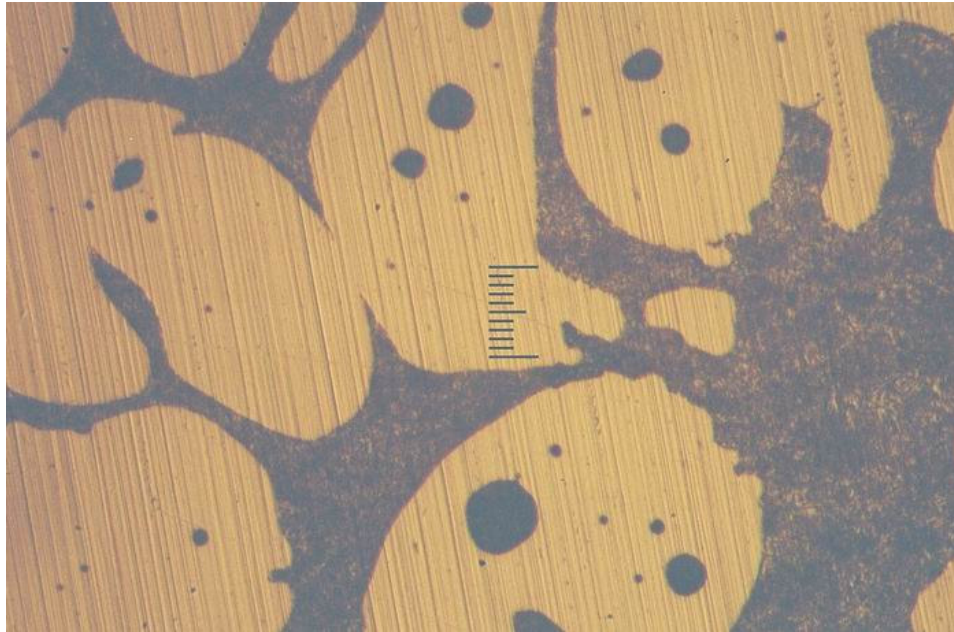


Figure 5.14. Eutectic microstructure of sample S6 (x500)

In order to evaluate globular mechanism more precise shape factor values were determined by analyzing the images with Image Tool program. The averages of the calculated shape factor (F) values were shown in table 5.1.

Table 5.1. Shape factor (F) values of the samples

Sample No	S1	S2	S3	S4	S5	S6
Shape Factor (F)	-	0,59	0,73	0,80	0,87	0,88

It can be said that the shape factor values increases gradually with changing the temperature from 570 to 580 °C. It is also noticeable from the values that increasing the holding time helps the globurization of the grains. With longer holding times the shape factor values converge to 1 which represents a perfect sphere. In contrast further increase in holding time results in grain coarsening in the microstructure and adversely effects the formability and the final mechanical properties of the product. As a result the holding time should be chosen carefully where maintaining the forming of globular structure together with preventing the coarsening of the primary grains.

Figures 5.15, 5.16 and 5.17 represent the microstructure of hot formed samples S7, S8 and S9. The images were similar to the raw material images and the grains were aligned

in the direction of deformation. Increasing the temperature from 450 °C to 500 °C showed no observable difference on the microstructure of the samples. In all of the samples the forming was accomplished by the deformation of solid primary grains rather than flow in the liquid intermetallic matrix. Because of this lower mechanical properties can be expected in hot formed products.

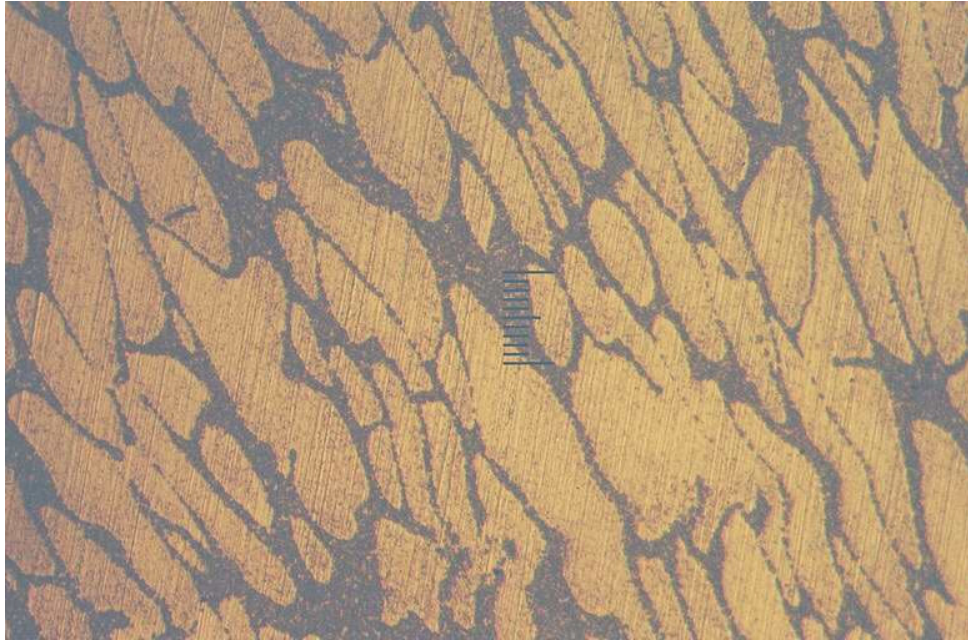


Figure 5.15. Microstructure of sample S7 (x500)

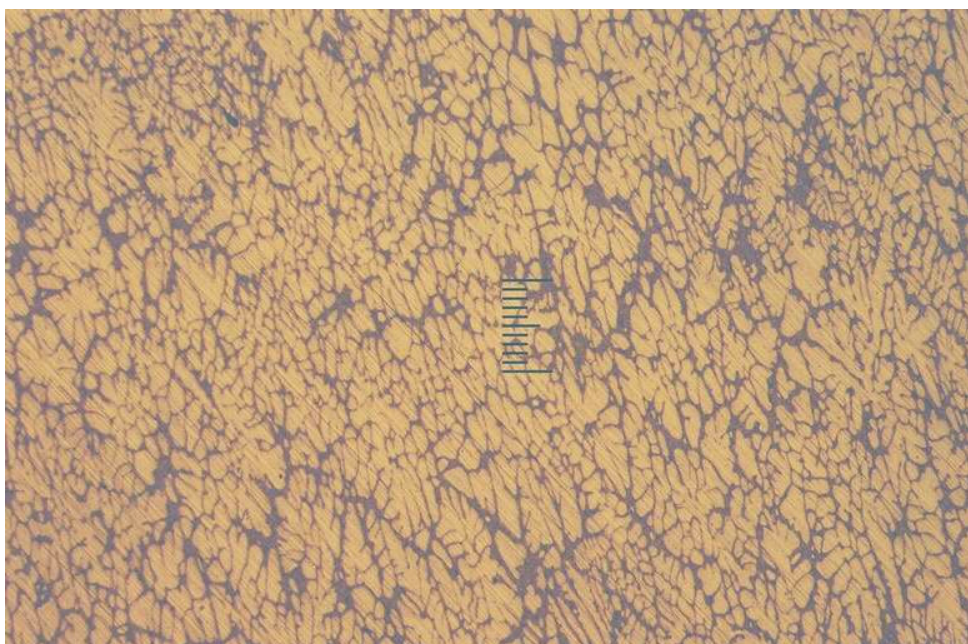


Figure 5.16. Microstructure of sample S8 (x100)

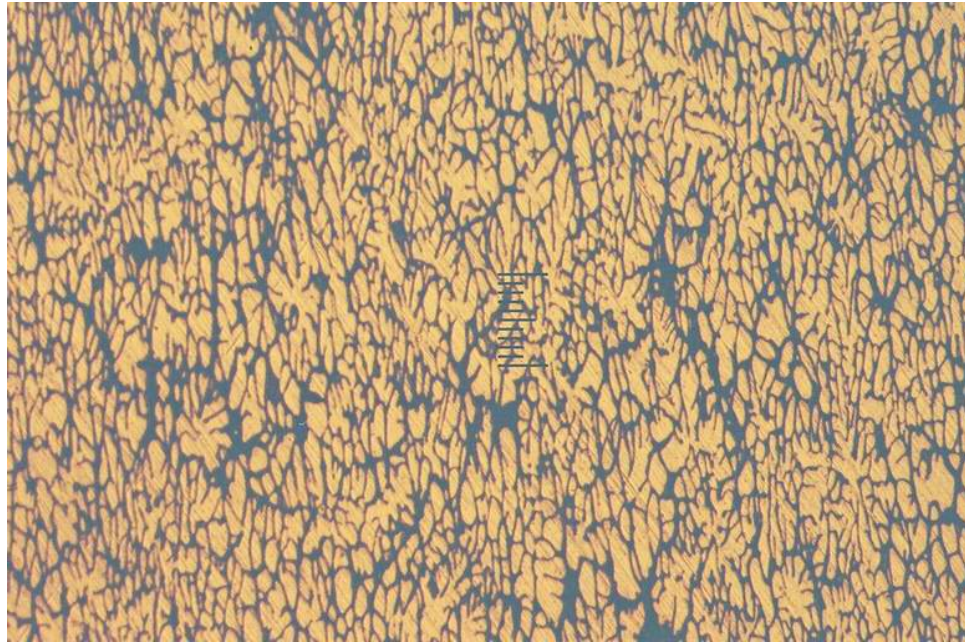


Figure 5.17. Microstructure of sample S9 (x100)

## 5.2. Mechanical Properties

After microstructural examinations Vickers Microhardness values of the samples were determined in order to observe the difference of mechanical properties between semi-solid forming and hot forming. The measurements were performed at 5 different points through the cross sectional height and width section of the samples. So hardness distribution across the sample was determined. Average of 3 measurements at each point was taken as the final value. Hardness measurements were made on the specimens that were formed in the shorter die. Figures 5.18, 5.19, 5.20 and 5.21 show the hardness of the semi-solid formed samples. The y axis refers to height while x axis refers to width of the samples.

As seen from the figures, generally the values were higher at the surface portions of the samples. This should be the result of direct pressing force by the punch and inner surface of the die to the product. On the other hand the results did not show general increasing or decreasing behavior through the sample. The hardness values range between 63-82 HV after semi-solid forming experiments.

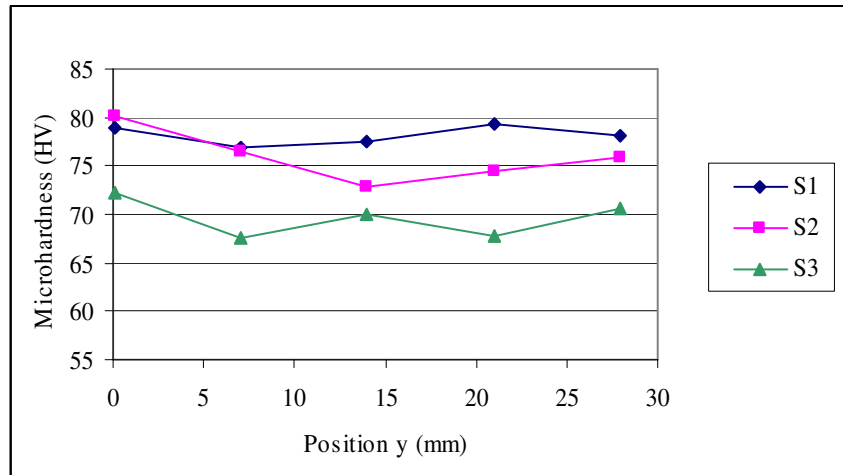


Figure 5.18. Vickers microhardness values of samples S1, S2 and S3 through height

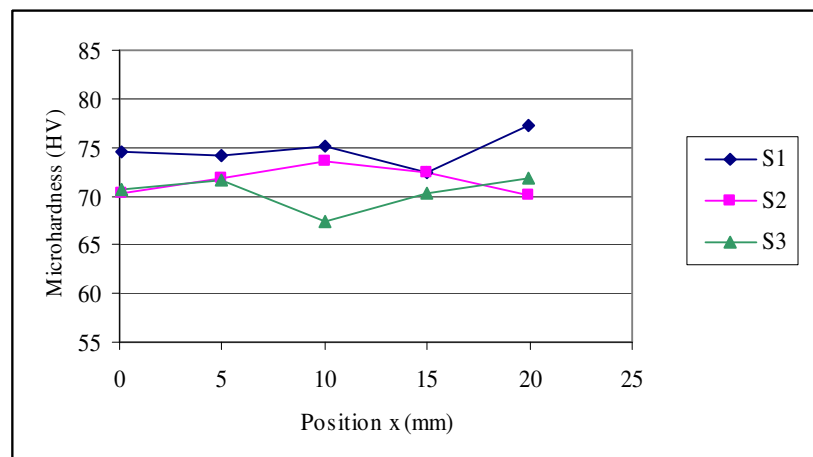


Figure 5.19. Vickers microhardness values of samples S1, S2 and S3 through width

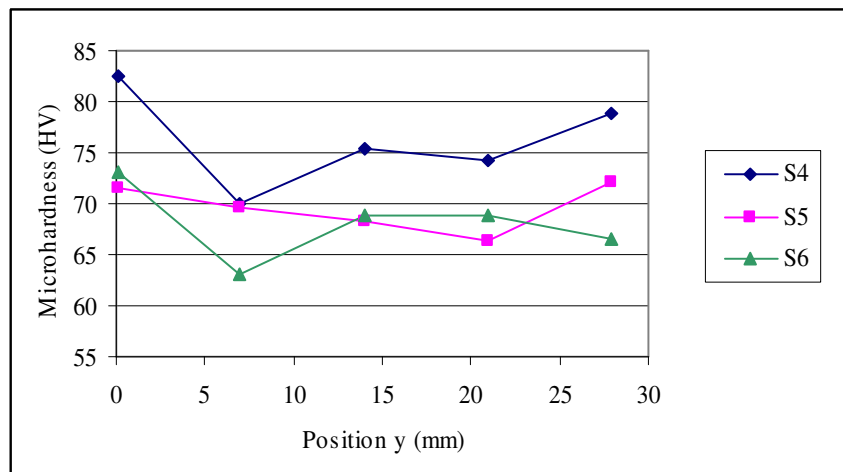


Figure 5.20. Vickers microhardness values of samples S4, S5 and S6 through height

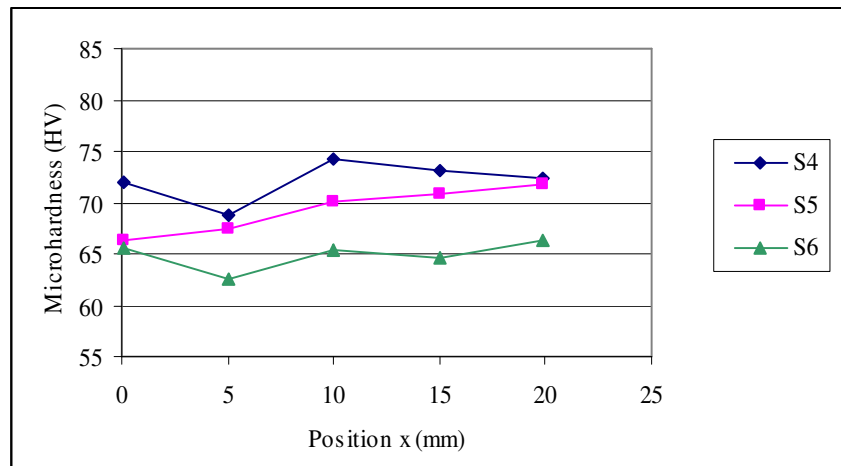


Figure 5.21. Vickers microhardness values of samples S4, S5 and S6 through width

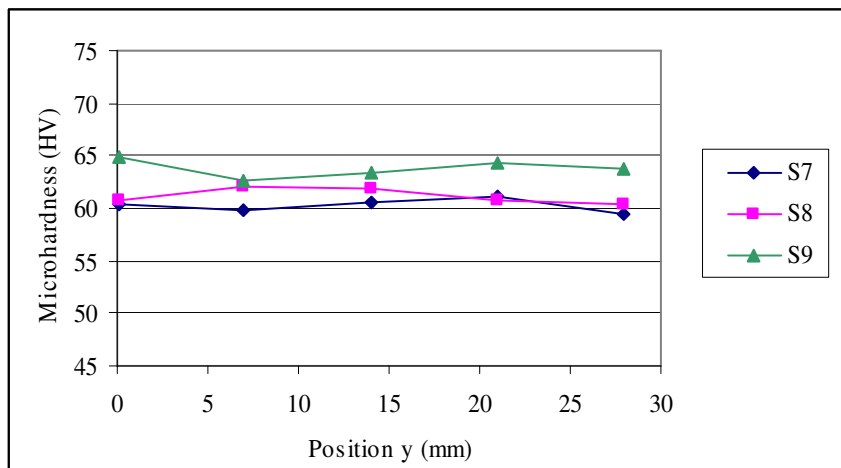


Figure 5.22. Vickers microhardness values of samples S7, S8 and S9 through height

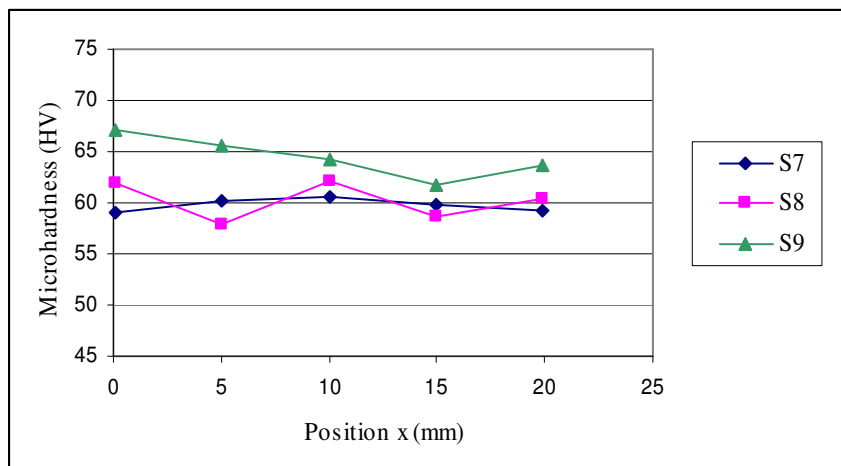


Figure 5.23. Vickers microhardness values of samples S7, S8 and S9 through width

The hardness values of hot-formed products were shown in Figures 5.22 and 5.23. The values were in the range of 58-67 HV. The values were more uniform compared to thixoformed products and there was no general increasing or decreasing tendency in the samples. As it can be seen from the figures hardness of the samples decrease with increasing temperature and highest hardness values were observed in sample S9 which has a forming temperature of 450 °C. Hardness of samples S7 and S8 were appear to be similar.

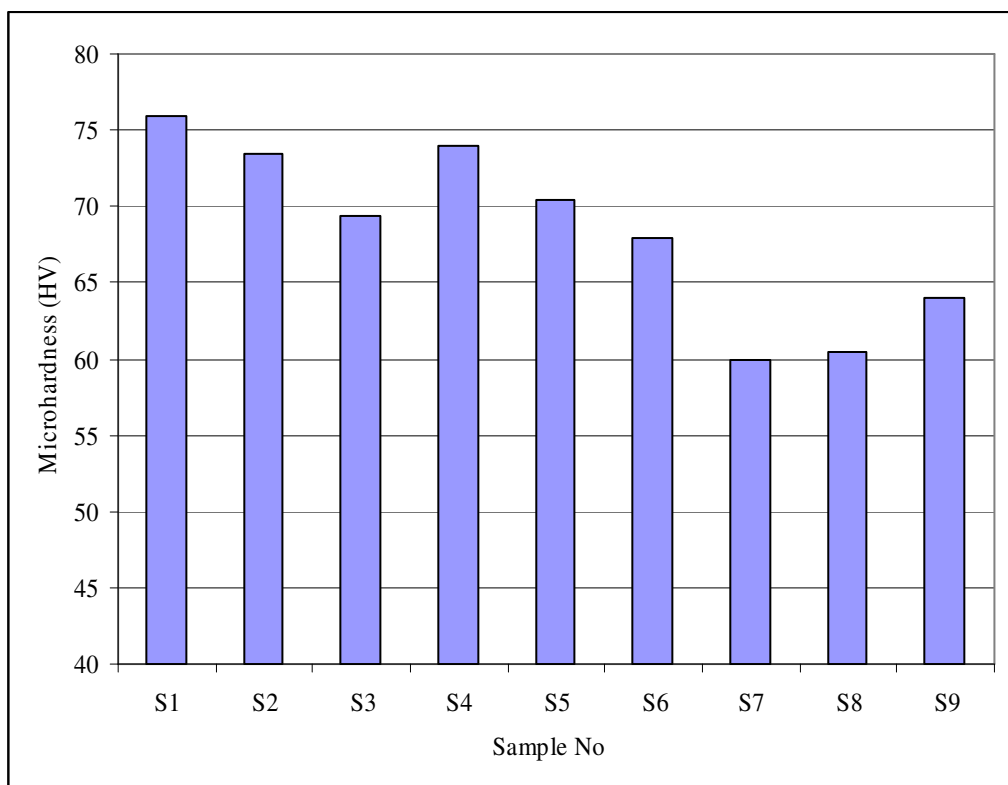


Figure 5.24. Average Vickers microhardness values of the samples

Figure 5.24 shows the average hardness values of the samples as a whole in order to make a comparison between semi-solid forming and hot forming experiments. It can be noticed from the figure that hardness values tend to decrease with increasing holding time in thixo-formed products S1, S2, S3, S4, S5 and S6. After 5 minutes of holding time the decrease became more observable. This could be the outcome of grain coarsening with the prolonged holding times. In addition to this, a slight decrease in hardness values was observed with increasing the forming temperature from 570 °C to 580 °C. All of the hot-formed specimens S7, S8 and S9 showed lower hardness levels than the semi-solid formed

ones. Therefore, it can be summarized that in semi-solid forming better mechanical properties were determined by means of hardness levels.

After microhardness measurements, tensile test were performed on the specimens and yield strength, tensile strength and elongation to fracture values were determined to make a further comparison between the mechanical properties of the samples. The tests were performed on the specimens S3, S5, S7 and S9.

Table 5.2. Tensile test results of the products

<b>Sample No</b>	<b>S3</b>	<b>S5</b>	<b>S7</b>	<b>S9</b>
<b>Yield Strength (MPa)</b>	64	79	60	67
<b>Tensile Strength (MPa)</b>	195	225	186	190
<b>Elongation (%)</b>	14,9	14,7	18	15,8

Table 5.2 shows the tensile test results of the products and Table 5.3 represents the tensile values found in the literature. The values indicate that semi-solid formed samples S2 and S5 gave better tensile properties when compared to the hot formed samples S7 and S9. This table demonstrates that semi-solid forming is beneficial for improving tensile properties compared to hot forming. The grains retained their shape during deformation by the help of liquid flow and the fine and equiaxed grains led to better mechanical properties in the product. Therefore the mechanical properties were better in thixo-formed products as expected. Also the results were similar to those found in the literature. However the results were not at best values as in the literature. This could be the result of grain coarsening and liquid penetration in the grains as a consequence of resistance furnace heating. In addition lower pressing forces on the experiments compared to the ones on the literature could be another reason for these findings. Sub-size specimens used in tensile test could be another reason. Better properties can be achieved with T6 heat treatment on the alloys.

In contrary with the tensile strength results better elongation values were determined in hot forming experiments. The improvement of tensile strength and elongation in forming is not expected together. Another observed difference between the two forming experiments was that necking was developed in the hot-formed samples. In semi-solid formed samples fracture occurred at the maximum stress value. On the other in the hot-

formed samples necking was observed and the tensile value at fracture was lower than the ultimate tensile result. In other words ultimate tensile strength was not observed in semi-solid formed samples. Low hardening rate was the reason of this necking situation.

Table 5.3. Mechanical properties of A356 aluminum alloy

	<b>Yield Strength (MPa)</b>	<b>Tensile Strength (MPa)</b>	<b>Elongation (%)</b>
<b>Semi-solid Forming (66,67,68)</b>	85-110	190-240	12-18
<b>Hot Forming (69)</b>	-	160	18

## 6. CONCLUSIONS

According to the results of the experiments it was established that determining a fine and globular microstructure for semi-solid forming is possible in resistance furnace heating. However care must be taken in transferring the reheated billets to the die in order to prevent the heat loss and oxide layer on the surface during the operation. In addition handling the billet at high liquid fractions is a major problem in thixoforming. Apart from these issues, resistance furnace heating can be used as an alternative method. Its advantages are the simplicity and lower costs compared to induction heating method.

After the experiments with different parameters fine and uniformly distributed grains in a liquid matrix was obtained at  $580^{\circ}\text{C}$  in 5 and 7 minutes of holding times. However after 5 minutes the grain coarsening and penetration of liquid phase inside the grains occurred at the samples. In addition the liquid fraction of the metal increased rapidly and this led to difficulties in handling the reheated billets. It was also found that reheating the billets to  $570^{\circ}\text{C}$  did not give satisfactory result for the operation. In thixoforming globular and solid grains in a liquid eutectic matrix is needed. Although the holding time was prolonged to 7 minutes, the obtained microstructure was not totally globular and the grain boundaries were not clear. This was because  $570^{\circ}\text{C}$  was below the eutectic temperature of the alloy and complete eutectic melting could not be reached. The best results were achieved by holding the samples for 5 minutes at  $580^{\circ}\text{C}$ . It was also enough for the homogeneity of temperature distribution across the billet and further increment was not necessary which will promote grain coarsening and adversely affects the mechanical properties. The microstructure of the hot-formed specimens was alike to the raw material and did not show any difference with different temperatures. The grains were aligned along the deformation direction.

After microstructural examinations mechanical test were performed on the products. Firstly hardness measurements were made on the formed samples. The results revealed that in semi-solid forming hardness values decrease with the increase in holding times. In addition to this, increasing the forming temperature from  $570^{\circ}\text{C}$  to  $580^{\circ}\text{C}$  resulted in a

slight decrease at the values. Besides, at hot formed experiments best results were achieved at the lowest forming temperature and a severe decrease in hardness was observed after 470 °C. It is clear from these findings that hot forming experiments should be done at lower temperatures. According to the hardness values of the final products it can be summarized that semi-solid forming of the A356 aluminum alloy gave better results than the hot forming. Secondly tensile tests were carried out on the samples. The tensile properties of semi-solid formed samples were better than the hot-formed ones. On the other hand hot forming gave better elongation levels. The results were also similar to the ones found on literature.

## REFERENCES

1. Office of Industrial Technologies Energy Efficiency and Renewable Energy, “Aluminum Project Fact Sheet”, <http://www.oit.doe/IOF/aluminum>
2. Atkinson, H. V., “Modeling the Semisolid Processing of Metallic Alloys”, *Progress in Materials Science*, Vol. 50, pp. 341-412, 2005.
3. Barkhudarov, M. R., “Advanced Simulation of the Flow and Heat Transfer Processes in Simultaneous Engineering”, <http://www.flow3d.com/pdfs/simeng.pdf>
4. Fan, Z., “Semi-solid Metal Processing”, *International Materials Reviews*, Vol. 47, No. 2, pp. 49-85, 2002.
5. Hirt, G., R. Cremer, T. Witulski and H. C. Tinius, “Lightweight Near Net Shape Components Produced by Thixoforming”, *Materials and Design*, Vol. 18, pp. 315-321, 1997.
6. Rovira, M. M., B. C. Lancini and B. H. Robert, “Thixoforming of Al-Cu Alloys”, *Journal of Materials Processing Technology*, Vol. 92, pp. 42-49, 1999.
7. Yang, Y. S. and Y. A. Tsao, “Viscosity and Structure Variations of Al-Si Alloy in the Semi-solid State”, *Journal of Material Science*, Vol. 32, pp. 2087-2092, 1997.
8. Flemings, M. C., “Behavior of Metal Alloys in the Semi-solid State”, *Metallurgical Transactions A*, Vol. 22A, pp. 957-981, 1991.
9. Vogel, A., R. D. Doherty and B. Cantor, “Solidification and Casting of Metals”, *The Metals Society*, pp.518-525, 1979.

10. Qin, R. S. and Z Fan, "Fractal Theory Study on Morphological Dependence of Viscosity of Semi-solid Slurries", *Materials Science and Technology*, Vol. 17, pp. 1149-1152, 2001.
11. Ji, S. and Z. Fan, "Solidification Behavior of Sn-15Pb Alloy Under High Shear rate and High Intensity of Turbulence", *Metallurgical and Materials Transactions*, Vol. 33A, pp. 3511-3520, 2002.
12. Ji, S., Z. Fan and M. J. Bevis, "Semi-solid Processing of Engineering Alloys by a Twin-screw Rheomoulding Process", *Materials Science and Engineering*, Vol. A299, pp. 210-217, 2001.
13. Seconde, J. F. and M. Suery, "Effect of Solidification Conditions on Deformation Behavior of Semi-solid Sn-Pb Alloys", *Journal of Materials Science*, Vol. 19, pp. 3995-4006, 1984.
14. Liua, D. B., H. V. Atkinson and R. L. Higginson, "Disagglomeration in Thixoformed Wrought Aluminium Alloy 2014", *Materials Science and Engineering A*, Vol. 392, pp. 73-80, 2004.
15. Chen, J. Y. and Z. Fan, "Modelling of Rheological Behaviour of Semi-solid Metal Slurries Part 1", 2001, <http://www.brunel.ac.uk/controls/common/275.pdf>.
16. Modigell M. and J. Koke, "Time-dependent Rheological Properties of Semi-solid Metal Alloys", *Mechanics of Time-Dependent Materials*, Vol. 3, pp. 15-30, 1999.
17. Tzimas, E. and A. Zavaliangos, "Mechanical Behavior of Alloys with Equiaxed Microstructure in the Semi-solid State at High Solid Content", *Acta Materialia*, Vol. 47, pp. 517-528, 1999.
18. Koke, J. and M. Modigell, "Flow Behaviour of Semi-solid Metal Alloys", *Journal of Non-Newtonian Fluid Mechanics*, Vol. 112, pp. 141-160, 2003.

19. Joly, P. A. and R. Mehrabian, "The rheology of a Partially Solid Alloy", *Journal of Materials Science*, Vol. 11, pp. 1393-1418, 1976.
20. Gilmer, R. B., N. A. Andreas and V. Entov, "Thixotropic Rheology of Semi-solid Metal Suspensions", *Journal of Materials Processing Technology*, Vol. 110, pp. 164-176, 2000.
21. Chris, S. R. and F. M. Patricio, "Slurry Based Semi-solid Die Casting", *Advanced Materials and Processes*, Vol. 159, pp.49-52, 2001.
22. Flemings, M. C., R. G. Riek and K. P. Young, "Rheocasting", *Materials Science and Engineering*, Vol. 25, pp. 103-117, 1976.
23. Spencer, D. B., R. Mahrebian and M. C. Flemings, "Rheological Behavior of Sn-15 Pct Pb in the Crystallization Range", *Metallurgical Transactions*, Vol. 3, pp. 1925-1935, 1972.
24. Brabazon, D., D. J. Browne and A. J. Carr, "Mechanical Stir Casting of Aluminium Alloys From the Mushy State: Process, Microstructure and Mechanical Properties", *Materials Science and Engineering*, Vol. A326, pp. 370-381, 2002.
25. Flemings, M. C., R. A. Martinez-Ayers, A. M. Figueredo and J. A. Yurko, "Metal Alloy Compositions and Process", *U.S. Patent*, 6,645,323, 2003.
26. Jung, B. I., C. H. Jung, T. K. Han and Y. H. Kim, "Electromagnetic Stirring and Sr Modification in A356 Alloy", *Journal of Material Processing Technology*, Vol. 111, pp. 69-73, 2001.
27. Vives, C., "Elaboration of Metal Matrix Composites from Thixotropic Alloy Slurries Using a New Magnetohydrodynamic Caster", *Metallurgical Transactions B*, Vol. 23B, pp. 189-205, 1992.

28. Zoqui, E. J., M. Paes and E. Sadiqi, "Macro and Microstructure Analysis of SSM A356 Produced by Electromagnetic Stirring", *Journal of Material Processing Technology*, Vol. 120, pp. 365-373, 2002.
29. Yang, Z., C. G. Kang and P. K. Seo, "Evolution of the Rheocasting Structure of A356 Alloy Investigated by Large-scale Crystal Orientation Observation", *Scripta Materialia*, Vol. 52, pp. 283-288, 2004.
30. Kenney, M. P., J. A. Courtois, R. D. Evans, G. M. Farnior, C. P. Kyonka, A. A. Koch and K. P. Young, "Semi-solid Metal Casting and Forging", *Metals Handbook, 9th edition*, Vol.15, Metals Park, OH ASM International, pp. 327-338, 1988.
31. Zhou, Y., J. Lu, N. S. Saluja, S. Singh and A. V. Riviere, "Processes for Producing Fine Grained Metal Compositions Using Continuous Extrusion for Semi-solid Forming of Shaped articles", *U.S Patent*, 6,120,625, 2000.
32. Ward, P. J., H. V. Atkinson, P. R. G. Anderson, L. G. Elias, B. Garcia, L. Kahlen and J. M. Rodriguez, "Semi-solid Processing of Novel MMCs Based on Hypereutectic Aluminium-silicon Alloys", *Acta Materialia*, Vol. 44, pp. 1717-1727, 1996.
33. Tzimas, E. and A. Zavaliangos, "Evolution of Near-equiaxed Microstructure in the Semi solid state", *Materials Science and Engineering A*, Vol. 289, pp. 228-240, 2000.
34. Manson-Whitton, E. D., I. C. Stone, J. R. Jones, P. S. Grant and B. Cantor, "Isothermal Grain Coarsening of Spray Formed Alloys in the Semi-solid State", *Acta Materialia*, Vol. 50, pp.2517-2535, 2002.
35. Flemings, M. C., "Behavior of Metal Alloys in the Semi-solid State", *Metallurgical Transactions A*, Vol. 22A, pp. 269-292, 1991.

36. Hogg, S. C., H. V. Atkinson and P. Kapranos, "Semi-solid Rapid Compression Testing of Spray-formed Hypereutectic Al-Si Alloys", *Metallurgical and Materials Transactions*, Vol. 35A, pp. 899-911, 2004.
37. Adachi, M., O. Kogushi, H. Sasaki, H. Yasunori, T. Sakamoto, S. Satoru and Y. Atsushi, "Method and apparatus of shaping Semi-solid metals", *European Patent*, 0745694B1, 1996.
38. Xia, Xia and G. Tausig, "Liquidus Casting of a Wrought Aluminum Alloy 2618 for Thixoforming", *Materials Science and Engineering A*, Vol. 246, pp. 1-10, 1998.
39. Haga, T. and S. Suzuki, "A Downward Melt Drag Single Roll Caster for Casting Semi-solid Slurry", *Journal of Materials Processing Technology*, Vol. 157-158, pp. 695-700, 2004.
40. Haga, T. and P. Kapranos, "Billetless Simple Thixoforming Process", *Journal of Materials Processing Technology*, Vol. 130-131, pp. 581-586, 2002.
41. Liu, D., H. V. Atkinson, P. Kapranos, W. Jirattiticharoean and H. Jones, "Microstructural Evolution and Tensile Mechanical Properties of Thixoformed High Performance Aluminium Alloys", *Materials Science and Engineering*, Vol. A361, pp. 213-224, 2003.
42. Douglas, A. G., "Aluminum Silicon Alloys", *Metals Handbook, 9th edition*, Vol.15, Metals Park, OH ASM International, pp. 159-167, 1988.
43. Jian, X., H. Xu, T.T. Meek. and Q. Han, "Effect of Power Ultrasound on Solidification of Aluminum A356 Alloy", *Materials Letters*, Vol. 59, pp. 190-193, 2005.
44. Abramov, V. O., Abramov, O. V. Abramov, B. B. Straumal and W. Gust, "Hypereutectic Al-Si Based Alloys with a Thixotropic Microstructure Produced by Ultrasonic Treatment", *Materials and Design*, Vol. 18, pp. 323-326, 1997.

45. Lapkowski, W., J. Sinczak and S. Rusz, "Feasibility of Metal Forming in Semi-liquid State", *Journal of Materials Processing Technology*, Vol. 63, pp. 260-264, 1997.
46. Cho, W.G. and C. G. Kang, "Mechanical Properties and Their Microstructure Evaluation in the Thixoforming Process of Semi-solid Aluminum Alloys", *Journal of Materials Processing Technology*, Vol.105, pp. 269-277, 2000.
47. Parkway Thixomolding, "Thixomolding Overview", 2003, [http://www.parkwayproducts.com/thixomolding/te\\_thixo.html](http://www.parkwayproducts.com/thixomolding/te_thixo.html).
48. Flender, E., M. Lipinski and E. Hepp, "New Developments for Process Modeling of Thixotropic Forming Process", *Proceedings of the 1st International Aluminum Casting Technology Symposium*, 1998, [http://www.foundrysoft.se/publications/1\\_99\\_Thixo.PDF](http://www.foundrysoft.se/publications/1_99_Thixo.PDF).
49. Wang, K. K., N. Wang and H. Peng, "Rheomolding a One-step Process for Producing Semi-solid Metal Castings with Lowest Porosity", *Proceedings of TMS Annual Meeting*, 1996.
50. Messmer, G., "Simulation of a Thixoforging Process of a Aluminum Alloy with Flow-3D", [http://www.thixoschmieden.de/misc/Veroeffentlichung\\_pdf/Mr%20Massiv01%20english.pdf](http://www.thixoschmieden.de/misc/Veroeffentlichung_pdf/Mr%20Massiv01%20english.pdf).
51. Jung, H. K., "The Induction Heating Process of Semi-solid Aluminium Alloys for Thixoforming and Their Microstructure Evaluation", *Journal of Materials Processing Technology*, Vol. 105, pp. 176-190, 2000.
52. Buynacek, C. J. and W. L. Winterbottom, "High Volume Semi-solid Forming of Aluminum Master Cylinders", 2000, <http://delphi.com/pdf/techpapers/2000-01-0060.pdf>.
53. Flemings, M. C., "Semi-solid Forming: The Process and the Path Forward", *Metallurgical Science and Technology*, Vol. 18, No. 2, pp.3-4, 2000.

54. Kang, C. G., Y. J. Jung and S. W. Youn, "Horizontal Reheating of Aluminum Alloys and Semi-solid Casting for a Near Net Shape Compressor Component", *Journal of Materials Processing Technology*, Vol. 135, pp. 158-171, 2003.
55. Kapranos, P., R. C. Gibson, D. H. Kirkwood and C. M. Sellars, "Induction Heating and Partial Melting of High Melting Point Thixoformable Alloys", *Proceedings of the 4th International Conference on Semi-solid Processing Alloys and Composites*, 1996.
56. Dughiero, F., M. Forzanand, S. Lupi, "Reheating 150 mm Billets of A356 Alloy for Thixo-processing", 2003, <http://www.modlab.lv/publications/mep2003/pdf/187.pdf>.
57. Omar, M. Z., E. J. Palmiere, A. A. Howe, H. V. Atkinson and P. Kapranos, "Thixoforming of a High Performance HP9/4/30 Steel", *Materials Science and Engineering*, Vol. A395, pp. 53-61, 2005.
58. Rosso, M., E. Romano and S. Barone, "Properties Improvement of Thixoformed Parts by Liquid Hot Isostatic Process", *Metallurgical Science and Technology*, Vol. 19, No. 1, pp. 28-33, 2001.
59. The Aluminium Federation of Southern Africa, 1999, "Hot Forming of Aluminum Alloys", <http://www.afsa.co.za/download/tech/intro3.pdf>.
60. Efundu Engineering Fundamentals, 2005, "Extrusion", [http://www.efunda.com/processes/metal\\_processing/extrusion.cfm](http://www.efunda.com/processes/metal_processing/extrusion.cfm).
61. Efundu Engineering Fundamentals, 2005, "Forging", [http://www.efunda.com/processes/metal\\_processing/Forging.cfm](http://www.efunda.com/processes/metal_processing/Forging.cfm).
62. Aluminim Pechiney, "Althix Billets", 1996.
63. Meles Griot, "Vickers Microhardness Test", 2005, <http://www.mellesgriot.com/glossary/wordlist/glossarydetails.asp?wID=232>.

64. National Instruments, “Mechanical Engineering Laboratory” 2003, [http://www.ni.com/pdf/academic/us/me105\\_lab3\\_2003.pdf](http://www.ni.com/pdf/academic/us/me105_lab3_2003.pdf).
65. ASTM E-8M-04 Standard, “Standard Test Methods for Tension Testing of Metallic Materials”, 2004.
66. Winterbottom, W. L., “Semi-solid Forming Applications: High Volume Automotive Products”, *Metallurgical Science and Technology*, Vol. 18, No. 2, pp. 5-10, 2000.
67. Leo, P. and E. Cerri, “Silicon Particle Damage in a Thixocast A356 Aluminum Alloy”, *Metallurgical Science and Technology*, Vol. 21, No. 1, pp. 27-31, 2003.
68. Siegert, K, A. Wolf and J. Baur., “Thixoforging of Aluminum and Brass”, 2000, [http://www.cct-bw.de/veroeffentlichung\\_pdf/wgp-beitrag\\_thixoforging2.pdf](http://www.cct-bw.de/veroeffentlichung_pdf/wgp-beitrag_thixoforging2.pdf).
69. Shiomi M., D. Takano, K. Osakada and M. Otsu, “Forming of Aluminum Alloy at Temperatures just Below Melting Point”, *International Journal of Machine Tools and Manufacture* Vol. 43, pp. 229-235, 2002.

## REFERENCES NOT CITED

- Kang, C. G., H. K. Jung and K. W. Jung, “Thixoforming of a Aluminum Component with a Die Designed by Process Simulation”, *Journal of material Processing Technology*, Vol. 11, pp. 37-41, 2001.
- Alexanderov, S., P. T. Wang and R. E. Roadman, “A Fracture Criterion of Aluminum Alloys in Hot Metal Forming”, *Journal of material Processing Technology*, Vol. 160, pp. 257-265, 2005.
- Gokhale, A. M. and G. R. Patel, “Analysis of Variability in Tensile Ductility of a Semi-solid Metal Cast A356 Alloy”, *Materials Science and Engineering A*, Vol. 392, pp. 184-190, 2005.
- Bigot, R., V. Favier and C. Rouff, “Characterization of Semi-solid Material Mechanical Behavior by Indentation Test”, *Journal of material Processing Technology*, Vol. 160, pp. 43-53, 2005.
- Lee, S. Y., J. H. Lee and Y. S. Lee, “Characterization of Al 7075 Alloys After Cold Working and Heating in the Semi-solid Range”, *Journal of material Processing Technology*, Vol. 111, pp. 42-47, 2001.
- Kopp, R., D. Neudenberger and G. Winning, “Different Concepts of Thixoforging and Experiments for Rheological Data”, *Journal of material Processing Technology*, Vol. 111, pp. 48-52, 2001.
- Chen, T. J., Y. Hao, J. Sun and Y. D. Li, “Effects of Processing Parameters on Tensile Properties and Hardness of Thixoformed ZA27 Alloy”, *Materials Science and Engineering A*, Vol. 382, pp. 90-103, 2004.

Kliauga, A. M. and M. Ferrante, "liquid Formation and Microstructural Evolution During Re-heating and Partial melting of an Extruded A356 Aluminum Alloy", *Acta Materialia*, Vol. 53, pp. 345-356, 2005.

Zoqui, E. J., M. T. Shehata, M. Paes, V. Kao and E. Es-Sadiqi, "Morphological Evolution of SSM A356 During Partial Remelting", *Materials Science and Engineering A*, Vol. 325, pp. 38-53, 2002.

Jung, H.K. and C. G. Kang, "Reheating Process of Cast and Wrought Aluminum Alloys for Thixoforging and Their Globularization Mechanism", *Journal of material Processing Technology*, Vol. 104, pp. 244-253, 2000.